Title
Substrate recognition and processing by the 26S proteasome

Author
Bashore, Charlene

Publication Date
2015

Peer reviewed|Thesis/dissertation

Substrate recognition and processing by the 26S proteasome

By

Charlene Bashore

A dissertation submitted in partial satisfaction of the

requirements for the degree of

Doctor of Philosophy

in

Molecular & Cell Biology

in the

Graduate Division

of the

University of California, Berkeley

Committee in charge:
Professor Andreas Martin, Chair
Professor John Kuriyan
Professor Kathleen Collins
Professor Matthew F Francis

Spring 2015

Substrate recognition and processing by the 26S proteasome

Abstract

Substrate recognition and processing by the 26S proteasome

by

Charlene Bashore

Doctor of Philosophy in Molecular and Cell Biology

University of California, Berkeley

Professor Andreas Martin, Chair

Cell survival fundamentally depends on protein degradation, which in eukaryotes is carried out to a large extent by the ubiquitin-proteasome system (UPS) [1,2]. Cells not only must maintain the proteome and degrade misfolded or damaged polypeptides, but degradation of regulatory and signaling proteins mediates numerous vital processes, ranging from transcription to cell division[3]. As the final destination in the ubiquitin-proteasome system, the essential 26S proteasome is a compartmental protease of the AAA+ family that mechanically unfolds and degrades protein substrates in an ATP-dependent manner. Most proteasomal substrates are marked for degradation and targeted to the proteasome by the enzymatic attachment of ubiquitin chains, which need to be removed by intrinsic deubiquitinases (DUBs) at the proteasome to allow efficient turnover.

The 26S proteasome recognizes post-translationally added polyubiquitin chains attached to substrates by a complex network of ubiquitination enzymes. Degradation of a substrate requires binding of a polyubiquitin chain to proteasomal ubiquitin receptors, engagement of an unstructured region followed by translocation and unfolding by an ATPase motor subcomplex, and removal of ubiquitin chains by deubiquitinases Rpn11 and Ubp6 prior to translocation into the degradation chamber. The 26S proteasome utilizes over thirty different subunits and distinct holoenzyme conformations to accomplish these tasks.

Here I investigate two distinct aspects that modulate proteasome function. The deubiquitinase Ubp6 has previously been shown to trim ubiquitin chains and affect substrate processing by the proteasome, but the involved mechanisms and its location in the 26S proteasome complex remained elusive. Here we show that Ubp6 deubiquitination strongly responds to interactions with the base ATPase and the conformational state of the proteasome. Our electron-microscopy studies revealed that ubiquitin-bound Ubp6 contacts the N-ring and AAA+ ring of the ATPase hexamer, placing it in close proximity to the deubiquitinase Rpn11. In complex with ubiquitin, Ubp6 inhibits substrate deubiquitination by Rpn11, stabilizes the substrate-engaged conformation of the proteasome, and allosterically interferes with the engagement of a subsequent substrate. Ubp6 may thus act as an ubiquitin-dependent timer to coordinate individual processing steps at the proteasome and modulate substrate degradation.

Secondly, although the mechanism of substrate proteolysis has been well characterized, little is known about how the processing steps prior to degradation culminate to give an overall degradation rate. The complexity of substrate processing and the requisite of proteasome function for cell viability pose a significant challenge to quantitative analysis. We have developed an *in vitro* system to prepare defined proteasomal substrates and designed assays to determine the rates of degradation and deubiquitination for a given substrate input. We used these tools to show that deubiquitination by Rpn11depends on translocation of the substrate polypeptide by the ATPase. Moreover we also observe that unlike prokaryotic ATP dependent protease ClpXP, unfolding is not rate limiting in degradation by the proteasome. Overall these studies provide insight on how the complex 26S proteasome functions to degrade such a diversity of substrates and is integral to the cell.

Table of Contents

Acknowledgements

I first and foremost would like to acknowledge and thank Andreas Martin for being my mentor and advisor throughout this degree. I will always be in awe of the brilliance and dedication to science that Andy has shown and passed on to his lab members. I would also like to thank my thesis committee—Professors John Kuriyan, Kathy Collins, and Matt Francis for their invaluable feedback and assistance throughout my doctoral research.

I must also acknowledge other faculty that have mentored me over the years. Dr. Jim Amonette is a rare scientist who thinks high school students are worth mentoring and guided me through my first steps in lab. Professor Peter Williams is a superlative mentor and educator, and Arizona State University is lucky to have such a person on their campus. Pete had unending patience for me as an undergraduate researcher and continues to be a source of support and mentorship to this day. Finally, I would like to thank Professor Jack Kirsch for many good conversations about science, music, and life over the past few years in Stanley Hall.

I am very lucky to have outstanding labmates. Robyn Beckwith paved the way for the Martin lab with her willingness to teach and fantastic sense of humor. Mary Matyskiela showed me the ropes and picked me up when I was down. Eric Estrin was my comrade-in-arms in Barker Hall and I admire how he fearlessly takes on projects in lab and in life. Jared Bard was the ideal baymate and offered insight, support, and cookies at critical moments of my PhD. Kris Nyquist always has brilliant ideas for any scientific endeavor and I'm grateful for the conversations we have had. I am always in awe of Brooke Gardner's ability to pinpoint the most important questions to try and answer and how to best present one's science to the outside world. I thank Evan Worden for inspiring me to work harder and for always making me laugh in lab. *Dziękuję* Michał Olszewski for helping me remember some Polish and for making me participate in every Stanley Hall fire drill. Ellen Goodall is the lab member we do not deserve and patiently keeps our freezers, FPLCs, and general lab functional in the face of constant chaos. I'm also grateful Mike Lawson chose the Martin lab as his adoptive family, as he has been a huge source of support and invaluable expert in structural biology.

I would like to thank my friends outside of graduate school. Christine Carroll has been the voice of reason since we were roommates in college, and I'm thankful we have managed to stay in touch and have some fun over the course of our PhDs. Amy Huzjak continues to wow me with her unstoppable work ethic and brilliant musical talent, and I've enjoyed our phone calls over the years. I'm also very thankful that Emily Hellmich did not decide our roommate ad was a craigslist scam, as she has been my closest friend throughout my time in Berkeley. I look forward to many more scones and conversations in the years to come.

I owe a special debt of gratitude to Dr. Camran Nezhat and his office at the Center for Special Minimally Invasive and Robotic Surgery at Stanford Medical School. The care I received from the outstanding staff and doctors in this office gave me my life back in the face of chronic pain.

I have an astonishingly caring and supportive family. My parents Joe and Tina Bashore have given everything they had to their daughters, and I owe them, quite literally, everything. I have a kick-ass sister who knows how to achieve the incredible and is also willing to ship 20lbs of fish from Pike Place Market under the guise of a 'fish raffle'. I hope we have more adventures together in the future and that the next time you remember to pack pants.

Finally, "acknowledge" seems inadequate for the one and only Matt Davis. You are the reason why I actually finished this endeavor, and you are easily the best thing that came out of it.

Chapter 1

An introduction to the ubiquitin-proteasome system

Chapter 1

Survival through destruction

Protein degradation is fundamental to cell survival. Cells must not only maintain the proteome and degrade misfolded polypeptides, but also degrade key signaling proteins that mediate cellular processes ranging from transcription to cell division. As the final destination in the ubiquitin-proteasome system (UPS), the 26S proteasome is a highly complex ATP-dependent protein-degradation machine and is essential across all eukaryotes.

It is the intricate, three-dimensional structure of a protein that imbues the ability to carry out a specific task in the cell. Polypeptide misfolding results in loss of function and toxicity to the cell, and so robust systems of quality control are requisite within all cells. Polypeptides that become damaged over their lifetimes are deleterious to cells and must be removed, broken down into amino acids, and recycled to form new proteins. Failure to do so is a hallmark of many neurodegenerative diseases. The UPS functions to remove misfolded polypeptides at every stage of their lifecycle: during protein synthesis at the ribosome[2,4,5], folding in the ER[6,7], or misfolding and aggregation after synthesis[8-10]. Components of the UPS monitor, label, and destroy proteins that no longer maintain the structure crucial to their function.

Errors in translation produce so-called defective ribosomal products and are the consequence of ribosome stalling or amino acid misincorporation[2]. A number of translational quality-control factors have been observed at the ribosome that mediate the ubiquitination of defective translated polypeptides and mark them for degradation[4,11,12]. The UPS also plays a major role in disposing misfolded polypeptides to maintain a healthy proteaome. A number of ubiquitin ligases have been shown to recognize intrinsically disordered polypeptides, and target them to the proteasome for removal[13]. Proteomic studies have suggested that unfolding of proteins during stress can expose otherwise buried recognition motifs for ubiquitination machinery, which then marks them for proteasomal destruction[10]. Failure to fold in the ER results in extraction of polypeptides via ATPase Cdc48/p97 and delivery to the proteasome for degradation. Kaganovich *et al.* reported the presence of juxtanuclear quality control compartments that formed under induction of proteotoxic stress[8,9]. These inclusions contain misfolded but soluble proteins that are surrounded by constituents of the UPS as well as folding chaperones. Kaganovich demonstrated proteasomal degradation of these substrates localized within juxtanuclear quality control compartments and showed co-localization of proteasomes with these compartments upon induction of misfolding stress.

However, ordered degradation of different regulatory proteins drives signaling events in almost every major cellular process. For example, degradation of cell cycle kinase inhibitors drives cell division[14,15]. Degradation of the protective molecule securin releases the protease separase during the metaphase to anaphase transition in cell division[16,17]. Separase then cleaves the bonds holding sister chromatids together, triggering chromatid release and

anaphase. A number of transcription factors are also regulated by the ubiquitin proteasome system. Inflammatory signals lead to the processing of transcription factor NfκB, resulting in transcription-factor import into the nucleus and the upregulated expression of inflammation response pathways[18].

Ubiquitin

The proteasome recognizes a post-translationaly attached polyubiquitin targeting signal on substrate proteins[19]. A cascade of enzymes conjugates the C-terminus of monomeric ubiquitin moiety via an isopeptide linkage to a nucleophilic lysine. This lysine can be on a target substrate or be one of the seven lysines on ubiquitin itself. Ubiquitin connected by different linkage types allow a distinct set of chain conformations as observed by structural and single molecule studies[20] (fig 1.1). Differing linkage types are reported to correspond to different cellular activities. For example, substrates carrying ubiquitin chains with many different linkages, including K-11 or K-48, are subjected *in vivo* to proteasome degradation[21], whereas K-63 linked ubiquitin chains correspond with DNA damage or other signaling events. However, *in vitro* the proteasome can robustly degrade both K-48, K-11 and K-63 linked ubiquitin chains[22].

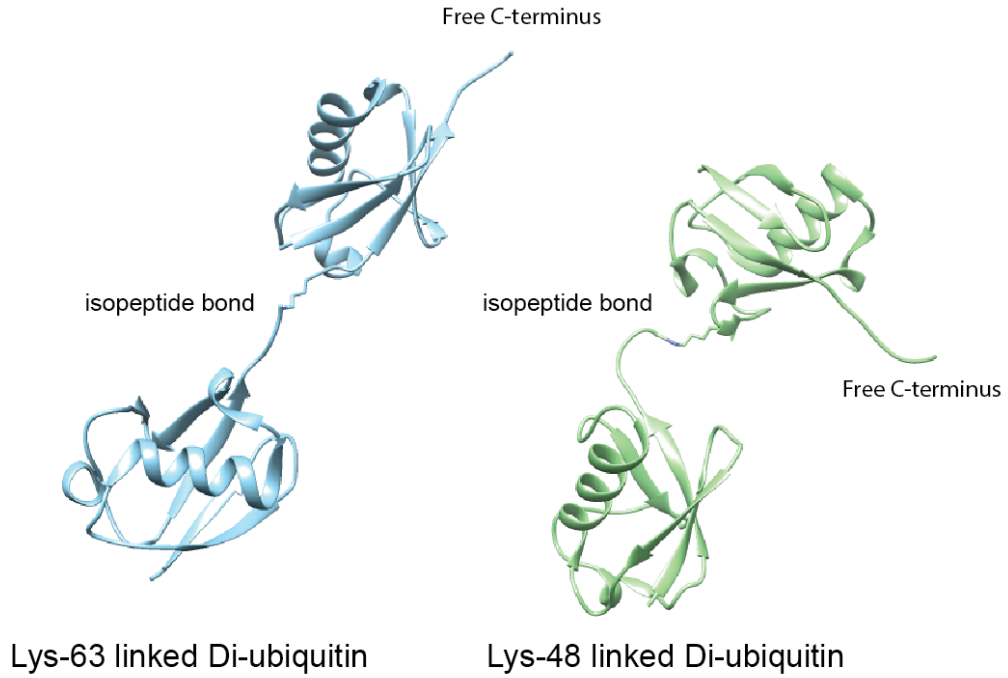

Figure 1.1 different ubiquitin linkage types have different conformations Structures of two ubiquitins linked by K63 (blue, PDB 3h7p) and K48 (green, PDB 2kde). The linkage types show different conformations, with K63 being more open and extended, while K48 di-ubiquitin adopting a more closed and compact shape.

The art of making a chain

A cascade of three enzymes form these isopeptide bonds (fig 1.2). First an E1 activating enzyme uses ATP hydrolysis to form a thioester bond between the C-terminus of ubiquitin and an active site cysteine, preparing the ubiquitin monomer for transfer to the active site cysteine of an E2 conjugating enzyme. The E2 then recognizes one of many E3 ligases. E3 ligases interacts with a specific substrate and facilitate the transfer of the new ubiquitin onto either a substrate lysine or a lysine on an ubiquitin already conjugated to the substrate. There are two main classes of E3s, which differ substantially in the mechanism of transfer of ubiquitin to the substrate. Homology to E6AP containing (HECT) ligases utilize an active site cysteine similar to the activating and conjugating enzymes. The HECT domain of the ligase generally determines the linkage type of ubiquitin chain[23]. In contrast, really interesting new gene (RING) ligases are generally multi-subunit scaffolds that position the E2 and the substrate in the correct orientation to facilitate direct discharge of ubiquitin from the cysteine of the E2 onto the lysine of the substrate. For RING E3 mediated ligation, it is the E2 that dictates chain specificity in polyubiquitination of the substrate[17,24].

Thus polyubiquitin is a highly heterogeneous post-translational modification. Any given substrate can have ubiquitin attached to one or more lysine residues, and the chain can be of variable lengths or linkage types. Certain substrates can also have ubiquitin chains of multiple linkage types, forming branched chains. The variability in length, linkage, and placement of ubiquitin chains is a result of the combination of substrate, E2, and E3 ligase, giving rise to a highly intricate molecular code that is interpreted by other proteins in the cell.

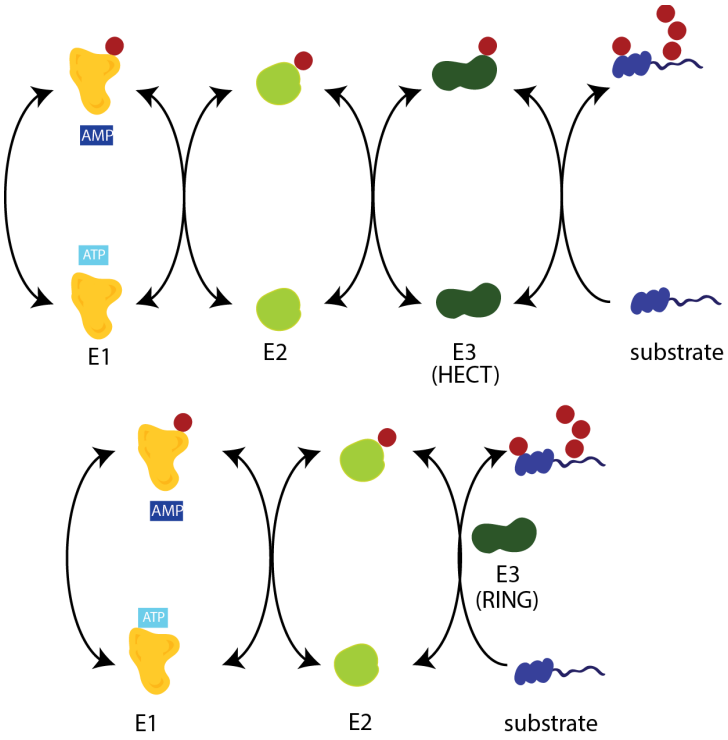

Figure 1.2. Ubiquitination by an enzyme cascade Ubiquitin ligation to a lysine requires a cascade of three enzymes. First, an E1 activating enzyme (orange) uses ATP hydrolysis to activate the C-terminus of ubiquitin, forming a thioester bond with an active site cysteine on the E1. The actvating E1 transfers the ubiquitin to the active site cysteine of an E2 conjugating enzyme (light green). The transfer of the ubiquitin to the substrate (purple) depends on the type of E3 ligase (dark green). HECT E3s use a third active site cysteine to take the ubiquitin from the E2 and place it on the lysine of the substrate. RING E3s act as scaffolds to position the E2 and the substrate to facilitate E2-mediated isopeptide bond formation between ubiquitin and substrate

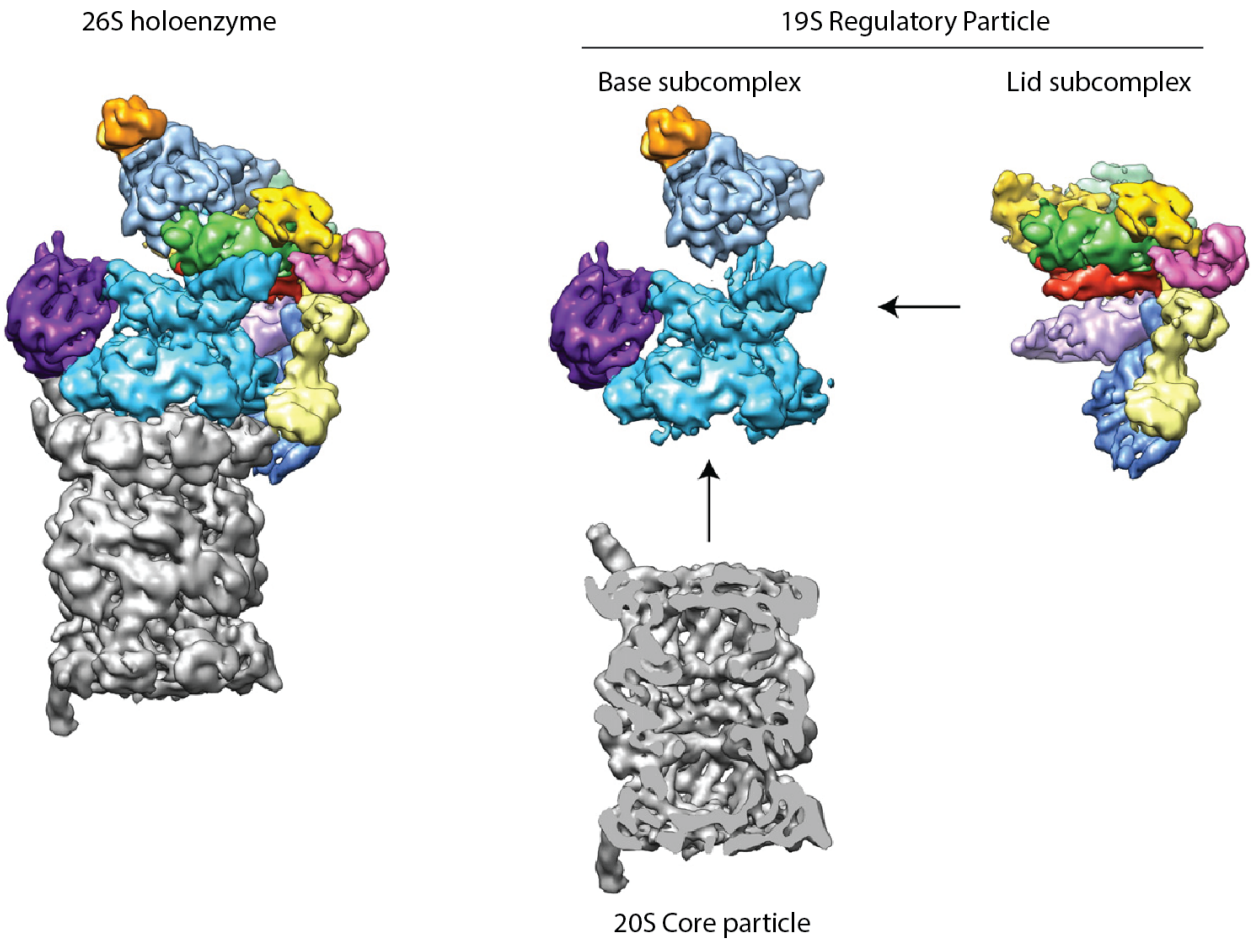

Figure 1.3. Subcomplexes of the 26S proteasome, (adapted from Matyskiela & Martin, 2012[25]) The 26S holoenzyme contains the 20S core particle (gray) that is capped by one or two 19S regulatory particles (colors). The 19S consists of two subcomplexes, base and lid. The base subcomplex contains the heterohexameric AAA+ motor (cyan) and non-ATPase subunits Rpn1, Rpn2, and Rpn13, while the lid subcomplex consists of 9 subunits including the deubiquitinase Rpn11 (green).

26S proteasome and its subcomplexes

The 26S proteasome is the major ATP dependent protease in eukaryotic cells[1]. The mega-dalton complex contains over 35 proteins present in one or two copies (Table 1). Peptide hydrolysis is carried out by a barrel-shaped 20S core particle (CP), and entrance into the degradation chamber is guarded by one or two 19S regulatory particles[26,27] (fig 1.3). The 19S regulatory particle consists of an ATP-dependent unfoldase referred to as the base and a scaffolding complex known as the lid. The subcomplexes of the 19S work together to facilitate substrate recognition, translocation, unfolding, and recycling of the polyubiquitin signal prior to peptide hydrolysis.

Table 1. Subunits of the 26S proteasome

Subunit	Domain/Description
Base subcomplex	
Rpt1	AAA+ domain subunit
Rpt2	AAA+ domain subunit
Rpt3	AAA+ domain subunit
Rpt4	AAA+ domain subunit
Rpt5	AAA+ domain subunit
Rpt5	AAA+ domain subunit
Rpn1	PC-repeat solenoid, binds Ubp6 and shuttle factors Rad 23, Ddi1, Dsk2
Rpn2	PC repeat solenoid, binds Rpn13
Rpn13	Ubiquitin binding by Pru domain
Lid subcomplex	
Rpn9	PCI domain subunit
Rpn5	PCI domain subunit
Rpn6	PCI domain subunit
Rpn7	PCI domain subunit
Rpn3	PCI domain subunit
Rpn12	PCI domain subunit
Rpn8	Inactive Jab1/MPN domain
Rpn11	Active Jab1/Mpn domain with JAMM motif deubiquitination active site
Rpn10	Receptor binding ubiquitin via UIM and lid via VWA domain
Core Particle	
α1-α7	Gating subunits
β1-β7	β1, β2, β5 contain proteolytic active sites

The 20S peptidase is by far the best-understood subcomplex of the proteasome, both structurally and functionally. It consists of two sets of heteroheptameric rings stacked in two copies to give a four-tiered barrel structure. The top and bottom rings of the barrel contain α subunits 1-7 that gate access to the proteolytic active sites. The α subunit N-termini restrict access into the pore until C-terminal tails of a proteasomal activator, for instance the base ATPase ring, bind into pockets at α subunit interfaces[28]. The two inner rings are comprised of seven β subunits, three of which have catalytic N-terminal threonines and function much like serine proteases. The β1 subunit shows glutamyl peptidase activity and cleaves after acidic residues, the β2 subunit shows trypsin-like activity and cleaves after arginine residues, and the β5 shows chymotrypsin-like activity and cleaves after hydrophobic

residues[29]. The three activities ensure through cleavage of the polypeptide chain translocated by the regulatory particle.

The lid is made up of 10 different subunits. Rpns 5,6,7,9, and 12 each contain a C-terminal Proteasome-Cyclosome-EIF3 (PCI) domain that interact with each other to form a horseshoe-shaped structure at the center of the lid[22,30,31]. Extending out like fingers from this horseshoe are the individual subunit N-termini, consisting of helix-turn-helix repeats. Rpn11 and Rpn8 do not contain a PCI domain, but instead a Jab1/Mpn domain that allows them to dimerize. Assembly of the lid from individual subunits is mediated through interactions of C-terminal helices into a twisted revolver-shaped helical bundle[32,33]. In the isolated lid, Rpn11 seems to be inactive, perhaps because Rpn5 curls up and occludes access to the active site[22]. Upon binding to the holoenzyme, Rpn5 moves away from Rpn11, making it more accessible to substrate. The ubiquitin receptor Rpn10 contacts Rpn9 and the Rpn8/11 dimer, which places this receptor close to the coiled-coil of base Rpts 4/5[22,32].

The base consists of six distinct ATP hydrolyzing subunits (Rpt 1-6) that form a hexameric ring and three non-ATPase subunits (Rpn1, 2, and 13). Cysteine cross-linking studies revealed that the six ATPases assemble in a specific order: Rpt1, Rpt2, Rpt6, Rpt3, Rpt4, Rpt5.[34] Unlike AAA+ hexamers that consist of two alternating subunits, like the mitochondrial Yta10/Yta12 or the perixomal dislocase Pex1/Pex6, the base is a fully heterohexameric AAA+ motor[35,36]. *In vitro* studies on the base show that the different subunits constitute a functional asymmetry in their contribution to substrate engagement, core binding, and ATP hydrolysis[37]. Each Rpt subunit consists of an N-terminal OB fold domain and a C-terminal AAA+ domain, which in the hexamer assembly form an N-Ring and a AAA+ ring, respectively[22]. EM studies of the proteasome holoenzyme show a dramatic spiral staircase arrangement of the AAA+domains, with Rpt3 at the top of the spiral, and Rpt2 at the bottom of the spiral[22]. Secondary structure prediction models and EM also show long coiled-coils extending from the N-termini of Rpt3 and Rpt6, as well as Rpt4 and Rpt5. EM structures revealed that the coiled-coil of Rpt3/Rpt6 provides a binding site for Rpn2 and the lid[22,32], whereas the coiled coil of Rpt4/Rp5 does not make many contacts to other proteasome subunits. However, the Rpt4/Rpt5 coiled coil is located close to the ubiquitin receptor Rpn10 and may provide a structure that positions the ubiquitin interacting motif (UIM) to interact with ubiquitin chains. Previous crosslinking studies suggested a cryptic binding site for ubiquitin in Rpt5, which may actually be due to the proximity to the receptor of Rpn10[38]. The non-ATPase subunits Rpn1 and Rpn2 act as scaffolds that assist in assembly of the base subcomplex and crucially contact other proteasome subunits. The two proteins are large, 100 kDa toroids that contain proteasome/cyclosome (PC) repeats, giving them a solenoid structure seen in EM and crystallographic studies[22,39]. Rpn1 docks to the ATPase subunits Rpts 1 and 2, and is known to interact with a number of proteasome factors including ubiquitin shuttle receptors and the deubiquitinase Ubp6, which use their ubiquitin-like (Ubl) domain to dock to Rpn1[40,41]. Rpn2 binds to the N-terminal coiled-coil of Rpts 3 and 6 and is positioned high above the unfoldase pore. Rpn2 binds to ubiquitin receptor Rpn13, and also appears to contact the critical deubiquitinase Rpn11.

Subcomplex communication

Although they form distinct subcomplexes, the lid, base, and core make extensive contacts to one another. Upon solving the architecture of the regulatory particle, Lander *et al.* found that the eponymous lid did not actually sit on top of the holoenzyme complex, but rather was integrated to the side and interacts with both base and core. Subunits Rpn5 and Rpn6 make contacts to alpha subunits in the core particle, which was seen by a combination of crosslinking and EM[22,42]. The lid has several contact points to the base unfoldase, as Rpn11 actually binds to Rpn2, and Rpn6 also makes contacts with Rpt3 in the base. The base interacts with the core through C-terminal tails on the Rpts. Three subunits, Rpts 2, 3, and 5, contain a conserved hydrophobic/tyrosine/unspecified amino-acid motif (HbYX) at their C-termini that dock into pockets formed by the α subunit ring of the core particle. Synthetic peptides containing this C-terminal motif open the gate of the core particle; moreover deletion of these tails in the base causes defects in core-particle binding. EM holoenzyme structures also show visible density for tails of the three Rpts docked into the α-ring binding pockets[28,37,43].

Ubiquitin receptors

The yeast 26S proteasome contains two ubiquitin-binding subunits that stoichiometrically co-purify with holoenzyme, Rpn10 and Rpn13. Rpn10 consists of an N-terminal von-Willebrand A (VWA) domain and a C-terminal alpha-helical UIM domain to interact with ubiquitin[44]. In *S. cerevisiae*, Rpn10 contains a single UIM, however in higher eukaryotes the receptor uses two of these motifs to interact with ubiquitin[45]. Rpn13 uses a novel pleckstrin-like receptor for ubiquitin (Pru) domain to interact with ubiquitin[46,47]. The Pru relies on two beta sheets stabilized by an alpha helix; three loops that bridge beta-strands are responsible for ubiquitin binding. This interface is significantly different from the alpha helical motif for Rpn10, but both receptors interact with the same hydrophobic patch on ubiquitin[1]. In higher eukaryotes, Rpn13 also serves as an interaction point for the deubiquitinase Uch37. As elucidated by structural studies, deubiquitination of Uch37 is activated by binding to Rpn13[48,49]. The *S. cerevisiae* proteasome does not contain Uch37, and therefore Rpn13's role seems to only involve ubiquitin recruitment. It should be noted that *in-vitro* degradation of substrates does not require Rpn13. Aside from these two intrinsic ubiquitin receptors, a number of transiently bound "shuttle receptors" also recruit ubiquitinated substrates to the proteasome. Rad23, Dsk2, and Ddi1 all utilize an ubiquitin-associated (UBA) domain to bind to ubiquitinated substrates, while an N-terminal ubiquitin-like (Ubl) domain binds the receptor to the proteasome[40,50]. Scaffolding protein Rpn1 has shown to pulldown with these transient cofactors and acts as a sort of 'landing pad' for the shuttle receptors and other factors. Intriguingly, deletion of all five known ubiquitin receptors in yeast is not lethal, suggesting that there is yet another 'cryptic' ubiquitin receptor within the proteasome[46,51].

Deubiquitinases

The lid houses Rpn11, which is the key deubiquitinase of the proteasome. It is essential for viability and has been shown to cleave at the base of a polyubiquitin chain[52,53]. Rpn11 is related to the thermolysine protease and uses a catalytic zinc ion to coordinate and activate the nucleophilic water in the active site[54]. Rpn11 uses two histidines to coordinate the

catalytic zinc in a HXH motif. Structure-function studies of the DUB show that in isolation the Rpn11-Rpn8 dimer does not have any linkage specificity, as it only makes contacts to the distal moiety in isopeptide-linked diubiquitin. This high promiscuity for the proximal moiety agrees with the model that Rpn11 cleaves the isopeptide bond at the base of an ubiquitin chain, right at the highly variable substrate polypeptides[42,55].

In *S. cerevisiae*, the proteasome contains one other associated deubiquitinase, Ubp6. Ubp6 is an ubiquitin-specific protease (USP) that uses an active-site cysteine to catalyze isopeptide-bond hydrolysis. It consists of an N-terminal ubiquitin-like (Ubl) domain and a C-terminal catalytic USP domain. The Ubl domain recruits Ubp6 to Rpn1[56], although the binding site for Ubp6 within the 100 kDa scaffold is still unclear. Ubp6 is thought to "trim" ubiquitin chains docked on the proteasome, in contrast to Rpn11 removing polyubiquitin from substrates at the base of chains. Ubp6's trimming activity has also been implicated in maintaining levels of free monomeric ubiquitin in cells[57,58].

Substrate requirements for degradation

The canonical degradation-targeting signal in yeast is comprised of at least 4 ubiquitin moieties linked by lysine 48. Thrower *et al.* used purified free ubiquitin chains of defined length to compete with degradation of a DHFR substrate genetically fused to a linear polyubiquitin chain. Competition kinetic assays showed that chains containing fewer than 4 ubiquitins have much weaker binding to the proteasome, while chains containing more than 4 ubiquitins do not exhibit a dramatic increases in affinity[19]. Multiple reports have also suggested that the proteasome efficiently degrades substrates with multiple but shorter ubiquitin chains[59]. Mass spectrometry studies of the ubiquitinated proteome indicate that most proteasome substrates have more than one lysine modified by polyubiquitin[60]. Although K48 is the canonical linkage type in yeast, studies have shown that all other linkages are degraded *in vivo*, except for K63 linked chains, which are required for efficient DNA repair and other signaling processes[21]. Nonetheless, K63 linked chains are efficiently degraded by the proteasome *in vitro*[22,37,61]. One explanation for this discrepancy is that other cellular factors may preclude K-63 linked chains from interacting with the proteasome, directing them away from a degradation pathway. One study has implicated ESCRT 0 as a K63 binding protein that may act in this capacity[62]. However much remains to be elucidated for the field to understand how ubiquitin-chain binding happens at the proteasome.

Aside from the ubiquitin chains that bind to ubiquitin receptors on the proteasome, a substrate must also contain an unstructured initiation region of at least 35 or 40 amino acids, which is long enough to span some of the distance from the ubiquitin receptor, through the N-ring of the base and to the internal pore loops of the AAA+ domain that grab and pull on the substrate[63]. It has been shown that the ubiquitin shuttle receptor Rad23 does not get degraded when bound to the proteasome, because it lacks this flexible initiation region, suggesting an explanation for how accessory factors can interact with the proteasome without undergoing degradation[64]. The additional need for an initiation region may also explain how the proteasome can selectively degrade substrates in a protein complex, as in the degradation of cyclin-dependent-kinase inhibitors during the cell cycle. Ubiquitination may

tether the entire complex to the proteasome, but only the subunit containing a flexible tail would be extracted and degraded[63]. Moreover, some studies suggest that the specific amino acid sequence of this initiation region is important. Polypeptides containing repetitive and simple amino acid sequences, so called "slippery sequences", can pose a challenge to efficient gripping by the pore loops and would impede engagement[65].

The geometry of this two-part degradation signal understandably impacts the efficiency of the overall degradation process. The distance between the ubiquitin tether and the initiation region could add an extra level of regulation of substrate turnover in the cell. Moreover, this geometry could change depending on whether a substrate is recruited to the proteasome by an intrinsic receptor or a shuttle receptor, as they are located in different parts of the holoenzyme. Inobe *et al.* showed that the length of the ideal initiation region may vary depending on the recruiting ubiquitin receptor[66]. This two-part degradation signal can also be supplied in *trans*. It has been found *in vitro* that the proteasome can degrade a client protein containing an unstructured region if that substrate is bound to a second partner containing the polyubiquitin tag[63]. The proteasome has also been shown to asymmetrically process complexes, as in the case of transcription factors Mga2 and Spt23[7,67]. The yeast NFκB homologues Spt23 and Mga2 are transcription factors that maintain unsaturated fatty acid levels in cell membranes. Mga2 exists as a dimer bound to the endoplasmic reticulum by a C-terminal anchor, and in its full-length version, p120, it is inactive. Ubiquitination results in partial degradation of one monomer in the dimer by the proteasome, creating a p90 product that is eventually released into the cytosol upon further processing by $Cdc48^{Ufd1/Npl4}$ and is imported into the nucleus to regulate transcription.

A handful of transcription factors use partial degradation as an activation mechanism. The best-established examples are the mammalian NFκB and the *Drosophila* Cubitus interruptus. One of the subunits of NFκB is synthesized as a larger precursor protein, p105. The added bulk of the subunit masks the nuclear localization signal for the transcription factor, thus keeping the complex inactive in the cytosol. Inflammation or stress recruits ubiquitination machinery to p105, resulting in its precise partial degradation to the active subunit p50. The partial degradation leads to the exposure of the nuclear localization signal, resulting in nuclear import and activation of transcription. Piwko *et al.* also showed in the case of Mga2 degradation that the proteasome does not engage a terminus. Instead the motor pulls on an unstructured loop between the C-terminal tail anchor and N-terminal domains of Mga2, demonstrating that the proteasome can handle multiple polypeptide chains to mediate internal degradation initiation[67].

Substrate processing and conformational changes

Substrate processing involves several steps (fig 1.4). First, polyubiquitin binds to proteasomal ubiquitin receptors. Ubiquitin chains tether the substrate to the proteasome as the unstructured initiation region eventually threads through the N-ring and reaches the spiral staircase of the AAA+ ring. The unfoldase contacts the polypeptide chain through pore loops, thus engaging the substrate. ATP hydrolysis provides the energy for

conformational changes of the base AAA+ ring to mechanically translocate the polypeptide chain, ultimately resulting in substrate unfolding. Concomitant with substrate unfolding is removal of polyubiquitin by Rpn11.

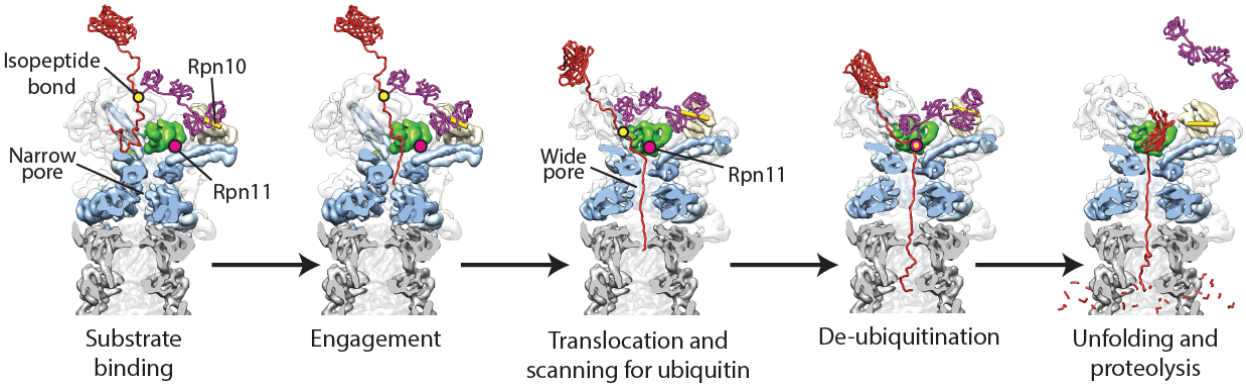

Figure 1.4. Substrate turnover requires multiple conformational states (from Matyskiela, et al, 2013[42]) EM structures of holoenzymes in the absence and presence of substrate predict a model for substrate degradation by the proteasome. Substrate binds via polyubiquitin chain to a ubiquitin receptor on the proteasome while the proteasome is in an apo state marked by a narrow, misaligned pore between base and core. Substrate threading through the N-ring is engaged by pore loops in the AAA+ ring of the base. This results in a substantial conformational change marked by a wide, coaxially aligned, central channel formed by base and core, and a shifting of Rpn11 to sit directly over the entrance of the pore. Translocation of the substrate polypeptide brings the isopeptide bond between a substrate lysine and the first ubiquitin of the chain to the active site of Rpn11 for cleavage. Concomitant with Rpn11 deubiquitination is the unfolding and proteolysis of the substrate.

Structural studies of the proteasome show that these processing steps are marked by distinct proteasomal conformations. Cryo EM of the substrate-free state shows that the N-ring and AAA+ ring of the base are offset from a coaxially alignment with the core particle[22,32]. However, the N-ring is positioned such that an unstructured region could thread into the pore. The AAA+ ring in this apo state is also marked by a steep spiral staircase arrangement of the Rpts. Mutagenesis of individual Rpts revealed that inactivation of subunits at the top of the spiral staircase in the apo configuration leads to bigger substrate-degradation defects and a lag in single turnover experiments, presumably due to a defect in substrate engagement[37]. Finally, the apo structure revealed an Rpn11 active site that was not oriented towards the unfoldase pore, but is instead partially occluded by the Rpt4/5 coiled-coil which would pose a challenge for hydrolysis of isopeptide bonds.

Matyskiela *et al.* used Rpn11-inactivated proteasomes purified from yeast incubated with a polyubiquitinated substrate containing a single lysine residue to capture a substrate-engaged state[42]. This state was marked by a significant rearrangement of the regulatory particle. The N-ring and AAA+ ring of the base coaxially align with the core particle to form a

continuous channel. The spiral staircase arrangement of the AAA+ domains flattens upon substrate engagement. Contacts between the AAA+ domains and the lid also change between the two states. Importnatly, Rpn11 shifts from a position occluded by the Rpt4/5 coiled-coil to sitting right above the central pore of the N-ring, placing it in an ideal location to scan for isopeptide bonds as the substrate polypeptide is translocated through the central channel. This engaged state also agreed with a structure of the holoenzyme incubated with the non-hydrolyzable ATP analogue ATPγS (fig s2.2)[68]. Underoben *et al.* did a large scale classification of over three-million particles and observed an intermediate third state[69]. Finally, Asano *et al.* used tomography to image proteasomes in live neurons, allowing an unprecedented look at the conformational state of various particles. They saw that the majority of proteasomes were in an apo conformation, indicating that at least in some cell types or conditions the proteasome is not overwhelmed with ubiquitintated substrates[70].

Ubp6 modulates proteasomal degradation

Ubp6 is a stably associated proteasomal deubiquitinase shown to modulate proteasomal function. This 60KDa ubiquitin specific protease (USP) uses an active site cysteine to cleave ubiquitin moieties off of substrates. Ubp6 has high sequence and structural conservation to its human homologue, Usp14[71]. Although Ubp6 has been shown to biochemically interact with Rpn1, efforts to localize either Ubp6 or Usp14 bound to proteasomes have failed. Moreover, Ubp6 has previously been shown to catalytically and non-catalytically affect the rates of proteasomal degradation, increase access to the 20S core particle, and stimulate rates of ATP hydrolysis[72-76]. Others have also reported that Ubp6 interferes with deubiquitination by Rpn11, which is critical to substrate degradation. However the field lacks mechanistic insight as to how Ubp6 interactions modulate proteasomal activity.

When bound to ubiquitin conjugates, Ubp6 has been shown to increase the ATP-hydrolysis rate of the base ATPase and increase access into the core peptidase. Furthermore, Ubp6 may affect substrate recruitment by trimming ubiquitin chains on substrates bound to the proteasome. This observation has led many to speculate that Ubp6 may act like a 'timer' by slowly decreasing the ubiquitin targeting signal on a substrate until it no longer has subsequent affinity to bind to the proteasome. However, Ubp6 seems to non-catalytically affect protein turnover as well. Mutating Ubp6's active-site cysteine results in decreased degradation and deubiquitination by Rpn11[72].

In vivo, modulation of Ubp6 or Usp14 activity dramatically alters cellular function. Loss of function of Ubp6 shows increased aneuploidy tolerance in yeast, presumably due to an increased proteasome capacity to turn over higher protein levels. Pharmacological inhibition of Usp14 has also shown to increase proteasome activity. Higher Usp14 expression in multiple cancer types has correlated with poorer prognoses, and knockdown of Usp14 in cancer cell lines slows cell growth and induces apoptosis[77,78]. Usp14 is also essential for maintaining ubiquitin levels at neuromuscular junction development[58]. Allosteric inhibition of proteasomal degradation is also potentially critical to maintain correct protein balance in cells. A detailed structural and mechanistic understanding of Ubp6's interactions with the

proteasome is therefore expected to provide important new insight into the role of this deubiquitinase in maintaining the proteome.

Open questions in the field

Several questions regarding substrate processing at the 26S proteasome remain unanswered. Although many reports have demonstrated that the deubiquitinase Ubp6 modulates the activity of the holoenzyme, little is known of the mechanistic underpinnings behind this interaction. Moreover, Ubp6 is the only proteasome subunit in *S. cerevisiae* that has not been localized by EM. Secondly, although recent structural studies have greatly increased our understanding of the architecture of the proteasome and shown how conformational changes facilitate the complex task of protein recognition, processing, and degradation, we still lack a biochemical understanding of the kinetics behind substrate processing by the 26S proteasome. We do not know whether engagement of the initiation region, unfolding of the substrate, or removal of polyubiquitin dictates the overall degradation rate for a substrate. Moreover, we do not understand whether the rate-limiting step changes for any given substrate input.

This dissertation addresses two of these questions. First, I examined the mechanism of how the deubiquitinase Ubp6 affects proteasomal activity. Through biochemical and structural approaches, I observed that ubiquitin binding to Ubp6 stabilizes the engaged conformation of the holoenzyme. We have localized Ubp6 and see that it surprisingly contacts the AAA+ ring of the base, placing it 30 Å from the deubiquitinase Rpn11. Moreover, we revealed that ubiquitin binding to Ubp6 exacerbates its inhibition of Rpn11 activity, suggesting that the close proximity of the two DUBs is detrimental to Rpn11.

Secondly, I took a substrate-based approach to investigate the different processing steps of proteasomal degradation and how modulating substrate thermodynamic stability or engagement affect degradation and deubiquitination. Overall, these studies inform us on how complex the mechanisms of substrate degradation are and how different factors may contribute to the highly regulated protein destruction so necessary for cell viability.

Chapter 2

The deubiquitinase Ubp6 controls conformational dynamics and substrate degradation by the 26S proteasome

Chapter 2

This work was done in collaboration with Corey Dambacher, Mary Matyskiela, and Gabe Lander. Corey Dambacher and Gabe Lander did the negative stain EM, and Mary Matyskiela designed and constructed the artificial recruitment system.

Abstract

Protein degradation by the 26S proteasome is essential across all eukaryotes. Substrates are targeted for degradation through the attachment of polyubiquitin chains that need to be removed by intrinsic proteasomal deubiquitinases prior to substrate unfolding and translocation into the proteolytic chamber. The deubiquitinase Ubp6 has previously been shown to trim ubiquitin chains and affect substrate processing by the proteasome, but the involved mechanisms and its location in the holoenzyme remained elusive. Here we show that Ubp6 deubiquitination strongly responds to interactions with the base ATPase and the conformational state of the proteasome. Our electron-microscopy studies revealed that ubiquitin-bound Ubp6 contacts the N-ring and AAA+ ring of the ATPase hexamer, placing it in close proximity to the deubiquitinase Rpn11. In complex with ubiquitin, Ubp6 inhibits substrate deubiquitination by Rpn11, stabilizes the substrate-engaged conformation of the proteasome, and allosterically interferes with the engagement of a subsequent substrate. Ubp6 may thus act as an ubiquitin-dependent timer to coordinate individual processing steps at the proteasome and modulate substrate degradation.

Introduction

Cell survival fundamentally depends on protein degradation, which in eukaryotes is carried out to a large extent by the ubiquitin-proteasome system (UPS) [1,2]. Cells not only must maintain the proteome and degrade misfolded or damaged polypeptides, but degradation of regulatory and signaling proteins mediates numerous vital processes, ranging from transcription to cell division [3]. As the final destination in the ubiquitin-proteasome system, the essential 26S proteasome is a compartmental protease of the AAA+ family that mechanically unfolds and degrades protein substrates in an ATP-dependent manner. Most proteasomal substrates are marked for degradation and targeted to the proteasome by the enzymatic attachment of ubiquitin chains, which need to be removed by intrinsic deubiquitinases (DUBs) at the proteasome to allow efficient turnover[52,53].

The *S. cervesiae* 26S proteasome consists of at least 34 different subunits that assemble into a 2.5 MDa complex. At the center of the holoenzyme is the barrel-shaped 20S core particle (CP) that sequesters the proteolytic active sites[79]. Access to the degradation chamber is controlled by the 19S regulatory particle (RP), which caps one or both ends of the 20S peptidase and can be further separated into the base and lid subcomplexes. The base contains three non-ATPase subunits, Rpn1, Rpn2 and Rpn13, as well as six distinct AAA+ ATPases (Rpt1-6) that form a heterohexameric ring with a central processing pore, constituting the unfoldase motor of the proteasome. ATP hydrolysis in the AAA+ domains of these ATPases is thought to drive conformational changes and propel movements of conserved pore loops to mechanically pull on substrate polypeptides and translocate them

through the central channel into the peptidase[80,81 82]. In addition to the AAA+ domain, each Rpt subunit contains a N-terminal OB-fold domain that in the hexamer assembles into a distinct N-ring above the AAA+ domain ring. The lid subcomplex acts as a scaffold bound to one side of the base and contains the metalloprotease Rpn11, which is the essential deubiquitinase of the proteasome [52,53]. The base and lid subcomplexes must work together to recognize, process, and ultimately deliver substrates to the proteolytic core particle for cleavage into small peptides. Substrate proteins modified with ubiquitin chains of different linkage types, in particular K11 and K48, but *in vitro* also K63-linked chains[21,60,83], are tethered to the proteasome by interacting with the intrinsic receptors Rpn10 and Rpn13 or transiently bound shuttle receptors[44,45,50,84,85]. Subsequently, the ATPase ring of the base engages an unstructured initiation region of the substrate and utilizes ATP hydrolysis to mechanically unfold and translocate the polypeptide. Concomitant with substrate translocation is the removal of ubiquitin modifications by the DUB Rpn11, which is localized above the entrance to the central pore of the base[22,32] .

Substrate degradation involves multiple conformational states of the proteasome regulatory particle. In the substrate-free state, the AAA+ domains of the Rpts adopt a steep spiral-staircase arrangement that may facilitate substrate engagement[37]. Engagement induces the transition to the actively translocating state that is characterized by a more planar spiral staircase arrangement of the Rpts as well as a coaxial alignment of the N-ring and AAA+ ring with the peptidase, creating a continuous central channel for substrate translocation into the degradation chamber[42,68]. Furthermore, during this conformational change of the regulatory particle, Rpn11 shifts to a central position above the entrance to the pore where it is ideally placed to scan for and remove ubiquitins from substrates as they are translocated by the base ATPases. Thus, we surmise that for every substrate turnover, the proteasome transitions from a substrate-free, engagement-competent state to an engaged state that facilitates processive translocation, unfolding, and deubiquitination. The proteasome has to switch back to the substrate-free conformation before the engagement of a subsequent substrate.

In addition to Rpn11, the 26S proteasome from *S. cerevisiae* contains another stably associated deubiquitinase, Ubp6, which shows high sequence and structural conservation with its human homologue, Usp14[71]. This 60 kDa ubiquitin specific protease (USP) uses an active site cysteine to cleave the isopeptide bonds within ubiquitin chains. Ubp6 is known to interact with Rpn1 of the base, but efforts to localize either Ubp6 or Usp14 in the context of the proteasome have failed[41,56]. Moreover, Ubp6 has been shown to catalytically and non-catalytically affect the rates of proteasomal degradation. Ubp6 interferes with the critical substrate deubiquitination by Rpn11, stimulates 20S gate opening and thus increases access to the degradation chamber, and enhances the rates of ATP hydrolysis[72-75]. However, the mechanisms by which Ubp6 modulates the activities of the proteasome remain poorly understood.

Depletion of Ubp6 or Usp14 activity has dramatic consequences *in vivo*. Loss of Ubp6 function, for example, increases aneuploidy tolerance in yeast, presumably due to an elevated

proteasome capacity for turning over higher protein levels, and pharmacological inhibition of Usp14 in human cells has been shown to stimulate proteasome activity[75,86,87]. In the hippocampus, loss of Usp14 binding to the proteasome results in higher degradation rates that interfere with presynaptic formation, which can be rescued by overexpression of a catalytically inactive mutant[88]. Thus, both the catalytic and non-catalytic effects of Ubp6 on proteasome activity have important implications in cellular protein turnover. Understanding the interactions of Ubp6 with the proteasome in structural and mechanistic detail is therefore expected to provide important new insights into the role of this deubiquitinase in maintaining the proteome.

In this study we used biochemical and structural approaches on reconstituted proteasome complexes to investigate the nature of Ubp6 interaction. We found that the deubiquitination activity of Ubp6 depends on binding to the base ATPase and responds to the conformational state of the proteasome. By engineering a substrate recruitment system independent of polyubiquitin, we were able to separate catalytic and non-catalytic effects of Ubp6 on proteasomal activities. We localized Ubp6 by electron microscopy and show that it contacts both the N-ring and AAA+ ring of the base in its substrate-engaged conformation, positioning this deubiquitinase directly facing Rpn11. The position of Ubp6 is consistent with our biochemical findings that the ubiquitin-bound deubiquitinase strongly inhibits Rpn11 deubiquitination activity, stabilizes the translocating conformation of the holoenzyme, and prevents engagement of subsequent substrates.

Results

Ubp6 deubiquitination activity responds to proteasome conformational states

The deubiquitination activity of Ubp6 has been shown to dramatically increase upon binding to the 26S proteasome[56,72,75]. To assess the mechanisms of this activation, we measured Ubp6 deubiquitination in the presence of purified proteasome subcomplexes[37] and 4-amino-methyl-coumarin-fused ubiquitin (Ub-AMC), a substrate that increases fluorescence upon cleavage (Fig. 2.1). Despite its known interaction with Ubp6, Rpn1 alone failed to stimulate Ubp6 activity, whereas purified base or holoenzyme induced a 300-fold increase in deubiquitination. Thus, full activation of Ubp6 requires contacts with other base subunits in addition to Rpn1 (Fig. 2.1a).

Interestingly, Ubp6 deubiquitination activity also responds to the conformational state of the proteasome. ATPγS was previously shown to invoke a conformation that is similar to the substrate-engaged state[42,68] (Fig. s2.1). We therefore reconstituted the proteasome in the presence of ATPγS, and observed a 1.9-fold increase in Ubp6 deubiquitination activity compared to the ATP-bound, substrate-free state of the proteasome (Fig. 2.1a). Importantly, this Ubp6 stimulation was also found for endogenous 26S holoenzyme purified from yeast, suggesting that the deubiquitinase indeed responds to an ATPγS-induced conformational change and not an alternative assembly state during *in-vitro* reconstitution (Fig. 2.1b). Proteasomes lacking Ubp6 or containing Ubp6 with a mutated active-site cysteine (C118A)

did not show this ATPγS-dependent stimulation of deubiquitination, indicating that the effect is solely caused by Ubp6 and not the other intrinsic deubiquitinase, Rpn11.

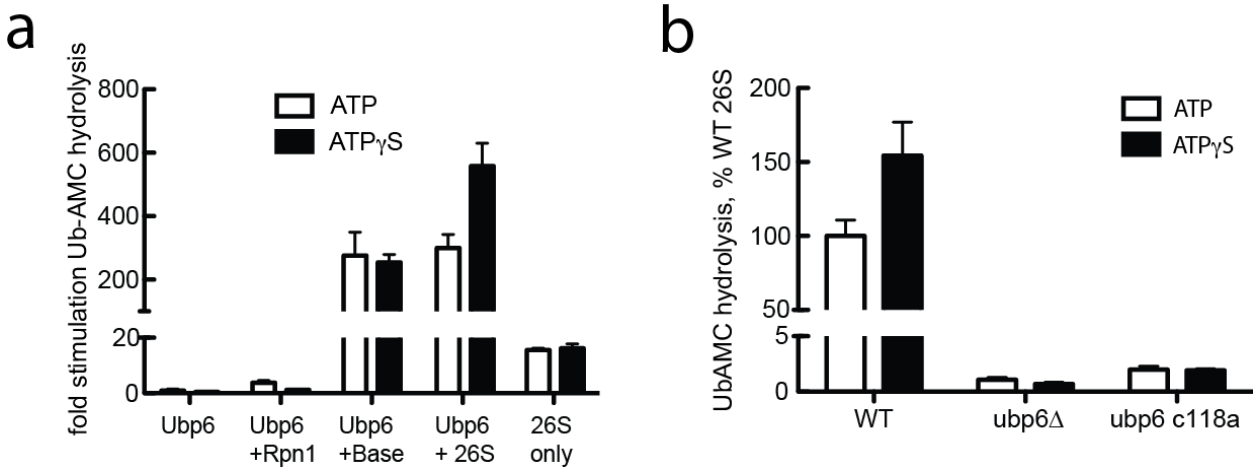

Figure 2.1. Ubp6 deubiquitination responds to the conformational state of the proteasome. Ub-AMC cleavage activity of Ubp6 was measured in response to interactions with the proteasomes holoenzyme or isolated subcomplexes. (a) Deubiquitination was assayed using proteasomes reconstituted with heterologously expressed base subcomplex purified from *E. coli* as well as core and lid subcomplexes purified from yeast. Ubp6 shows 300-fold activation when binding to either isolated base subcomplex or reconstituted holoenzyme, but not when interacting with Rpn1 alone. Inducing the engaged state of the proteasome by adding non-hydrolyzable ATPγS results in an additional 1.9-fold stimulation of Ubp6 deubiquitination activity, whereas Rpn11 shows no response. (b) Deubiquitination was measured using proteasomes purified from yeast strains with either wild-type, deleted, or inactive (C118A) Ubp6, showing that the stimulatory effect of ATPγS described in (a) is not due to *in-vitro* holoenzyme assembly. Only proteasomes from a wild-type Ubp6 strain responded to the presence of ATPγS with a 1.5-fold increase in deubiquitination. Error bars show SEM of three separate experiments.

Previous studies had shown that polyubiquitin-bound Ubp6 stimulates the ATPase rate of the proteasome[74]. This observation, together with our findings that ATP- and ATPγS-bound proteasomes differentially stimulate the deubiquitination activity of Ubp6, suggest that Ubp6 may play a role in the conformational dynamics of the holoenzyme. The function of Ubp6 in ubiquitin processing during substrate degradation, however, complicates a detailed analysis of such potential allosteric effects. To deliver substrates to the proteasome in an ubiquitin-independent manner, we therefore developed an artificial recruitment system by fusing a permuted single-chain variant of the dimeric substrate adapter $SspB_2$ to the N-terminus of the ATPase subunit Rpt2 (Fig. 2.2a). In bacteria, $SspB_2$ recruits substrates to the AAA+ protease ClpXP by recognizing a portion of the 11 amino acid ssrA tag[89]. Including this ssrA tag in our model substrates enables their ubiquitin-independent targeting to $SspB_2$-fused reconstituted proteasomes (Fig 2.2b), which are also still capable of degrading ubiquitinated

substrates (Fig. s2.2). The $SspB_2$-fused proteasomes allowed us to compare how ubiquitin binding to Upb6 and substrate engagement by the AAA+ ring stimulate ATP hydrolysis, and assess whether these processes affect the same or distinct conformations of the proteasome. To enforce an ubiquitin-bound state of Ubp6, we used the catalytically inactive C118A mutant and incubated it with purified lysine-48 linked ubiquitin dimers[90]. Ubp6 C118A led to a 1.8-fold increase of proteasome ATPase activity only in the presence but not in the absence of di-ubiquitin (Fig. 2.2C), with comparable effects also observed for ATPase stimulation of the isolated base subcomplex (Fig. s2.3). The ATPase response of $SspB_2$-fused proteasomes to ubiquitin-bound Ubp6 C118A strongly resembled the behavior of wild-type proteasomes (Fig. s2.4), confirming that the $SspB_2$-fusion construct is well suited to separate ubiquitin-related processes from other aspects of substrate degradation. To analyze the substrate-induced stimulation of ATP hydrolysis, we used the $SspB_2$-fused proteasomes in combination with an ssrA-tagged, permanently unfolded model protein that can get engaged and rapidly translocated without the extra burden of protein unfolding. Processing of this substrate caused a 3.3-fold increase in the ATPase rate of reconstituted proteasomes (Fig. 2.2c). Importantly, the addition of Ubp6 C118A and di-ubiquitin did not lead to a further increase, suggesting that substrate and ubiquitin-bound Ubp6 stimulate ATP hydrolysis by inducing or stabilizing a similar proteasome state, albeit to a different extent. Our previous structural comparison between substrate-free and substrate-engaged proteasomes suggest that the ATPase stimulation upon substrate engagement is caused by a switching of the AAA+ ring from a steep spiral staircase to a more planar conformation with uniform Rpt-subunit interfaces[42]. Ubiquitin-bound Ubp6 may thus also partially induce or stabilize this engaged conformation of the Rpt ring, which would be consistent with the observed reciprocal stimulation of Ubp6 deubiquitination activity by ATPγS-bound proteasomes.

In support of this hypothesis, we found that substrate engagement and translocation also stimulates Ubp6 deubiquitination activity, albeit not as strongly as trapping the base in a permanently engaged state with ATPγS (Fig. s2.5). Unfortunately, the ATPγS-bound state prevents substrate engagement and therefore made it impossible to assess whether the ATPase stimulation caused by substrate engagement and ATPγS binding are indeed non-additive, as expected based on the strong similarities between the corresponding proteasome structures[42,68].

In summary, our data suggest that ubiquitin binding to Ubp6 and substrate engagement by the base result in the same proteasome state, marked by an increased ATPase rate and higher Ubp6 deubiquitination activity.

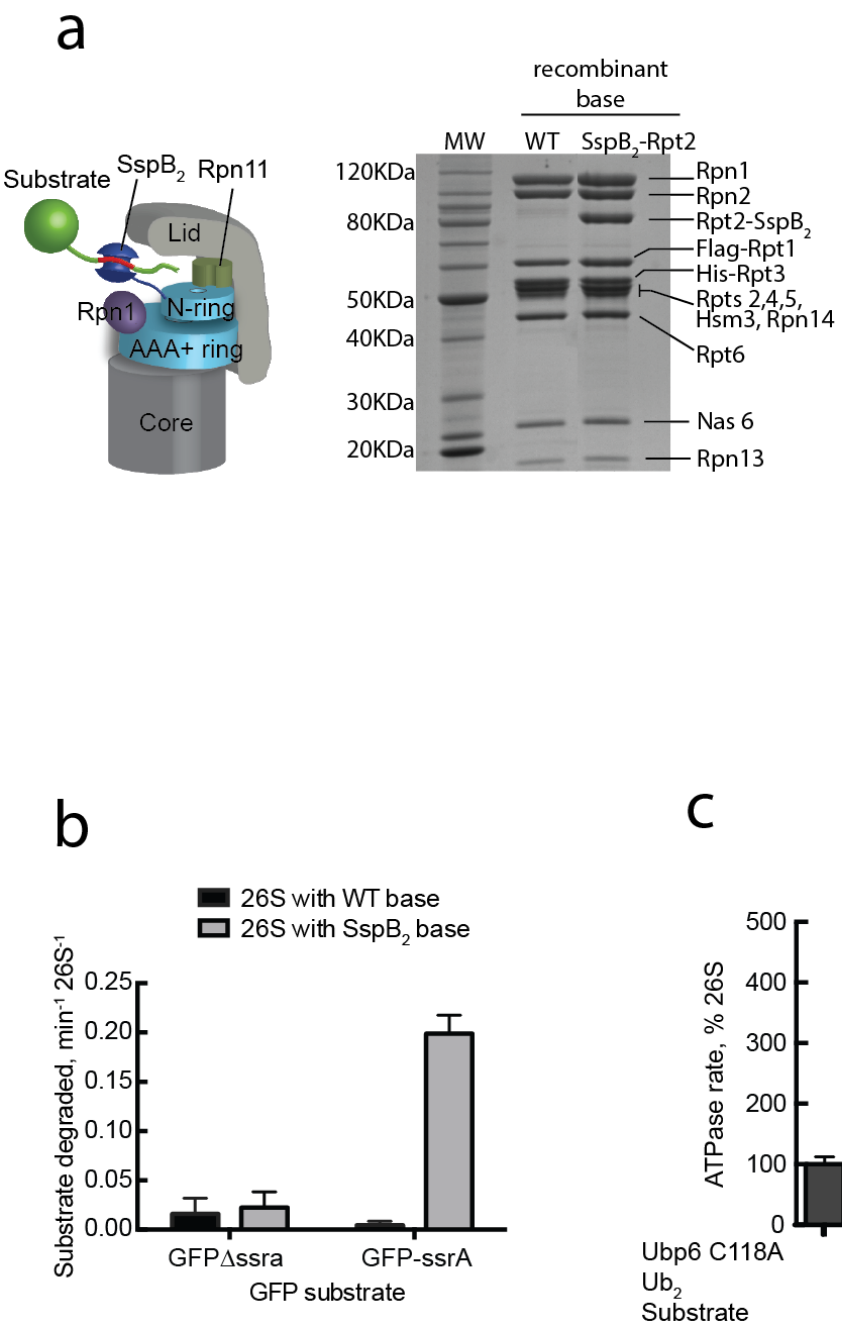

Figure 2.2 Ubp6 allostery is connected to substrate engagement. To separate ubiquitin processing from substrate engagement and translocation, we designed an ubiquitin-independent recruitment system by fusing a linked permutant of the bacterial dimeric substrate adapter $SspB_2$ to Rpt2 of the base. (a) Schematic of a $SspB_2$-fused proteasome recruiting an ssrA tagged substrate and SDS-PAGE of *E. coli*-expressed base subcomplex with either wild-type or $SspB_2$-fused Rpt2. (b) Degradation of a GFP model substrate containing the ssrA recognition motif was measured using proteasomes reconstituted with either wild-type or $SspB_2$-fused base complexes. Degradation only occurs when the $SspB_2$-fused base encounters a ssrA-containing substrate. (c) Ubiquitin-bound Ubp6 and substrate translocation stimulate the ATPase rate of $SspB_2$-fused proteasomes. The addition of substrate results in a 3.3-fold stimulation that is not

further increased by ubiquitin-bound Ubp6. Error bars represent SEM of at least three independent experiments.

Ubp6 binds to the Rpt hexamer of the base

Previous biochemical studies reported that Ubp6 is tethered to the proteasome through interactions of its N-terminal Ubl domain with the Rpn1 subunit of the base, yet attempts to visualize and localize Ubp6 bound to the proteasome have been unsuccessful[22,32]. The Ubl and the catalytic USP domains of Ubp6 are connected by a flexible 23 amino-acid linker[71], which may allow the deubiquitinase to sample a larger space around the regulatory particle for removal of ubiquitin chains docked on ubiquitin receptors Rpn10 or Rpn13. In addition to this mobile domain architecture of Ubp6, the high intrinsic flexibility of Rpn1, as indicated by consistently lower local resolutions in EM reconstructions[22,32], likely hampered the localization and visualization of proteasome-bound Ubp6.

Given the observed functional crosstalk between ubiquitin-bound Ubp6 and the base ATPase, we concluded that trapping Ubp6 in an ubiquitin-bound state might stabilize it on the proteasome for our EM structural studies. We therefore covalently modified Ubp6's active-site cysteine with ubiquitin vinyl-sulfone[91] and incubated the resulting Ubp6-UbVS with proteasomes in the presence of either ATP or ATPγS. ATP-bound proteasomes with Ubp6-UbVS exhibited a large degree of conformational heterogeneity (Supplementary Fig. 6), which was clearly observed in the 3D classification of the dataset. Although we could distinguish multiple 3D structures representing a continuum of different conformational states of the regulatory particle (Fig. s2.6), none of these reconstructed proteasomes in the presence of ATP contained sufficient particles to accurately localize the Ubp6 density. A 3D refinement of the combined dataset shows the holoenzyme in the apo conformation with diminished density in certain areas of the lid and especially the base, likely indicating the presence of proteasome particles in the engaged or hybrid states (Fig. s2.7). Previous reconstructions of the proteasome with ubiquitin-free Ubp6 did not show such heterogeneity, suggesting that ubiquitin-bound Ubp6 may partially induce alternate conformations. This would be consistent with its stimulation of base ATP hydrolysis. Importantly, we also detected additional weak density next to Rpn1 that contacts the ATPase hexamer and may correspond to a mobile Ubp6-UbVS.

In contrast to the ATP-bound complex, proteasomes incubated with ATPγS and Ubp6-UbVS exhibited less conformational heterogeneity and complete absence of the apo conformation, enabling 3D reconstructions of the holoenzyme in the engaged state (Fig. 2.3, Fig. s2.8). This reconstruction shows an extra, defined density of appropriate size to accommodate the catalytic domain of Ubp6 or human Usp14 (Fig. 2.3a). Usp14 and Ubp6 share high structural conservation[71], and we therefore generated a homology model of ubiquitin-bound Ubp6 based on the crystal structure of Usp14-ubiquitin aldehyde (PDB-ID: 2ayo), which was then docked into the additional electron density of the ATPγS-bound proteasome complex. Strikingly, the ubiquitin-bound Ubp6 binds directly to the ATPase hexamer of the base, primarily interacting with Rpt1 (Fig. 2.3a, e). In the docked model, the N-terminus of the ubiquitin-bound catalytic domain is positioned close to the density

observed between Ubp6 and Rpn1 (Fig. s2.9), which likely originates from the linker connecting the catalytic domain with the Ubl domain. Ubiquitin-bound Ubp6 contacts both the N-Ring and the AAA+ ring, which in the engaged, translocation-competent state of the base are coaxially aligned with the core particle. Ubp6's position at the periphery of the N-ring places it directly in front of Rpn11, separated by ~30 Å. Especially in its ubiquitin-bound state, Ubp6 may thus sterically occlude Rpn11's access to ubiquitinated substrates, which could explain its previously reported inhibitory effects on Rpn11 DUB activity[72]. Interestingly, this location of the Ubp6 density and its presence in the engaged conformation of the proteasome agree with a previously unspecified density in substrate-processing proteasomes observed by EM tomography of neurons[70].

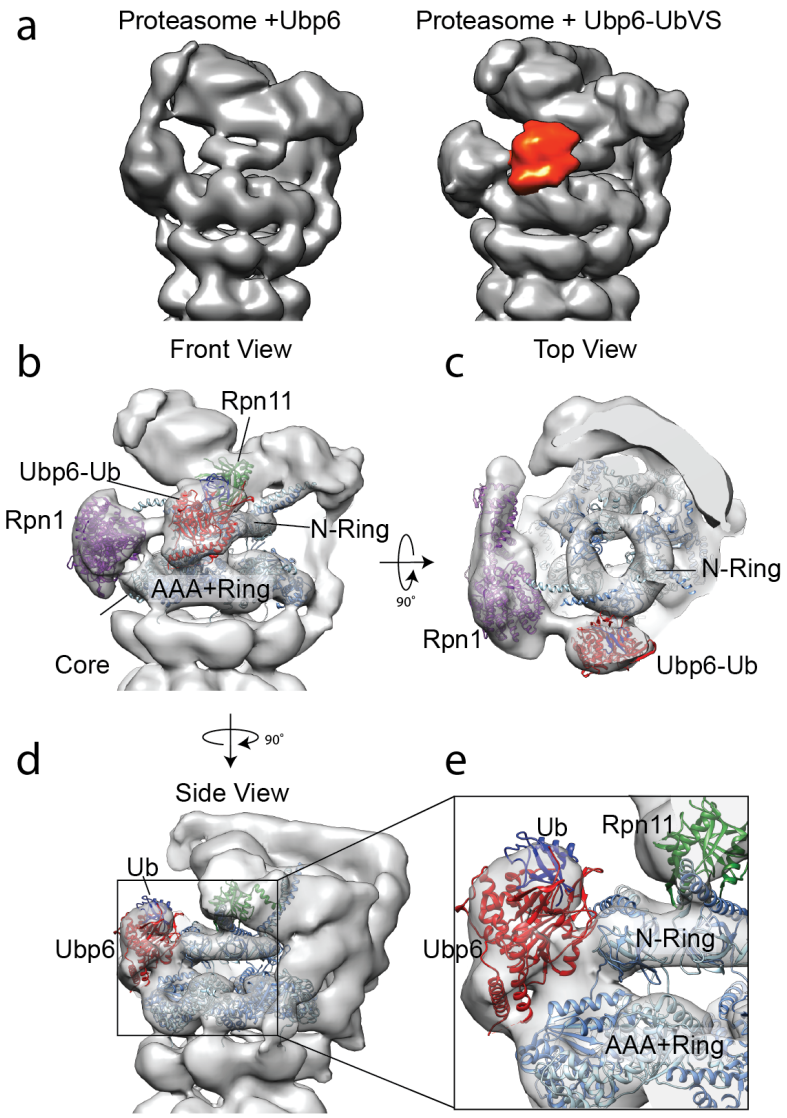

Figure 2.3 Ubiquitin-bound Ubp6 interacts with the Rpt hexamer of the base. (a) 3D reconstructions of the proteasome holoenzyme in complex with ATPγS and ubiquitin-free (left) or permanently ubiquitin-bound Ubp6 shown in red (right). (b-e) PDB models of various RP

subunits were docked into the 3D electron density map obtained from negatively stained samples. Rpn1 is shown in purple (PDB 4CR4 Chain Z), Rpn11 in green (PDB 4O8X), and the ATPase ring in blue (PDB 4CR4, Chains H-M). The Ubp6-Ub homology model was docked into the corresponding density of the 22.3-Å resolution map (Ubp6 is shown in red, ubiquitin in blue). PDB models for all Rpt proteins of the base are alternately colored in two different shades of blue. (b) Front view of the RP. Connecting density is observed between Rpn1 and the catalytic domain of Ubp6, which contacts the Rpt ring directly in front of Rpn11. (c) Top view of the RP. Ubp6 makes specific contacts with the N-terminal domain of Rpt1. (d) Side view of the RP. Ubp6 bridges the N-ring and the AAA+ ring in their coaxially stacked, engaged conformation. The N-domain residues of Rpt1 appear to interact with surface loops of Ubp6, while the AAA+ domain of Rpt1 contacts two C-terminal helices of Ubp6. This architecture places Ubp6 in close proximity to Rpn11 (~20 Å), with its bound ubiquitin only ~30 Å from the Rpn11 active site. (e) Zoomed-in view of (d), highlighting the Ubp6-base interface and proximity to Rpn11.

Ubp6 affects proteasomal conformational dynamics

Given the specific interaction of ubiquitin-bound Ubp6 with the ATPase ring in its engaged, translocation-competent conformation, we wanted to characterize Ubp6's effects on substrate degradation independent of ubiquitin processing. We therefore measured the ubiquitin-independent, $SspB_2$-mediated degradation of a permanently unfolded model substrate as well as a folded GFP model substrate in the presence or absence of Ubp6 (Fig. 2.4a). In contrast to the previously reported inhibition of ubiquitin-dependent substrate degradation[72], ubiquitin-free Ubp6 C118A had minimal effect on ubiquitin-independent degradation. However, Ubp6 C118A bound to di-ubiquitin inhibited substrate turnover. This inhibition was observed for degradation of both the folded and unfolded substrates, indicating that ubiquitin-bound Ubp6 does not affect the protein-unfolding abilities of the proteasome. In its ubiquitin-bound state, Ubp6 thus increases the ATPase rate of the base but slows substrate degradation. One possible explanation is that Ubp6 stabilizes the engaged, translocation-competent state of the proteasome and inhibits the reversion back to the apo conformation capable of engaging a new substrate. To test this hypothesis we analyzed degradation of the GFP substrate by $SspB_2$-fused proteasomes in the presence of ubiquitin-free or ubiquitin-bound Ubp6 under single-turnover conditions (excess enzyme over substrate), where measured fluorescence signals follow a single-exponential decay (Fig. 2.4b). Indeed, we observed no effect on single-turnover degradation, consistent with a scenario in which ubiquitin-bound Ubp6 might stabilize, but not strongly induce the substrate-engaged state, allowing efficient engagement of the first substrate. In contrast, multiple-turnover degradation was strongly inhibited by ubiquitin-bound Ubp6 (Fig. 2.4c). For degradation in the presence of only di-ubiquitin or ubiquitin-free Ubp6, the single-turnover rate constants agree well with the k_{cat} values of multiple turnover. These data thus suggest a model where substrate engagement with the AAA+ ring induces the engaged conformation, which is then stabilized by ubiquitin-bound Ubp6, preventing the return to the apo, engagement-competent conformation until ubiquitin dissociates.

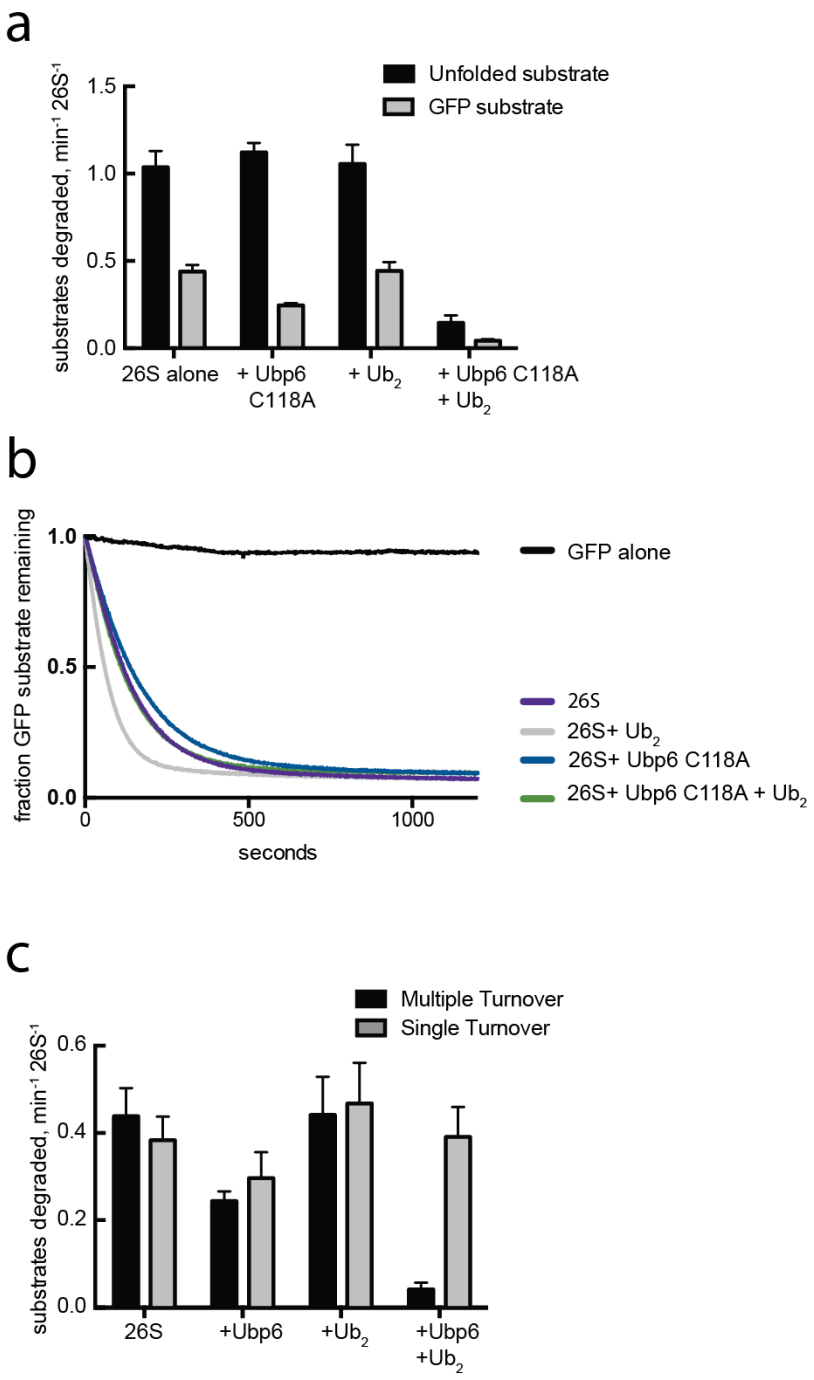

Figure 2.4 Ubiquitin-bound Ubp6 stabilizes the substrate-engaged conformation of the proteasome. Ubiquitin-independent substrate delivery to the proteasome reveals that ubiquitin-bound Ubp6 allosterically inhibits multiple- but not single-turnover degradation. (a) Multiple-turnover degradation of a permanently unfolded model substrate and a GFP fusion substrate by reconstituted $SspB_2$-Rpt2 proteasomes in the absence or presence of Ubp6 C118A and di-ubiquitin (Ub_2). Ubp6 C118A or Ub_2 in isolation had nominal effects on ubiquitin-independent degradation, whereas ubiquitin-bound Ubp6 C118A strongly impeded degradation of both substrates. Error bars show SEM of at least three independent experiments. (b) Single-turnover degradation of the GFP fusion substrate by saturating amounts of reconstituted $SspB_2$-

Rpt2 proteasomes in the absence or presence of Ubp6 C118A and Ub_2. Curves shown are representative of three individual experiments. (c) Comparison of rate constants for degradation of the GFP fusion substrate under multiple- and single-turnover conditions shown in (a) and (b). Rate constants for single turnover degradations were determined from a single exponential regression of data; error bars represent SEM of three individual experiments.

Ubp6 inhibition of ubiquitin-dependent degradation

Most substrates are targeted to the proteasome by attached polyubiquitin chains, which have to be removed by Rpn11 to allow efficient degradation[52,53]. We were thus interested in whether the close proximity of ubiquitin-bound Ubp6 to Rpn11 inhibited Rpn11-mediated deubiquitination and therefore ubiquitin-dependent substrate degradation. We directly analyzed the deubiquitination activity of Rpn11 by measuring Ub-AMC cleavage of holoenzymes with no Ubp6, Ubp6 C118A, or ubiquitin-aldehyde (UbH)-modified wild-type Ubp6 (Fig. 2.5a). Covalent modification of Ubp6 with UbH ensured an ubiquitin-bound state without adding free di-ubiquitin that would compete in the Rpn11 Ub-AMC cleavage assay. Ubp6-UbH inhibited Rpn11 by 85 %, whereas catalytically inactive Ubp6 C118A showed only 45 % inhibition. As a model substrate for the degradation experiments we used a lysine-less variant of superfolder GFP [92] fused to an unstructured region that contained a single lysine for *in vitro* ubiquitination, thus reducing potential substrate heterogeneity due to multiple chain placements. To ensure a permanently ubiquitin-bound state of Ubp6, we modified its active site with ubiquitin-vinyl sulfone (Ubp6-UbVS). Importantly, Ubp6-UbVS behaves similarly to di-ubiquitin-bound Ubp6 based on the stimulation of proteasomal ATP hydrolysis (Fig. s2.4). Substrate degradation was measured under single- and multiple-turnover condition using proteasomes purified from an ubp6Δ yeast strain with added-back wild-type Ubp6, Ubp6 C118A, or Ubp6-UbVS (Fig. 2.5 b,c). It is worth noting that in contrast to ubiquitin-independent degradation, all ubiquitin-dependent single-turnover traces followed a double exponential decay, which is consistent with our previously published data[37]. We attribute this behavior to potential heterogeneity in the ubiquitin modification of individual substrate molecules, with shorter ubiquitin chains affecting proteasome binding and processing kinetics. In agreement with earlier reports[72,75], we observed ~ 37 % slower multiple-turnover degradation in the presence of wild-type Ubp6 and a 48 % reduction in rate when the catalytically dead C118A mutant was bound to the proteasome (Fig. 2.5c). Similar to the results for ubiquitin-independent degradation, there were no significant defects in single turnover, consistent with our model that, upon ubiquitin binding, Ubp6 may stabilize the engaged proteasome conformation, prevent switching back to the substrate-free conformation, and inhibit engagement of a subsequent substrate for multiple turnover. Proteasomes in complex with Ubp6-UbVS exhibited almost no detectable degradation in both multiple and single turnover (Fig. 2.5b,c). This behavior suggests a model in which permanently ubiquitin-bound Ubp6 binds to the ATPase ring right after the substrate has entered the pore and induced the engaged conformation. The position of Ubp6 in proximity to Rpn11 would sterically prevent Rpn11 access to the ubiquitin-modified lysine of our model substrate. Since the proteasome encounters this modified lysine before the GFP moiety, inhibiting ubiquitin-chain removal by Rpn11 would stall translocation and prohibit GFP unfolding. Despite a 45 % inhibition of Rpn11 activity by Ubp6 C118A, we did not

observe defects in single-turnover substrate degradation. It is possible that the catalytically inactive Ubp6 C118A is not ubiquitin-bound during degradation of the first substrate, but holds on to ubiquitin after Rpn11 cleavage, affecting Rpn11 deubiquitination and stabilizing the engaged state in multiple turnover. Alternatively, the on- and off-rates for uncleaved ubiquitin on Ubp6 C118A may still allow ubiquitin-chain binding and cleavage by Rpn11, but significantly inhibit the base switching back to the pre-engaged state for multiple turnover. As a control, we verified that the proteasome did not engage and degrade any of the Ubp6 variants, which would also inhibit degradation of our model substrate (Fig. s2.10).

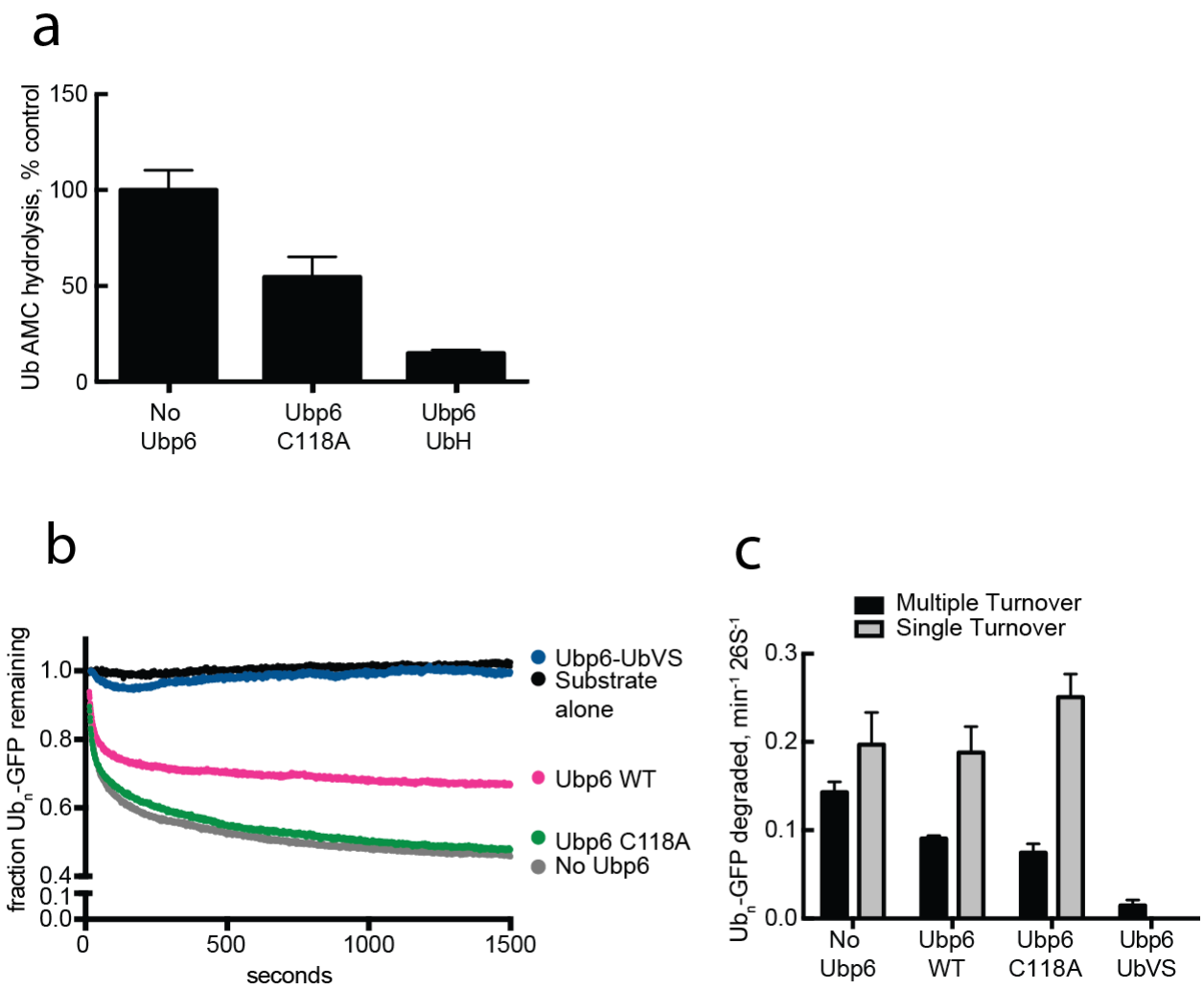

Figure 2.5 Ubp6 affects ubiquitin-dependent degradation.
(a) Ubiquitin binding to Ubp6 strongly inhibits Rpn11 deubiquitination activity. Buffer, Ubp6 C118A, or wild-type Ubp6 were treated with ubiquitin aldehyde (Ub-H) followed by N-ethylmaleimde (NEM) and DTT to ensure complete inactivation of Ubp6. After buffer exchange, samples were added to Ubp6-free holoenzymes purified from yeast. Rpn11 deubiquitination activity was measured by Ub-AMC cleavage, indicating ~ 45 % inhibition by C118A Ubp6 and ~ 85 % inhibition by permanently ubiquitin-bound Ubp6-UbH. (b,c) To examine the effects of Ubp6 on ubiquitin-dependent substrate degradation, the same GFP fusion substrate used for ubiquitin-independent turnover was *in-vitro* ubiquitinated on an engineered single lysine residue.

(b) Single-turnover degradations of the polyubiquitinated GFP fusion substrate were measured with saturating amounts of proteasome holoenzyme that was purified from an Ubp6-knockout yeast strain and had no Ubp6, wild-type Ubp6, Ubp6 C118A, or ubiquitin-vinylsulfone-fused Ubp6 (Ubp6-UbVS) added back. Ubp6-UbVS abrogated degradation, whereas wild-type and C118A Ubp6 permitted substrate single-turnover. (c) Comparison of rate constants for single- and multiple-turnover degradation of the ubiquitinated GFP model substrate. Notably, the presence of cleavage-deficient C118A Ubp6 inhibits degradation in multiple turnover, but not in single turnover.

Discussion

Our biochemical and structural data show that, besides its role in ubiquitin cleavage, Ubp6 affects proteasomal substrate degradation by allosterically interfering with distinct proteasome functions in an ubiquitin-dependent manner. Prior to substrate engagement by the base, Ubp6 is tethered via its Ubl domain to Rpn1, while its catalytic USP domain appears to be rather mobile and sampling a larger area. Interactions of Ubp6 with the base ATPase stimulate its deubiquitination activity, which further increases upon proteasome engagement of a substrate polypeptide. Ubiquitin-bound Ubp6 binds and stabilizes this substrate-engaged, translocation-competent conformation of the proteasome by interacting with both the N-ring and the AAA+ ring of the base, thereby maintaining their coaxial alignment with the 20S core. The interaction with the base places ubiquitin-bound Ubp6 in close proximity to Rpn11, where it interferes with Rpn11-mediated substrate deubiquitination.

Our results suggest a model in which substrate engagement acts as a switch to induce the translocation-competent state of the proteasome, which is then regulated by ubiquitin-bound Ubp6 in two ways: the inhibition of Rpn11 and the interference with conformational switching back to the substrate-free state (Fig. 2.6). Ubp6 would inhibit Rpn11 deubiquitination and therefore slow substrate degradation if it interacts with ubiquitin before Rpn11 has removed all modifications from a translocating substrate. Such coordination between Ubp6 and Rpn11 activities may be important for complex substrates containing multiple, very long, or branched polyubiquitin chains that need to be co-translocationally trimmed by Ubp6. After Rpn11 has cleaved off all ubiquitin modifications and a substrate has been completely unfolded and translocated, Ubp6 may trap the engaged conformation of the proteasome and prevent the engagement of a subsequent substrate until it is no longer occupied with ubiquitin. This mechanism would be important for Ubp6-mediated clearance of polyubiquitin chains from the several ubiquitin receptors before the proteasome commits to the degradation of a new substrate, and it would agree with Ubp6's role in maintaining high levels of free ubiquitin in the cell[58,93].

In our studies we either saturated ubiquitin-binding to catalytically dead Ubp6 or used covalent ubiquitin fusions to exaggerate the effects on proteasomal functions. However, given the fast kinetics of ubiquitin cleavage by Ubp6 compared to Rpn11, wild-type Ubp6 that is processing ubiquitin modifications would not be expected to severely slow

proteasomal substrate degradation. Ubp6 may rather act as a timer, not only as previously suggested by trimming of ubiquitin chains and thus affecting the persistence time of substrates at the proteasome, but in an ubiquitin-dependent manner by allosterically coordinating the various substrate-processing steps at the proteasome and preventing stalling of substrates with complex ubiquitin modifications.

Our EM structural work provides the first visualization of ubiquitin-bound Ubp6 in the context of the 26S proteasome. Future higher-resolution structures will be required to elucidate the detailed mechanisms involved in the reciprocal stimulation of Ubp6 deubiquitination and base ATPase activities. It will also be interesting to investigate how Ubp6 coordinates with other proteasome-bound cofactors, for instance the ubiquitin ligase Hul5[56,94,95] or ubiquitin shuttle receptors Rad23, Ddi1, and Dsk2[41,50,96,97], in fine-tuning substrate processing by the 26S proteasome.

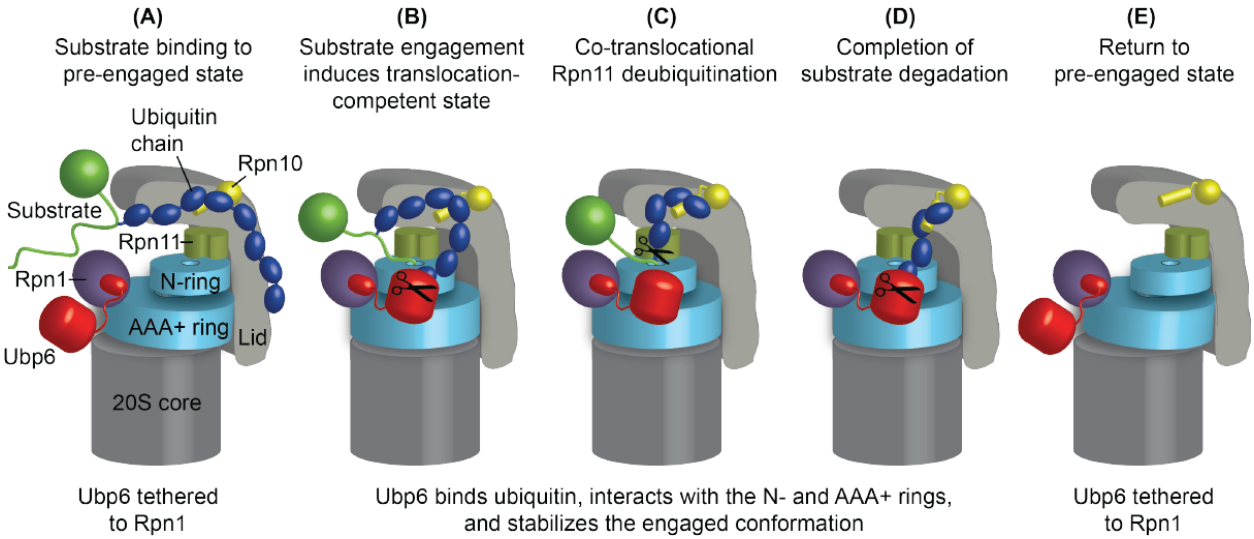

Figure 2.6 Figure 6. Model for Ubp6 acting as an ubiquitin-dependent timer to allosterically control proteasome conformational changes, Rpn11 deubiquitination, and substrate degradation. (a) Ubiquitin-chain binding to an intrinsic receptor, e.g. Rpn10, tethers a substrate to the proteasome. Ubp6 is bound to the proteasome via its Ubl domain interacting with Rpn1. (b) Engagement of the unstructured initiation region of the substrate by the ATPase hexamer induces a conformational switch of the regulatory particle to a substrate-engaged, translocation competent state, which is characterized by a coaxial alignment of Rpn11, N-ring, AAA+ ring, and 20S core. If ubiquitin-bound, for instance during debranching or trimming of ubiquitin chains, Ubp6 interacts with and stabilizes the engaged state of the ATPase hexamer by bridging the N-ring and AAA+ ring. In this state, ubiquitin-bound Ubp6 inhibits Rpn11-mediated deubiquitination and consequently substrate degradation. (c) Translocation moves the ubiquitin-modified lysines of the substrate into the Rpn11 active site for co-translocational ubiquitin-chain removal. (d) Even after complete substrate translocation, ubiquitin-bound Ubp6 stabilizes the engaged conformation of the

proteasome, prevents switching back to the engagement-competent state, and thus interferes with the degradation of the subsequent substrate. Such trapping of the engaged state would allow Ubp6 to clear ubiquitin chains from proteasomal receptors before the next substrate is engaged and degradation is initiated. (e) As soon as it is no longer occupied with ubiquitin, the catalytic domain of Ubp6 releases from the N-ring and AAA+ ring, and allows the regulatory particle to return to the pre-engaged state for the next round of substrate degradation.

Accession Codes

The cryo-electron microscopy density maps for the 26S proteasomes in the presence and absence of ubiquitin-bound Ubp6 can be found at the Electron Microscopy Data Bank under accession numbers 13349 and 30908, respectively.

Acknowledgements

We thank the members of the Martin lab for helpful discussions, Chris Padovani for purified ubiquitin dimers, and Robyn Beckwith for proteasome base subcomplexes. We are also grateful to Tom Wandless (Stanford School of Medicine) for providing the lysineless GFP construct and Kris Nyquist for cloning the GFP model substrate used in degradation assays. C.B. acknowledges support from the NSF Graduate Research Fellowship, and M.E.M. acknowledges support from the American Cancer Society. This research was also funded in part by the Damon Runyon Cancer Research Foundation, the Pew Scholars program, the Searle Scholars program, and the National Institutes of Health to G.C.L. A.M. acknowledges support from the Searle Scholars Program, start-up funds from the University of California Berkeley Molecular & Cell Biology Department, the National Institutes of Health the National Science Foundation CAREER Program.

Author Contributions

C.B., M.E.M., and A.M. designed, expressed, and purified proteasome components, and performed biochemical experiments. C.M.D. and G.C.L. performed the electron microcopy, data processing, and segmentation analyses. All authors contributed to experimental design, data analyses, and manuscript preparation.

Methods

Yeast strains

Yeast lid and holoenzyme were purified from strain YYS40 (genotype *MAT***a** *ade2-1 his3-11,15 leu2-3,112 trp1-1 ura3-1 can1 Rpn11::Rpn11*-3× Flag(His_3)[61]. Core particle was prepared from either strain RJD1144 (genotype *MAT***a** *his3Δ200 leu2-3,112 lys2-801 trpΔ63 ura3-52 PRE1*-Flag-His_6::*Ylpac211(URA3)*[98] or strain yAM14 (genotype *MAT***a** *ade2-1 his3-11,15 leu2-3,112 trp1-1 ura3-1 can1-100 bar1 PRE1::PRE1*-3× Flag*(KanMX)*,[37]). To generate *UBP6* deletion strains, the kanMX6 sequence was integrated at the respective genomic locus,

replacing the gene in YYS40[22]. To generate the *UBP6* C118A strain, a C118A copy of Ubp6 was cloned into pRS305 and was integrated into the *UBP6* deletion strain at the *leu2* locus.

Purification of yeast holoenzyme and subcomplexes

Wild-type and mutant proteasome was purified from *S. cerevisiae* essentially as described.[22,42] In summary, holoenzyme, lid, and core particle were purified from yeast strains listed above. Lysed cells were resuspended in lysis buffer containing 60 mM HEPES, pH 7.6, 50 mM NaCl, 50 mM KCl, 5 mM $MgCl_2$, 0.5 mM EDTA, 10% glycerol, and 0.2% NP-40. Holoenzyme lysis also included an ATP-regeneration mix (5 mM ATP, 0.03 mg/ml creatine kinase and 16 mM creatine phosphate). Complexes were bound to anti-Flag M2 affinity resin (Sigma) and washed with wash buffer (60 mM HEPES, pH 7.6, 50 mM NaCl, 50 mM KCl, 5 mM $MgCl_2$, 0.5 mM EDTA, 10% glycerol, 0.1% NP-40 and 500 mM ATP). Core particle was washed with wash buffer containing 500mM NaCl, and Lid was washed with wash buffer containing 1M NaCl. Complexes were eluted with Flag peptide and separation by size-exclusion chromatography over Superose-6 in gel-filtration (GF) buffer (60 mM HEPES, pH 7.6, 50 mM NaCl, 50 mM KCl, 5 mM $MgCl_2$, 0.5 mM EDTA and 0.5 mM ATP) containing 5% glycerol.

Recombinant expression and purification of proteins and complexes

Base subcomplexes were expressed and purified from *E. col* as previously described.[37] Nine integral subunits (Rpn1, Rpn2, Rpn13, Rpts-1-6,) and four assembly chaperones (Rpn14, Hsm3, Nas2 and Nas6) were expressed with rare tRNAs at overnight at 18˚C after induction with 0.5mM IPTG. Cells were harvested by centrifugation and resuspended in nickel buffer (60mM HEPES, pH 7.6, 100mM NaCl, 100mM KCl, 10% glycerol, 10mM $MgCl_2$, 0.5 mM EDTA, and 20mM imidazole) supplemented with 2 mg ml^{-1} lysozyme, protease inhibitors, (aprotinin, pepstatin, leupeptin and PMSF) and benzonase (Novagen). Cells were lysed with by freeze-thaw cycles and sonication, and clarified by centrifugation. A two-step affinity purification of the base subcomplex was performed using nickel–nitrilotriacetic acid (Ni-NTA) agarose (Qiagen) to select for His_6-Rpt3 and anti-Flag M2 resin (Sigma-Aldrich) selecting for Flag-Rpt1. 0.5 mM ATP was present in all purification buffers. The Ni-NTA and anti-Flag M2 columns were eluted with nickel buffer containing 250 mM imidazole and 0.15 mg ml^{-1} 3× Flag peptide, respectively. The Flag column eluate was concentrated and run on a Superose 6 size exclusion column (GE Healthcare) equilibrated with gel filtration buffer (60 mM HEPES, pH 7.6, 50 mM NaCl, 50 mM KCl, 10% glycerol, 5 mM $MgCl_2$, 0.5 mM EDTA, 1 mM DTT and 0.5 mM ATP).

The GFP fusion substrate construct was cloned into a pET Duet (Novagen) vector, and consisted of a lysinesless superfolder GFP [92], lysineless titin I27 V15P domain, and a random coil containing the ssrA sequence and the PPXY motif. *E. coli* Bl21-star (DE3) cells were transformed with the construct and grown in Terrific Broth (EMD Millipore) at 30 °C. Cells were induced with 0.5mM IPTG at an OD_{600} of 1-1.5 and expression went for 5 hours at 30 °C.

The unfolded substrate was cloned into a pET 28A (Novagen) vector and consisted of a lysineless, disulfide-less N1 domain from gene-3-protein[99] fused to a random coil containing an ssrA tag, ppxy motif, and a lysineless strepII tag. WT Ubp6 was amplified from genomic (W303) DNA, and cloned into pET Duet with an N-terminal His_6 tag. C118A mutation was made by around-the-horn PCR. *E. coli* Bl21-star (DE3) cells were transformed with either the N1 construct or the Ubp6 constructs and grown in Terrific Broth at 37 °C. Cells were induced with 0.5mM IPTG at an OD_{600} of 0.6 and expression continued overnight at 18 °C.

GFP, unfolded substrate, or Ubp6 expressing cells were harvested by centrifugation and resuspended in nickel buffer (above) supplemented with 2mg ml^{-1} lysozyme, benzonase (Novagen), and protease inhibitors (aprotinin, pepstatin, leupeptin and PMSF). Cells were lysed by freeze thaw and sonication. Lyates were clarified by centrifugation at 15,000 rpm for 20 minutes at 4 C. Proteins were purified using Ni-NTA affinity chromatography followed by size exclusion chromatography on a Superdex 200 (GE Healthcare) using nickel and gel filtration buffers mentioned above.

Construction of the $SspB_2$ permutant base

To allow ubiquitin-independent substrate delivery to the proteasome, we created a base variant that is fused to a linked permutant dimer of the E.coli substrate adaptor SspB. A wild-type SspB monomer consists of a globular domain and a C-terminal tail of 38 residues. In simple dimer fusions, where we connected the C-terminus of the globular domain of one SspB monomer with the N-terminus of the second SspB monomer, the linker interfered with ssrA substrate binding to $SspB_2$. We therefore constructed a circular permutant SspB monomer, in which we created a new N-terminus at residue L26 and connected the preceding N-terminal helix to the C-terminus of the globular domain, and fused this monomer to the N-terminus of a second, wild-type SspB monomer. The connectivity of this covalently fused dimer is: (L26-D111) - GGASG - (S4-Q25) - GGGTGG - (wild-type monomer). This $SspB_2$ dimer was then fused to the N-terminus of Rpt2 of the base.

Ubiquitin purification and dimer synthesis

Ubiquitin was expressed and purified as previously described[100,101]. Briefly, Rosetta II (DE3) pLysS *Escherichia coli* cells were transformed with a pET28a vector containing the ubiquitin gene from *S. cerevisiae* under control of a T7 promoter. Cells were grown in Terrific Broth supplemented with 1% glycerol at 37 °C until OD_{600} = 1.5–2.0 and were induced with 0.5 mM IPTG overnight at 18 °C. The lysis buffer contained 50 mM Tris-HCl, pH 7.6, 0.02% NP-40, 2 mg mL^{-1} lysozyme, benzonase (Novagen), and protease inhibitors (aprotinin, pepstatin, leupeptin and PMSF). Cells were lysed by sonication and 20 min incubation at room temperature. Lysate was clarified by centrifugation at 15000 rpm. Clarified lysate was precipitated by adding 60%perchloric acid to a final concentration of 0.5%, and the solution was stirred on ice for a total of 20 min. A 5-mL HiTrap SP FF column (GE Life Sciences) was used for cation-exchange chromatography, and ubiquitin fractions were pooled and exchanged into Ub storage buffer (20 mM Tris-HCl, pH 7.6, and 150 mM NaCl) by repeated dilution and concentration.

Lys-48 ubiquitin dimers were synthesized and purified as previously described[90].

Preparation of Ubiquitin fused Ubp6

50μM WT Ubp6 protein was reacted with 75uM ubiquitin vinyl sulfone or Ubiquitin Aldehyde (R&D Systems) in GF at 37 °C. For the experiment in 5D, which required complete inhibition of the active site cysteine, buffer, wild-type Ubp6, or C118A Ubp6 were reacted with ubiquitin aldehyde (R&D systems) for seven hours at 37˚C in the dark. Ubp6-UbH was further reacted with 500μM NEM for 30 min at 30 C, followed by quenching with 5mM DTT for another 30 min at 30 C. Ubiquitin-aldehyde, NEM, and DTT were removed by dilution and concentration in an Amicon 30K MCWCO concentrator (EMD Milipore).

Ubiquitin AMC hydrolysis assays

Ubiquitin-AMC (R&D systems) hydrolysis was measured in a QuantaMaster spectrofluorimeter (PTI) by monitoring an increase of fluorescence emission at 435 nm with an excitation at 380nm. Reactions using reconstituted proteasome used 100nM Ubp6, 150nM Rpn1, 150nM recombinant base, 300nM CP, 300nM Lid, 300nM Rpn10, 20μM unfolded substrate, and 3-10uM Ub-AMC. Reactions using proteasomes purified from yeast used 100nM proteasome. Reactions were carried out either in the presence GF buffer (see above) with 1mM DTT and 1x ATP regeneration system or 1mM ATPgS. Samples were incubated at 30°C for 5-10 minutes prior to the addition of substrate to ensure Ubp6 association and nucleotide exchange.

ATPase assays

ATPase activity was quantified by an NADH-coupled ATPase assay. Reconstituted proteasomes, (200nM base, 600nM core, 600nM lid, 600nM Rpn10) Ubp6, (200nM) Ub_2^{K48} (20uM), and unfolded gene-3-protein substrate (20uM) were incubated with 1× ATPase mix (3 U ml^{-1} pyruvate kinase, 3 U ml^{-1} lactate dehydrogenase, 1 mM NADH and 7.5 mM phosphoenol pyruvate) at 30 °C. Reactions were done in GF buffer (see above) with 1mM DTT. Absorbance at 340 nm was monitored at 30 °C for 600 s at 1-s intervals by a UV-vis spectrophotometer (Agilent).

Multiple and Single turnover ubiquitin independent degradation assays

26S proteasomes were reconstituted using recombinant, heterologously-expressed $SspB_2$-Rpt2 base, recombinant Rpn10, and lid and core subcomplexes purified from yeast. Multiple turnover degradations were done with 200nM CP, 600nM Lid, 600 nM base, 600nM Rpn10, 900nM Ubp6 and 20uM Ub_2^{K48}. Reactions were done in the presence of 1x ATP regeneration system (5 mM ATP, 0.03 mg ml^{-1} creatine kinase, 16 mM creatine phosphate) in gel filtration buffer with 1mM DTT. Single turnover reactions were done with 3uM $SspB_2$-Rpt2 base, 4.5uM lid, 4.5uM base, 4.5uM Rpn10, 9uM Ubp6, 20uM Ub_2^{K48}, and 300nM substrate in the presence of 1x ATP regeneration system in gel filtration buffer with DTT and ATP regeneration system. GFP single- and multiple-turnover degradation activities

were monitored by the loss of GFP fluorescence (excitation, 467 nm; emission, 511 nm) using a QuantaMaster spectrofluorimeter (PTI) Single turnover curves were fit to a single exponential in GraphPad Prism 6.

To track degradation of an unfolded substrate, purified N1 fusion substrates were labeled on a single cysteine with Alexa 647 maleimide at pH 7.2 for 3 hours at room temperature in the dark, before quenching unreacted dye with DTT. Free dye was removed on a Superdex 200. Substrate degradation was measured by taking time-points of a reaction at 30 °C and assessed by SDS-PAGE followed by imaging on a Typhoon Trio (GE) with a 633 laser and 670BP emission filter. Band intensity was quantified using Image Quant software. Degradation reactions consisted of 8uM substrate against proteasomes reconstituted as above with either $SspB_2$-Rpt2 base or WT base to correct for any non-specific, $SspB_2$ independent substrate cleavage.

Preparation of Ubiquitinated substrates

GFP substrates (20uM) were modified with polyubiquitin chains by 5uM yeast Uba1, 5uM yeast Ubc1, 5uM Rsp5, 1x ATP Regeneration system, and 300uM ubiquitin. Reaction was carried out in a thermocycler for 2 hours at 25 C, then overnight at 4C.

Multiple and Single turnover ubiquitin dependent degradation assays

GFP constructs were ubiquitinated overnight and then used the next day without freezing. Single- and multiple-turnover degradation activities were monitored by the loss of GFP fluorescence (excitation, 467 nm; emission, 511 nm) using a QuantaMaster spectrofluorimeter (PTI) as above. Multiple turnover reactions consisted of 300nM purified proteasomes from a ΔUbp6 strain, 600nM Ubp6, and 2μM substrate. Single-turnover reactions consisted of 3μM proteasome, 6μM Ubp6, and 300nM substrate.

Electron microscopy

Samples of 26S-bound Ubp6-UbVS were diluted to ~25 nM in 60 mM HEPES pH 7.6, 50 mM NaCl, 50 mM KCl, 5 mM $MgCl_2$, 0.5 mM EDTA, 1 mM TCEP and either 1 mM ATP or 1 mM ATPgS (Sigma). A thin layer of carbon was applied to 400-mesh Cu-Rh maxtaform grids (Electron Microscopy Sciences) by chemical vapor deposition, and grids were subsequently exposed to a 95% Ar/5% O2 plasma for 20 seconds to glow-discharge/activate the carbon surface. Grids were pre-treated with 4 μl of 0.1% poly-L-lysine hydrobromide (Polysciences) to prevent preferred orientation of 26S particles on carbon. Poly-L-lysine solution was then wicked away, grids were washed with 4 μl of H_2O, and 4 μl of sample was applied. 252 and 357 images of negatively stained (2% uranyl formate) 26S-Ubp6-UbVS complexes in the presence of ATP or ATPgS, respectively, were collected at a nominal magnification of 52,000 X on an F416 CMOS 4K X 4K camera (TVIPS) with a pixel size of 2.05 Å/pixel at the sample level. Images were acquired on a Tecnai Spirit LaB_6 electron microscope operating at 120keV, with a random defocus range of -0.5 μm to -1.5 μm and an electron dose of 20e-/$Å^2$. Data were acquired using the Leginon automated image acquisition software [102].

Processing

All image preprocessing and 2D analysis was performed using the Appion image-processing pipeline [103]. CTF was estimated using CTFFIND3, and only micrographs having a CTF confidence greater than 80% were used for processing. Particle picking was performed using the template-based FindEM software[104]. Micrographs were phaseflipped using EMAN's "applyctf" function, and particles were extracted with a box size of 384 pixels. Pixel values 4.5 sigma above or below the mean were replaced with the mean intensity of the extracted particle using XMIPP. Multiple rounds of iterative MSA/MRA was used for 2D classification and alignment of the particles, and class averages containing single-capped proteasomes, as well as damaged, aggregated, or false particles, were removed, resulting in a dataset containing 24,411 and 18,565 double-capped proteasome particles in presence of 1mM ATP and 1mM ATPgS, respectively. 3D classification and 3D refinement were performed with C2 symmetry imposed using RELION v1.31[105]. The 3D reoconstructions for proteasomes in the presence of ATP and ATPgS resolved to 24.2 Å and 22.3 Å, respectively, according to a gold standard Fourier Shell Correlation at 0.143. Low resolution intensities were dampened using a SPIDER script in order to more clearly visualize domain features.

3D modeling

An atomic model of yeast Ub-bound Ubp6 was constructed by superimposing the yeast Ubp6 crystal structure (PDB 1VJV) onto the stucture of the human Rsp14 structure bound to Ubiquitin (PDB 2AYO), using UCSF Chimera's "MatchMaker" tool. These structures have high structural homology, and the resulting hybrid structure did not exhibit any clashes between the Ubiquitin and Ubp6. This Ubp6-Ub model was docked into the density putatively corresponding to Ubp6. PDB 4CR4 was used for docking other 26S core, base and lid subunits into the ATPgS electron density map obtained here, with the exception of the Rpn8-Rpn11 dimer, for which PDB 4O8Y was used. All docking of PDB structures was performed using the "Fit in Map" tool of UCSF Chimera, and this software was also used to generate all figures displaying the EM density [106].

Supplementary information

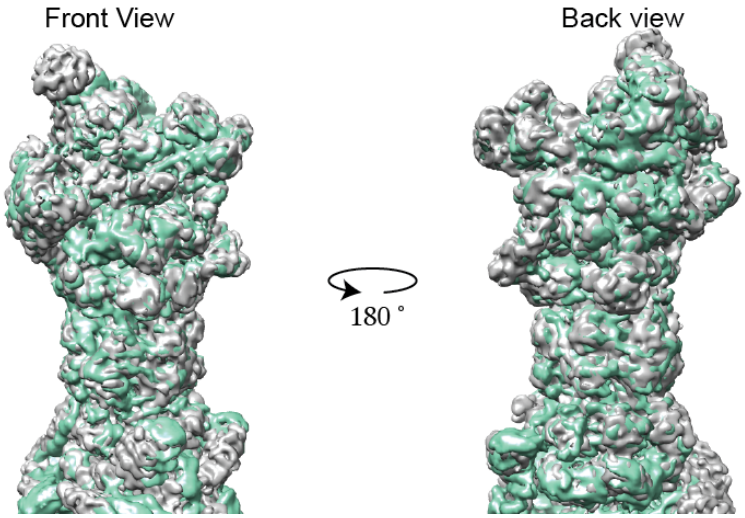

Figure s2.1 ATPγS induces holoenzyme conformation identical to substrate.
EM reconstruction of the ATPγS bound proteasome agrees with EM reconstruction of substrate-translocation proteasome. Font and back views of reconstructions of ATPγS bound proteasome (EMDB 2596, gray) and substrate-bound proteasome (EMDB 5669, cyan) that were aligned in chimera using the "fit in map tool"

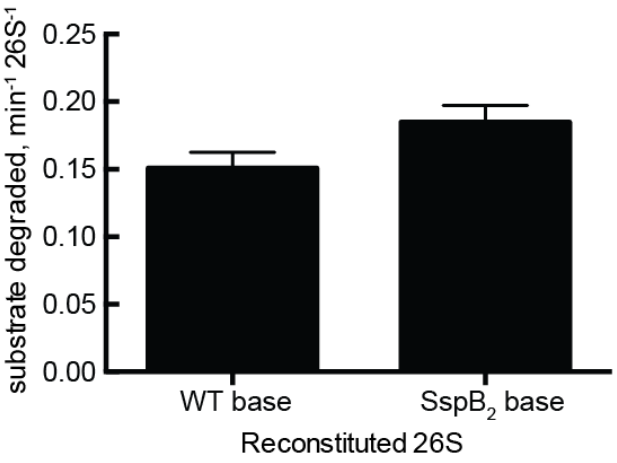

Figure s2.2 Proteasomes reconstituted with $SspB_2$-Rpt2 base are competent to degrade ubiquitinated substrate. 200nM WT or $SspB_2$-Rpt2 base was assembled into proteasomes with 600nM lid, Rpn10 and CP. Degradation of 2μM ubiquitinated EGFP substrate was measured by loss of fluorescence at 511nm.

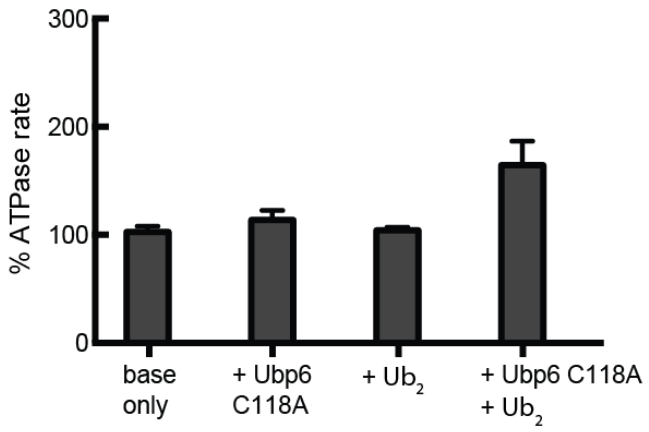

Figure s2.3 Ubp6 stimulates ATPase rate of the isolated base subcomplex. ATPase rates of purified recombinant base were measured in the presence of Ubp6 C118A, di-ubiquitin, and Ubp6 C118A with di-ubiquitin. Error bars show SEM of at least three independent experiments

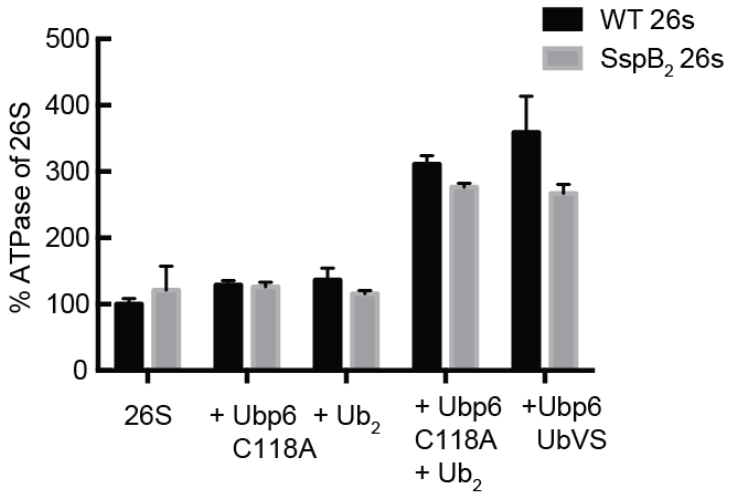

Figure s2.4 Ubp6 similarly stimulates ATPase rate of proteasomes reconstituted with WT base or $SspB_2$-Rpt2 base. Proteasomes were reconstituted with 200nM WT or $SspB_2$-Rpt2 base and 600nM Lid, Rpn10, and CP. 900nM Ubp6 and/or 20μM di-ubiquitin were added to show similar stimulations of ATPase rate with the wild-type or $SspB_2$-Rpt2 base. Di-ubiquitin with Ubp6 stimulated proteasomes similarly to UbVS-Ubp6. Error bars represent SEM of at least three independent experiments.

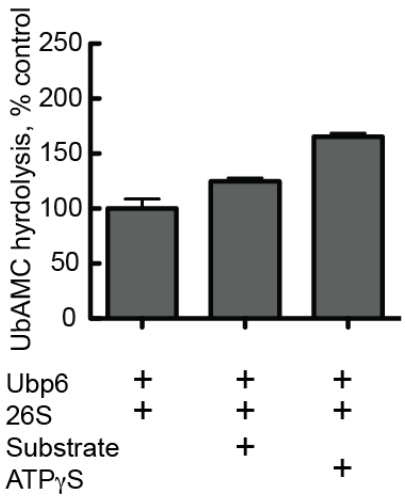

Figure s2.5 Substrate translocation by the proteasome stimulates Ubp6 deubiquitination. Wild-type Ubp6 activity was measured with proteasomes reconstituted with $SspB_2$-Rpt2 base. Addition of saturating amounts of an unfolded substrate increases Ubp6 deubiquitination, although not as much as the addition of ATPγS. Error bars represent SEM of at least three independent experiments.

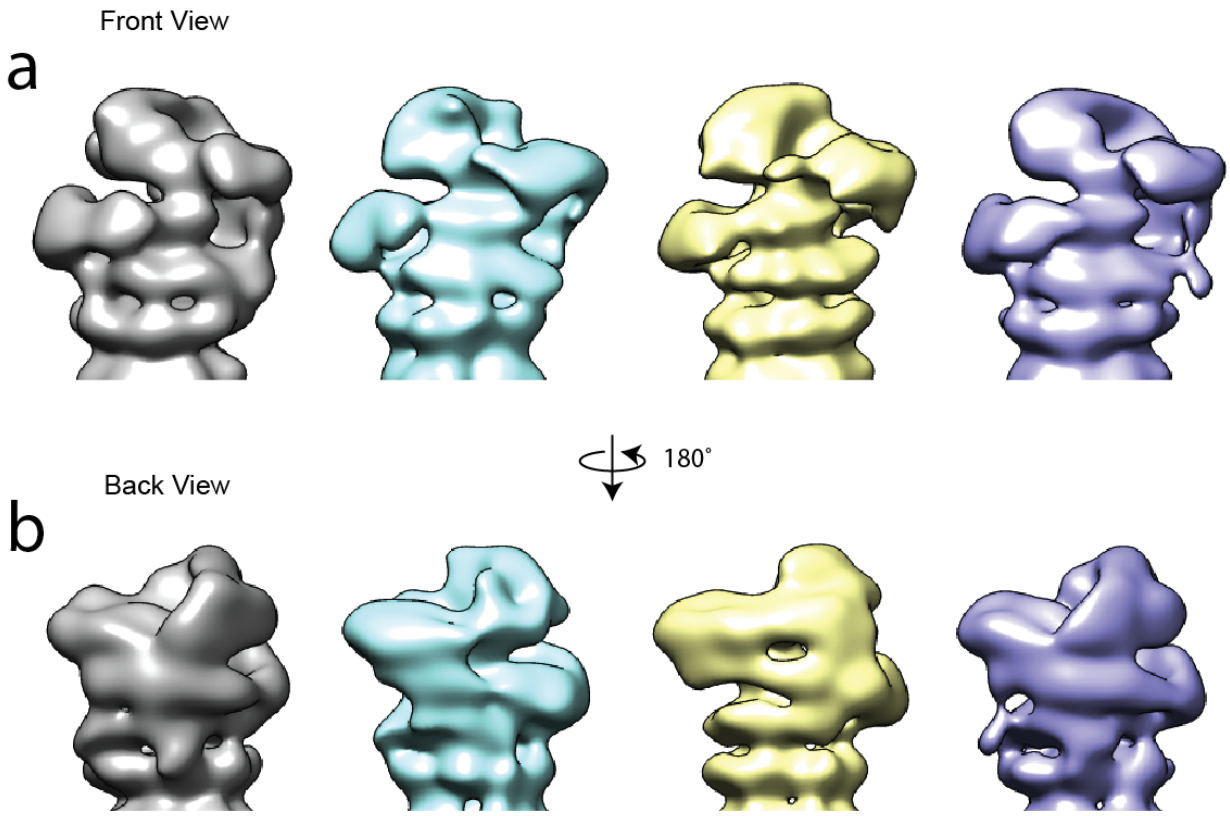

Figure s2.6 3D classes in ATP bound, Ubp6-UbVS proteasomes.
(A) Front and (B) back views of different proteasome conformations seen in 18000 particles by negative stain EM.

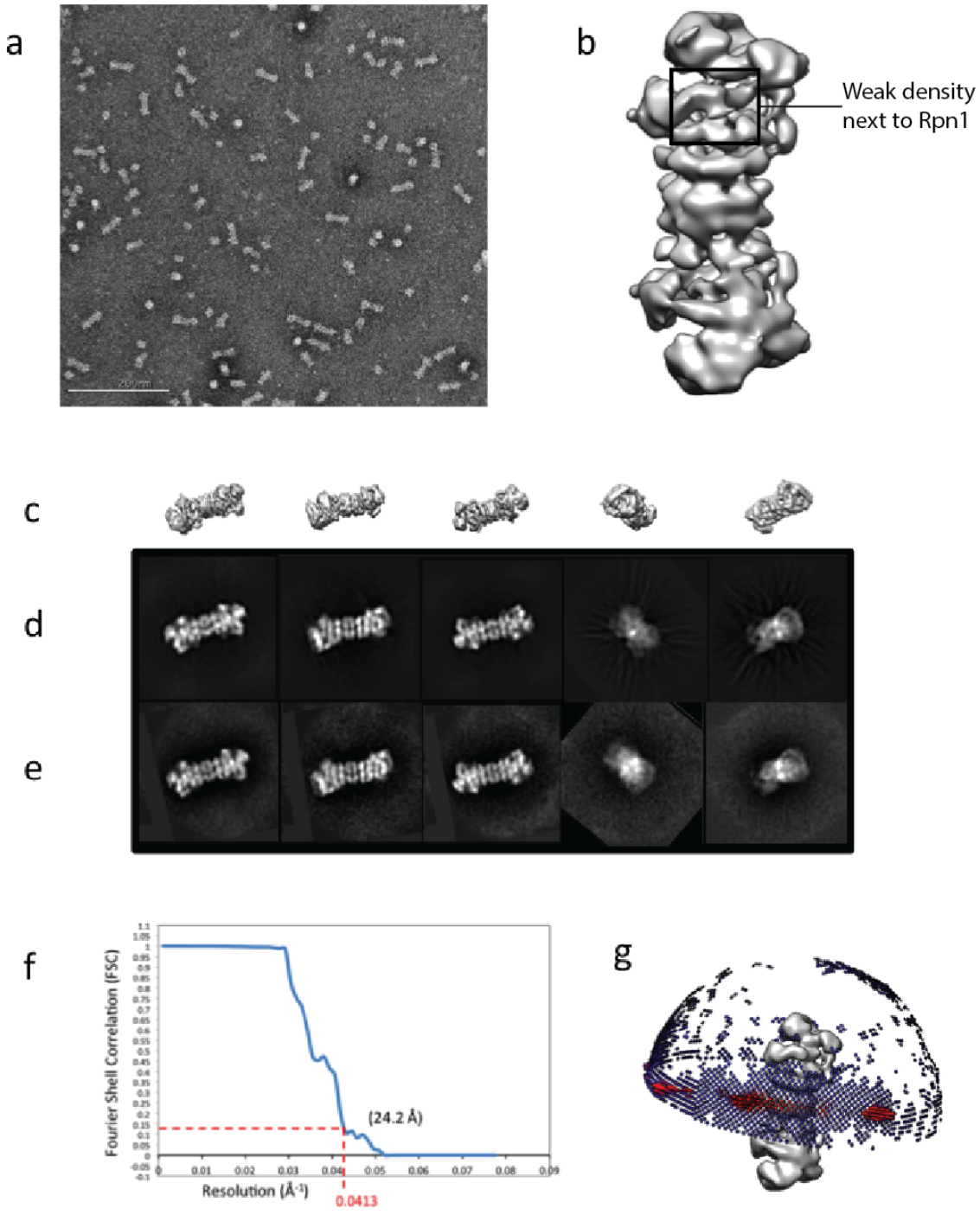

Figure s2.7 Ubp6-UbVS proteasome structure in ATP.
(a) raw micrograph of the grids. (b) sharpened reconstruction shows holoenzymes in an apo state. (c) Differential projections of the 3D model to match the 2D projections shown. (d) 2D projections calculated from the 3D model. (e) reference-free 2D classes from actual data set. (f) FSC curve. (g) Angular distribution plot (Euler plot)

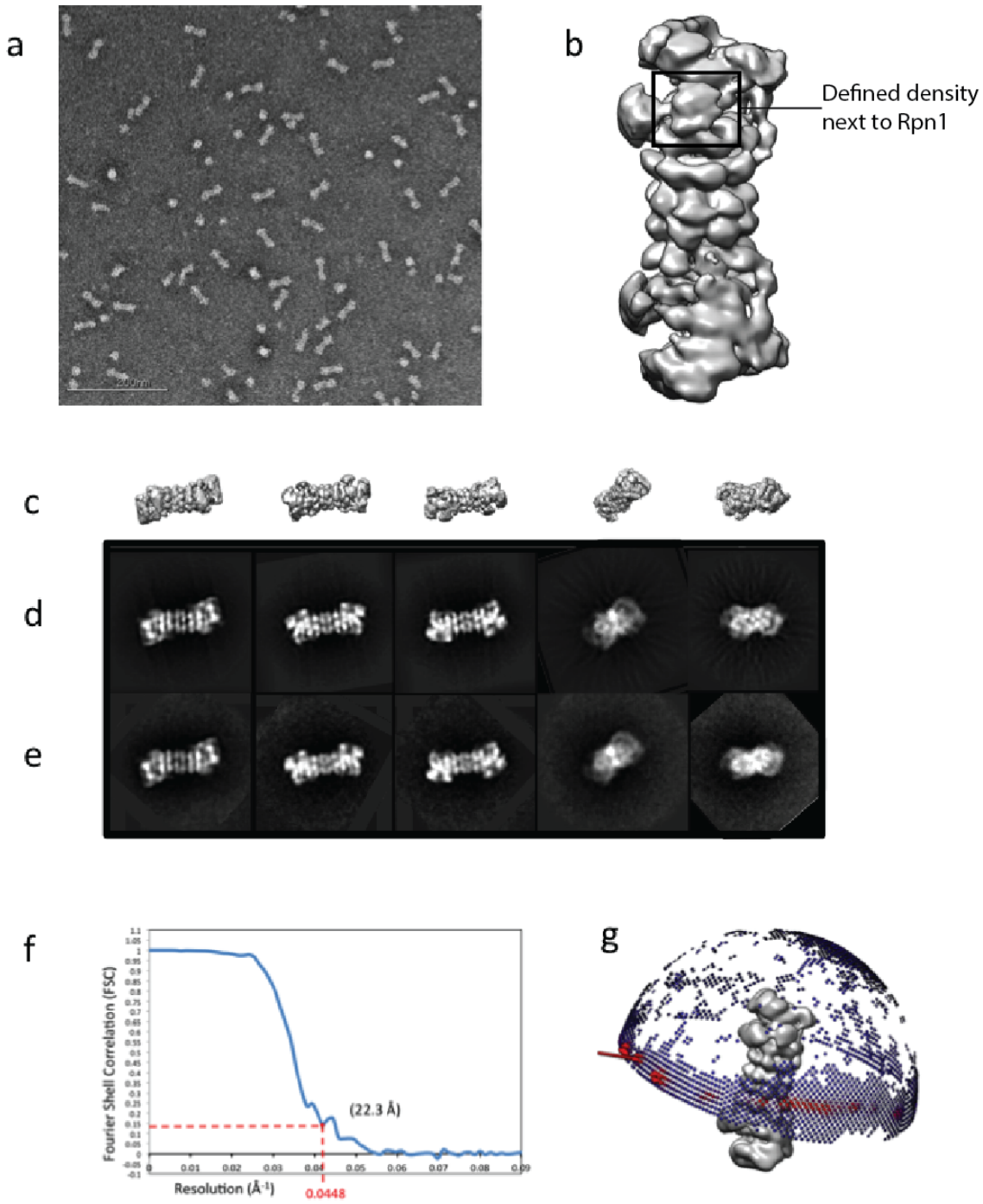

Figure s2.7 Ub-Ubp6 proteasome structure in ATPγS.
(a) raw micrograph of the grids. (b) sharpened reconstruction shows holoenzymes in an engaged conformation, with density for Ubp6 as shown in figure 2.3. (c) Differential projections of the 3D model to match the 2D projections shown. (d) 2D projections calculated from the 3D model. (e) reference-free 2D classes from actual data set. (f) FSC curve. (g) Angular distribution plot (Euler plot)

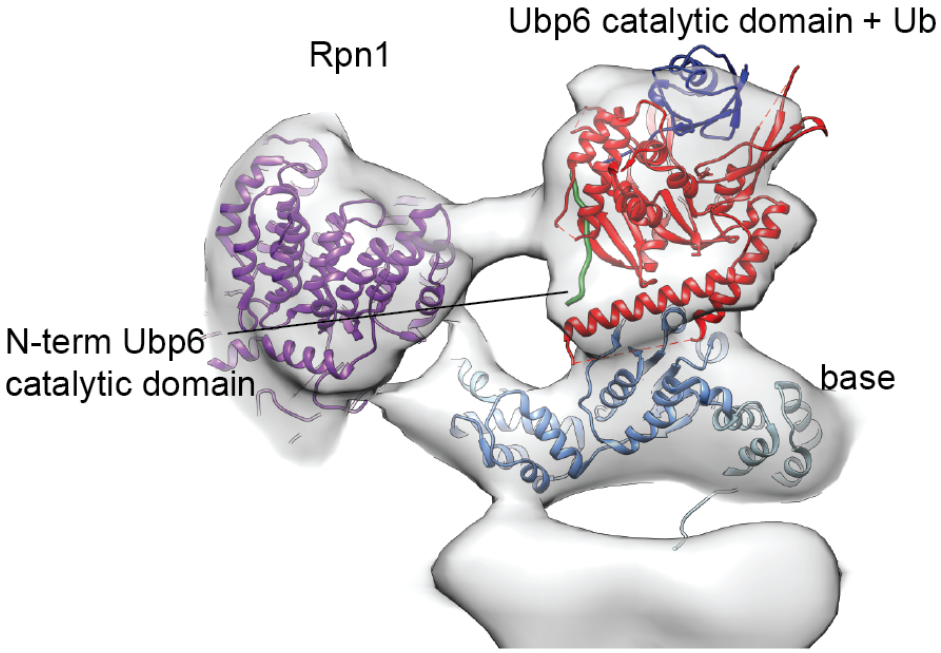

Figure s2.9. Zoomed-in view of docked Ubp6-UbVS model. Docked Ubp6-UbVS model (see methods, PDB 1VJV) in EM density places the N-terminus of the catalytic domain of Ubp6 near the connecting density between Ubp6 (red) and Rpn1 (purple, PDB 4CR4 chain Z). The N-terminal region of the Ubp6 catalytic domain (residues 104 to 114) are shown in green.

Supplementary Figure 10:

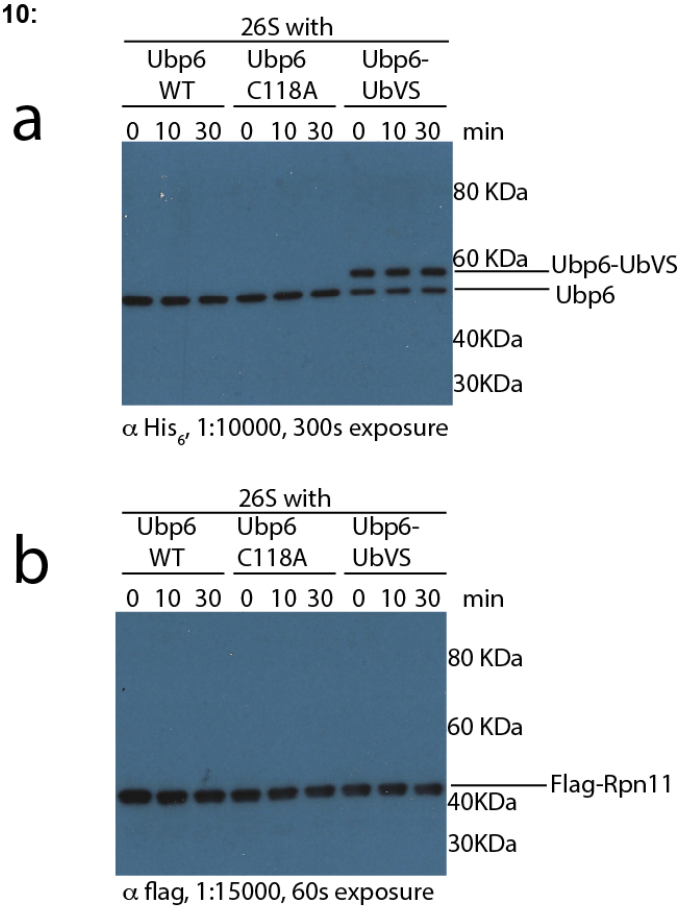

Figure s2.10 Ubp6 is not degraded by the proteasome.
100nM purified holoenzymes lacking Ubp6 were mixed with His_6-tagged WT, C118A or Ub-VS treated WT Ubp6 and incubated at 30˚ C with ATP regeneration system. (a) Ubp6 was visualized by western blot detecting His_6. Holoenzyme levels were detected by blotting against Flag-tagged Rpn11.

Chapter 3

Substrate recognition and processing at the proteasome

Chapter 3

Introduction

Cells depend on regulated protein destruction, both to maintain homeostasis and to drive signaling. The 26S proteasome is the major ATP dependent protease in eukaryotes and is integral to cell survival. As the final destination in the ubiquitin-proteasome system, the proteasome recognizes a wide variety of substrates marked for degradation by a post-translationally added polyubiquitin signal.

The proteasome recognizes polyubiquitin chains that bind to a number of ubiquitin receptors intrinsically or transiently associated with the 26S holoenzyme. Ubiquitin can be conjugated in a variety of lengths and linkages through a complex network of activating, conjugating, and ligating enzymes (Chapter 1). A substrate may also be ubiquitinated on more than one lysine, resulting in multiple chains that the proteasome must process. As many have shown, the proteasome degrades substrates with all types of ubiquitin linkages *in vitro* or *in vivo*,[21,22,37,83] and thus recognizes a highly diverse targeting signal, which is in contrast to its prokaryotic counterparts that recognize discrete amino acid sequence motifs[89,107]. Previous studies indicated that robust proteasome binding requires a minimum of four ubiquitins that have the length to span the distance between the ubiquitin receptor and the pore to the unfoldase[19,22,32]. Polyubiquitin removal is also required for substrate degradation. The proteasomal deubiquitinase Rpn11 performs the requisite isopeptide-bond hydrolysis, cleaving at the base of the chain and allows completion of substrate translocation and unfolding[52,53]. Structural studies show that Rpn11 shifts upon substrate engagement to a position directly over the unfoldase pore, acting as a gatekeeper scanning for isopeptide linkages.[42,68]

Aside from the targeting polyubiquitin chains, proteasomal substrates show a wide range of functional and structural diversity. For example, many cyclin-dependent kinase inhibitors are metastable or intrinsically disordered.[10,108] In contrast, a handful of transcription factors are known to be partially degraded and released to modulate transcription, suggesting that a part of the release signal includes a stable domain the proteasome cannot unfold[67].

These complexities led me to take a substrate-based approach to deconvolute the kinetics and coordination of substrate processing by the 26S proteasome. By developing a substrate ubiquitination and purification system, I can probe degradation *in vitro*. Combining this approach with a FRET-based deubiquitination assay, I was able to dissect the relationship between polypeptide translocation by the base and Rpn11 deubiquitination. Finally, by preparing substrates with defined thermodynamic stability and chain location, I was able to see that unfolding is likely not the rate-limiting step in substrate degradation by the proteasome.

Results

Development of a defined degradation system

I designed a modular substrate that allowed us to define the thermodynamic stability of the folded moiety as well as the lysine placement for ubiquitination (fig 3.1). The N1 domain of the gene-3-protein from bacteriophage fd is an established model protein for protein folding studies. It exhibits a two state folding mechanism and there are numerous characterized mutants with different thermodynamic stabilities available[99]. Moreover, previous studies had shown that the N1 domain had the same unfolding transition when the C-terminal N2 domain of gene-3-protein was unfolded, suggesting that fusing a C-terminal unstructured initiation region to the domain would not affect its foldedness[109]. I selected three N1-domain mutants of varying thermodynamic stabilities and removed all lysine residues. The domain was fused to an unstructured region, which is required for engagement and also contained the recognition motif for ubiquitination machinery. A single lysine was placed at the N-terminus of the protein to yield a single ubiquitin chain that is upstream of the folded domain when considering proteasome degradation starting at the flexible C-terminal tail. A single cysteine residue was also placed N-terminal to the N1 domain to allow fluorescent labeling and tracking of the substrate (fig 3.1a). The substrate was ubiquitinated *in vitro* using purified E1, E2, and E3 enzymes (fig 3.1b). To prevent the potential presence of a ubiquitin modification at the protein N-terminus, thrombin was used to cleave off the N-terminal His_6 tag from the substrate. The substrate N-terminal His_6 tag, E1, and E2 enzymes were captured by paramagnetic nickel particles. This yielded a substrate separated from the ubiquitination machinery with a chain only attached to the single substrate lysine (fig 3.1c,d). Degradation of this substrate could then be monitored by SDS-PAGE, following the fluorescent dye attached to the substrate (fig 3.1e). Quantifying the depletion of ubiquitinated substrate bands allowed for calculation of initial rates of degradation at a given substrate concentration.

This substrate and assay design has several advantages: it allows preparation of polyubiquitinated substrates at μM concentration, and different ubiquitinated species are well resolved by SDS-PAGE. Moreover, in contrast to genetically encoded linear ubiquitin fusions that utilize mutations to prevent hydrolysis during expression, ubiquitinating the substrate *in vitro* yields a native substrate amenable to more meaningful interpretation of deubiquitination kinetics. This system also allows unprecedented control over the location of the ubiquitin chain, ensuring a single location for polyubiquitin attachment.

In spite of these advances, quantifying substrate degradation still faces major challenges. Although ubiquitin placement is well defined, an ubiquitinated substrate still consists of a population of species with different numbers of ubiquitin moieties attached, which likely affects substrate affinities for the proteasome as well as turnover kinetics. The ratios between the species can also vary with each preparation, making consistent analysis difficult. Moreover, the creation and purification of substrates with chains long enough to be efficiently recognized by the proteasome (i.e. chains with at least 4 ubiquitins) is not robust. The chimeric E6AP/Rsp5 ligase makes primarily K-48 linked ubiquitin chains[23], but it can

also make other chain linkages, creating a potential for branched ubiquitin chains and adding extra variability. This heterogeneity poses a substantial challenge to ensuring equivalent ubiquitination, and each substrate preparation had to be carefully examined. Differences in ubiquitination between substrates did strongly influence the observed rate of degradation and deubiquitination (data not shown), complicating the confident interpretation of data. Nonetheless, careful preparations of ubiquitinated substrates have allowed us to better understand how the proteasome coordinates the processing steps of unfolding, translocation, and deubiquitination.

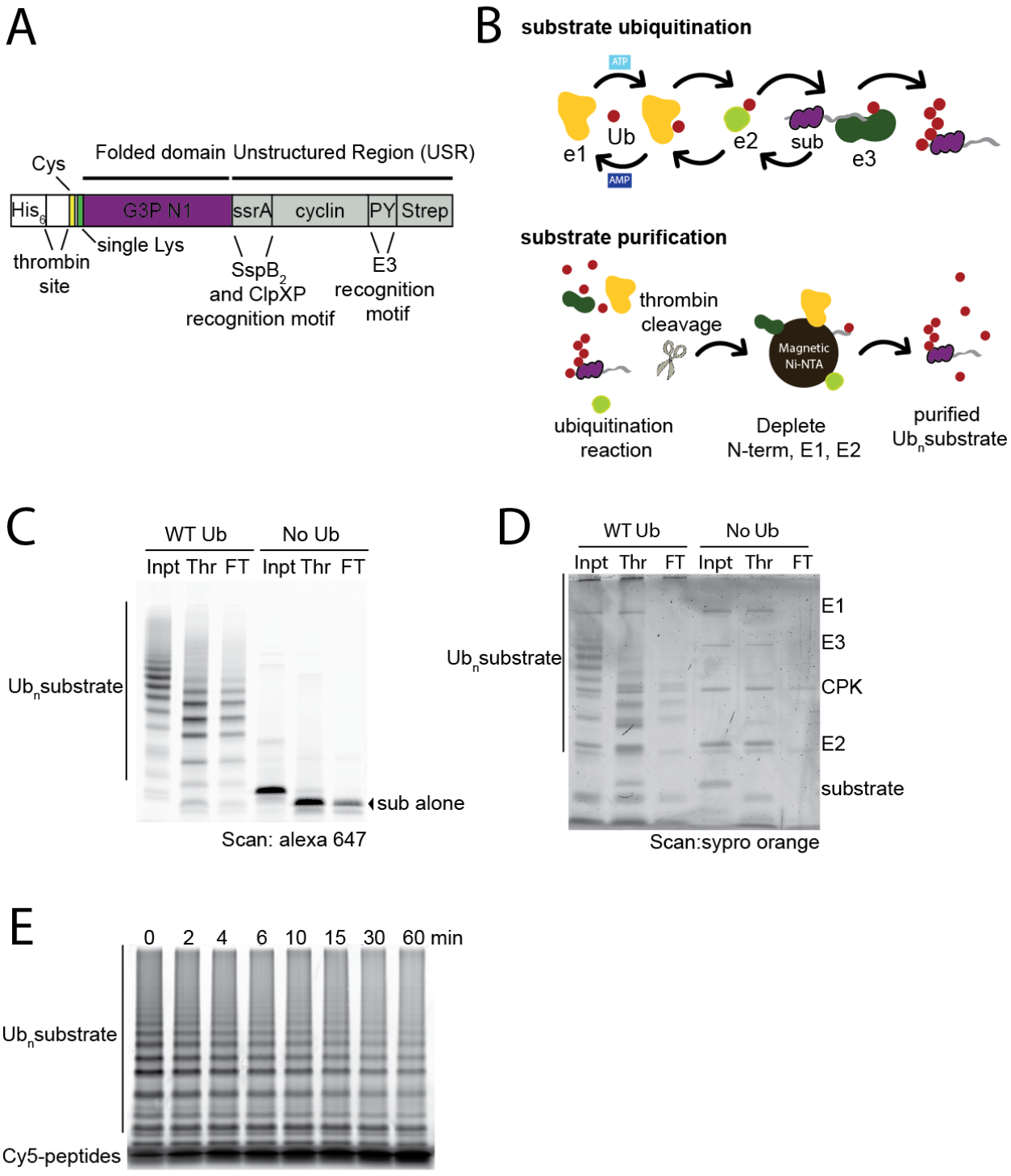

Figure 3.1 Substrate and assay design.
Substrates were designed using the N1 domain from the gene-3-protein from bacteriophage fd. (A) Schematic of substrates containing a single folded domain (purple), a single cysteine for fluorescent labeling, a single lysine for polyubiquitination, an unstructured region (gray), and two affinity tags for purification. (B) Outline of substrate ubiquitination and purification of ubiquitin conjugates. E1 (yellow), E2 (light green), E3 (dark green), ubiquitin (red), ATP, and substrate

(purple/gray) are mixed to create substrates ubiquitinated both on the N-terminus and at a single lysine. The N-terminus is cleaved with thrombin, and ubiquitination components and the N-terminus of the substrate are depleted by incubation of the reaction with paramagnetic nickel particles. (C) Gel showing the separation of the ubiquitinated and thrombin-cleaved substrate detected by Alexa 647 florescence. (D) Sypro-orange stain of the gel in (C) shows a depletion of E1, E2, and E3 from ubiquitinated sample. (E) Representative degradation timecourse. Ubiquitinated substrate was incubated with proteasome holoenzyme and an ATP regeneration system at 30˚C. Disappearance of ubiquitinated species is observed by SDS-PAGE and imaging of the Alexa-647 label on the substrate.

Measuring Deubiquitination

To assay Rpn11 deubiquitination directly, I developed a FRET-based deubiquitination assay (fig 3.2). I introduced a cysteine to the N-terminus of ubiquitin and labeled it with a donor fluorophore (Alexa 555) using maleimide chemistry. Ubiquitinating an acceptor- (Alexa 647) labeled substrate results in FRET between the ubiquitin and the substrate that ceases upon Rpn11 hydrolysis of the isopeptide bond (fig 3.2c). Michaelis-Menten analysis of deubiquitination in multiple-turnover shows a k_{cat} value that is similar to the degradation rate observed for wild-type ubiquitin measured by SDS-PAGE, but an increased K_M, perhaps due to the fluorophore on ubiquitin somewhat interfering with binding to the proteasome receptor (fig 3.2c, fig 3.5c). The higher sensitivity of a fluorescent readout as opposed to SDS-PAGE or western-blot analysis permits measurement of single-turnover kinetics as well as multiple-turnover kinetics, allowing me to witness a single deubiquitination event, instead of a multiple turnover reaction that would read out the rate-limiting step over repeated substrate degradation events. Single-turnover reactions resulted in a double exponential decay of the FRET signal, similar to what was previously seen in the single turnover degradation of ubiquitinated GFP substrates in chapter 2 and in previous work[37] (fig 3.2d). We attribute this behavior to the heterogeneity in polyubiquitin chain length on the substrate. If we assume the k_{slow} and k_{fast} constants represent the processing of substrates with chains of suboptimal or optimal length, the average rate constant for the substrate population would correlate to the V_{max} from multiple-turnover reaction, which we indeed observe (fig 3.2c).

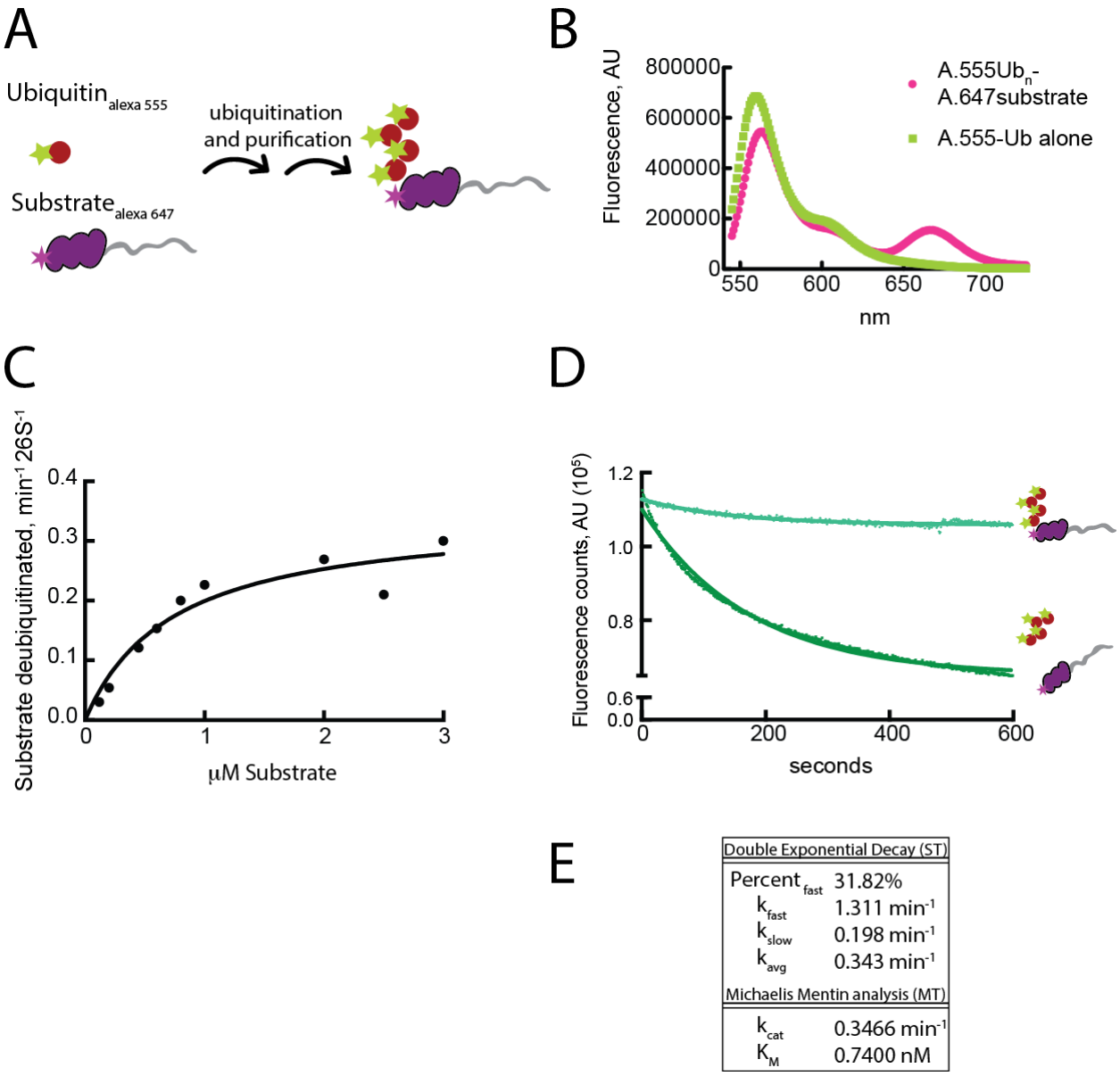

Figure 3.2. Development of a FRET-based deubiquitination assay
(A) Schematic of the doubly labeled ubiquitinated substrate. Alexa 647 labeled substrates (purple, magenta star) are ubiquitinated with N-terminally labeled Alexa 555 ubiquitin (red, green star), allowing FRET between the ubiquitin and substrate. (B) Emission spectra of ubiquitin and ubiquitinated substrate upon excitation at 527nm. Ubiquitin alone shows no emission at 650nm, but ubiquitinated substrate does, demonstrating FRET between ubiquitin and substrate fluorophores. (C) Michaelis-Menten curve of substrate deubiquitination. Substrate deubiquitination in multiple turnover shows a similar V_{max} as the degradation of a substrate with unlabeled ubiquitin (Fig 3.4) but an increased K_M, presumably due to the labeled ubiquitin binding less tightly to the proteasome. (D) Single turnover deubiquitination shows double-exponential loss of signal upon incubation with saturating amounts of holoenzyme. (E)

comparison of the rate constants from (D) with the k_{cat} from (C) show strong kinetic similarities between the two experiments.

Deubiquitination by Rpn11 is translocation dependent

An outstanding question in the field was whether Rpn11 substrate deubiquitination is translocation dependent. Previous studies had suggested Rpn11 activity depended on ATP hydrolysis, connecting translocation of a substrate to Rpn11 deubiquitination[4,52]. Moreover, localization of Rpn11 in substrate-free and translocating conformations show Rpn11 moves right over the pore of the N-Ring where it could feasibly scan for isopeptide bonds as the base translocates the substrate[22,42]. Our single-lysine substrate deubiquitination assay allowed us to investigate this directly (fig 3.3). In the presence of an unstructured region required for engagement the substrate is degraded and deubiquitinated in an exponential manner, however inclusion of ATPγS instead of ATP in the reaction hinders base translocation and results in a loss of exponential decay. To ensure that the other deubiquitinase, Ubp6, did not contribute to loss of FRET, we repeated these experiments with Δ Ubp6 proteasomes, and see the same trend (fig 3.3b). Moreover, a lack of the unstructured engagement region on the ubiquitinated N1-domain substrate also abrogated exponential decay of the FRET signal (fig 3.3b). However, this deletion of the initiation region still resulted in more deubiquitination than when ATPγS was present, which we presume is connected to breathing of the folded domain of the substrate, resulting in an unstructured region that could be engaged and initiate degradation by the proteasome. Indeed, analysis of the reactions by SDS-PAGE shows more products for the degradation of a substrate without an unstructured region in the presence of ATP than for a full-length substrate in the presence of ATPγS (fig 3.3b). These data support a translocation dependent model of Rpn11 deubiquitination as previously suggested. It also agrees with EM structures showing that Rpn11 shifts over the pore in an engaged state, acting as a gatekeeper to remove any isopeptide bonds from translocating substrates. Without active translocation through the pore, Rpn11 does not remove polyubiquitin chains.

Unfolding is not rate limiting for degradation

Our *in-vitro* system gave us the opportunity to assess whether unfolding is rate-limiting in substrate degradation. I first utilized substrates with different variants of the G3P N1 domain, each lacking disulfide bonds and containing a different set of mutations established to give a range of thermodynamic stabilities[99] (fig 3.4a). I removed all lysine residues from each variant and fused them to our substrate backbone (C-terminal unfolded initiation region, N-terminal extension with His tag, single Cys and Lys residues). Thermal denaturation measured by circular dichroism as well as wavelength scans indicated that one was completely unfolded above 25 °C, whereas the other one showed a midpoint for thermal unfolding at 52 °C (data not shown). To assess the stability of these variants against mechanical unfolding by a well-characterized, simpler ATP-dependent protease in the absence of ubiquitin processing, I fused an ssrA tag to the C-terminus and measured degradation by ClpXP. ClpXP has been shown to degrade titin substrates at different rates according to their thermodynamic stabilities[99]. ClpXP degraded the least stable variant at a rate of 4.5 $min^{-1}enzyme^{-1}$, which agrees with the degradation rate for unfolded and

carboxymethylated titin[110] (fig 3.4 b). ClpXP degraded the folded N1 substrate more slowly at a rate of 3 min^{-1}enzyme^{-1}. To minimize any potential effect an ubiquitin chain may have on stability, I placed the lysine adjacent to and upstream of the N1 domain (fig 3.4a). I ubiquitinated and purified the folded and unfolded substrates to assess the role of unfolding in proteasomal degradation by SDS-PAGE. Contrary to the k_{cat} values observed for degradation by ClpXP, both substrates show similar degradation rates with similar Michaelis-Menten kinetics (fig 3.4c-f). This pattern was also observed for ubiquitinated proteasome substrates containing folded and unfolded titin (data not shown). This suggests that unfolding is not rate limiting for proteasomal degradation.

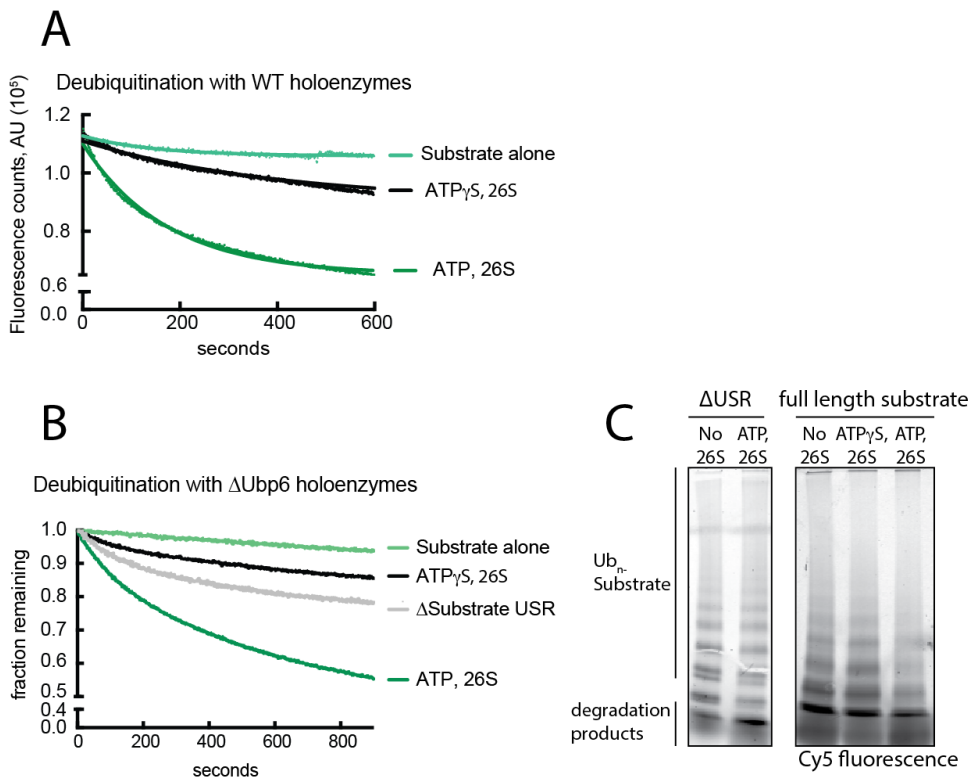

Figure 3.3 Deubiquitination by Rpn11 is translocation dependent
(A) Deubiquitination under single-turnover conditions monitored by FRET signal shows a double-exponential decay in the presence of ATP but not ATPγS. (B) ΔUbp6 holoenzymes show an identical pattern, suggesting that this activity is Rpn11 dependent. Moreover, either stopping translocation with ATPγS or deleting the unstructured region (USR) of the substrate abrogates exponential loss of signal. (C) Representative gel of reactions after degradation shows minimal processing of substrate lacking an unstructured region or substrate incubated with ATPγS.

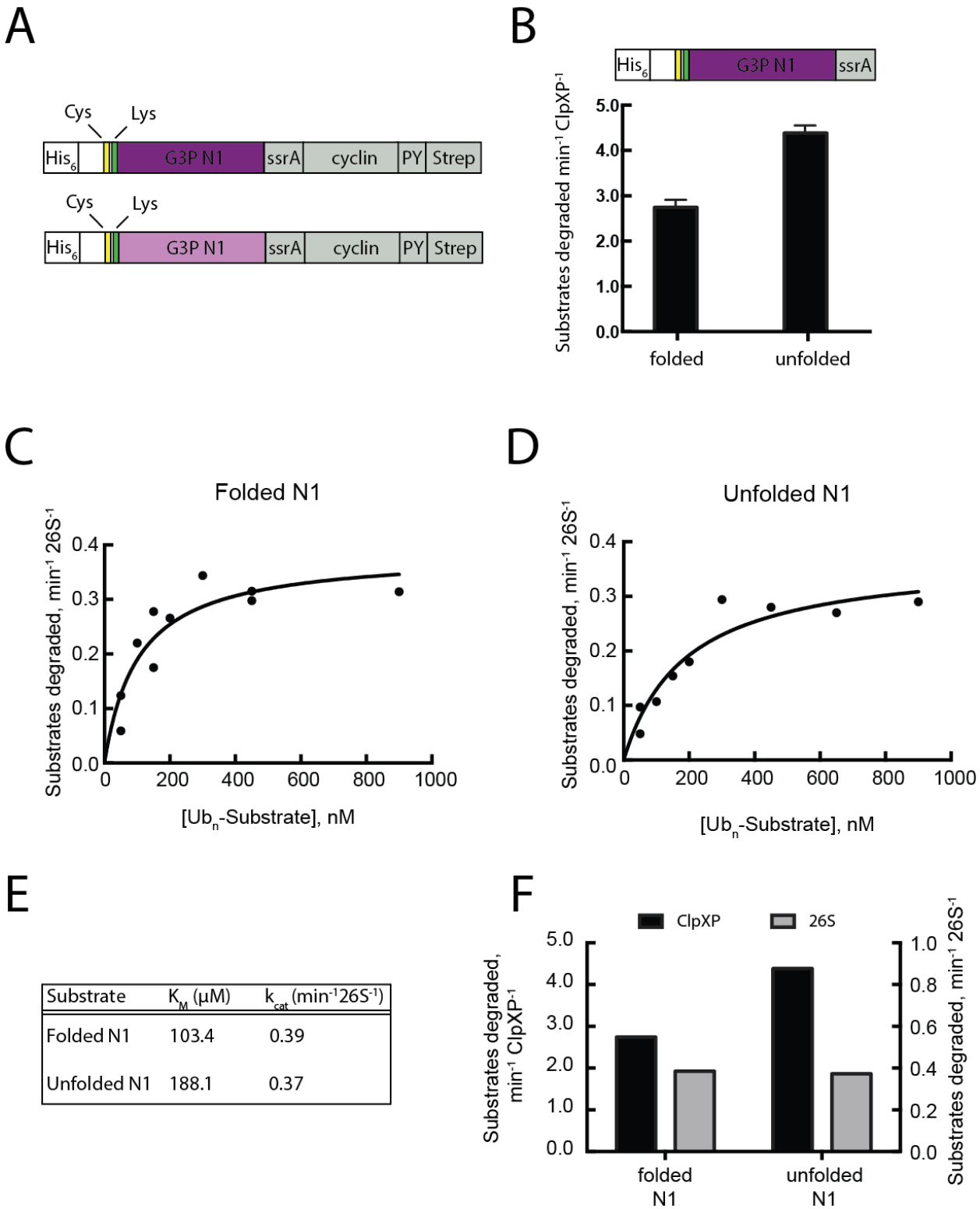

Figure 3.4 Unfolding does not determine degradation kinetics by the proteasome. (A) Schematic showing two substrates with two different N1 domains. (B) ClpXP degradation of the unfolded N1 domain shows a rate comparable to rates for other unfolded substrates of similar lengths, but is significantly slower for the folded N1 domain. (C) and (D) Michaelis-Menten

curves of proteasomal degradation measured by SDS-PAGE shows no significant differences between the folded and unfolded substrates. (E) K_M and k_{cat} from (C) and (D). (F) Comparison of rates for proteasome- and ClpXP-mediated degradation.

Thermodynamic stability of the folded substrate moiety does not affect Rpn11 deubiquitination

To further investigate the impact of unfolding on substrate processing, we turned to our FRET-based deubiquitination assay to examine processing kinetics in single and multiple-turnover, and expanded our N1 domain variants with a third variant that ClpXP degraded more slowly, at a rate of 2 min^{-1}enzyme^{-1} (fig 3.5a, b). Thus the three G3P fusion substrates represented variable degrees of mechanical unfolding that should show a difference in proteasomal degradation if unfolding is rate-limiting. By placing a lysine upstream of the N1 domain we can observe Rpn11-dependent deubiquitination after N1 unfolding, both under single- and multiple turnover conditions. Since Rpn11 activity is translocation dependent, any change in substrate translocation rate due to unfolding would affect the kinetics of Rpn11 cleavage. Moreover, since we confirmed by SDS-PAGE that these substrates show no release of deubiquitinated or partially degraded products, we surmise that deubiquitination is a valid proxy for degradation. Michaelis-Menten curves reveal very similar behavior for all three substrates in multiple turnover degradation (fig 3.5 b,c). Moreover, all three substrates show identical single turnover curves (fig 3.5 d). This result indicates that for these model substrates unfolding has no impact on degradation rate, and that some other processing step dictates the rate of degradation.

Is deubiquitination rate limiting?

To separate the effects of polyubiquitin processing from the other substrate degradation steps, we developed an ubiquitin-independent recruitment system (Chapter 2). We fused a permutant of the dimeric substrate adaptor $SspB_2$ from *E. coli* to the base unfoldase (fig 2.2). In *E. coli*, SspB2 delivers ssrA-tagged substrates to the ClpXP protease. Its fusion to the base allowed us to deliver ssrA-tagged model substrates to the proteasome and observe proteasomal degradation independent of polyubiquitin. We compared degradation of the unfolded N1 fusion substrate and a folded, single-lysine GFP fusion substrate in ubiquitin-independent and ubiquitin-dependent degradation (fig 3.5e). The ubiquitin independent system degraded both substrates more quickly than the ubiquitin dependent system. This finding suggests that deubiquitination is rate limiting, since it is unlikely that an artificially engineered recruitment system improves substrate engagement over a naturally evolved recruitment system.

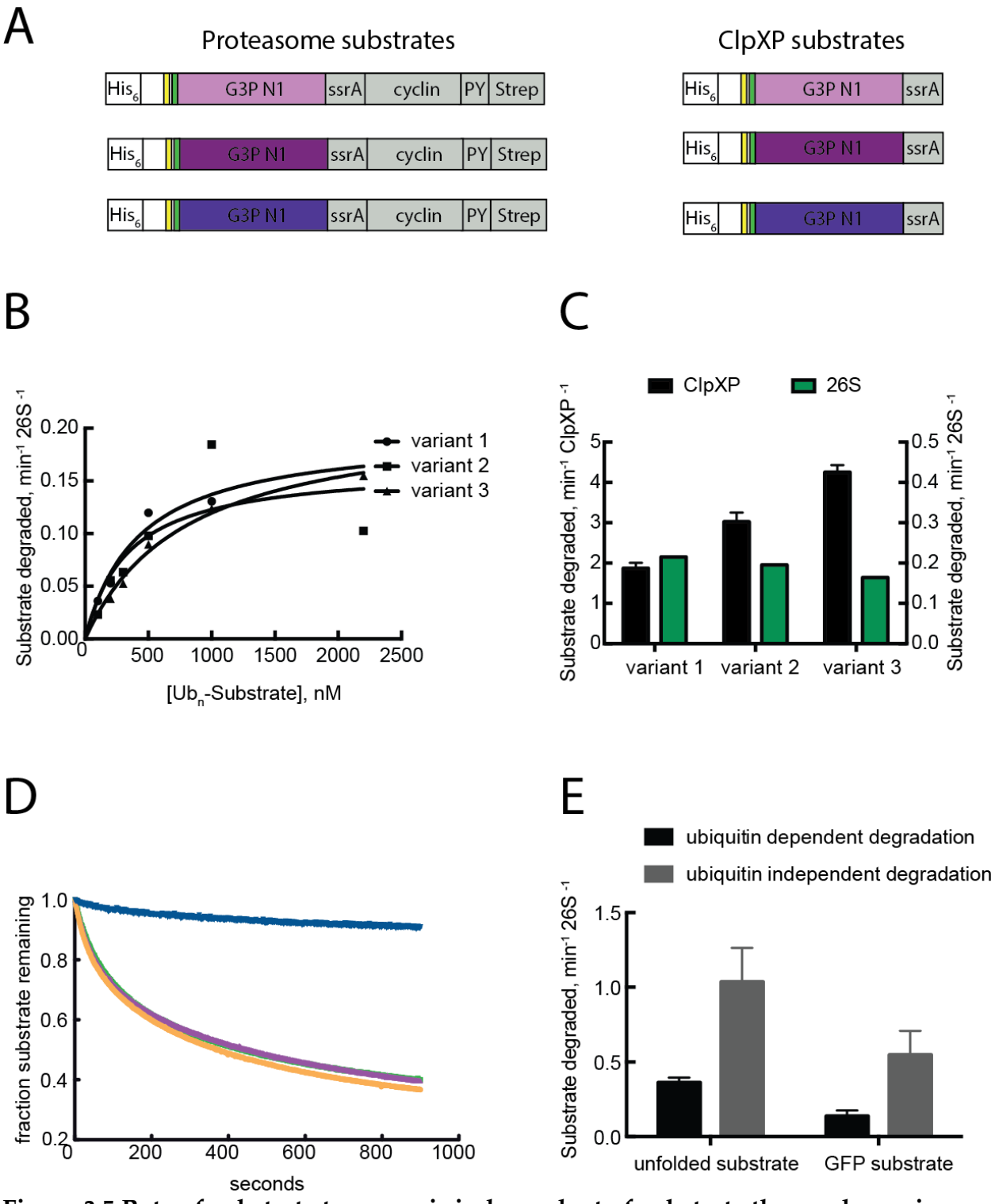

Figure 3.5 Rate of substrate turnover is independent of substrate thermodynamic stability. (A) Design of substrates to compare degradation by the 26S proteasome and ClpXP. (B) Michaelis-Menten analyses of ubiquitinated substrates by FRET shows that the three different N1 variants are turned over similarly. (C) ClpXP degradation rate compared to rates for deubiquitination and degradation by the proteasome indicate that ClpXP degrades the three

variants with different kinetics, whereas the proteasome processes them at similar speeds. (D) Single-turnover deubiquitination of substrates. Since the ubiquitin chain is upstream of the folded domain and deubiquitination by Rpn11 is translocation dependent, the identical traces of the three variant reactions suggests that substrate turnover by the proteasome is not rate limiting. (E) Degradation of polyubiquitinated substrates by the proteasome is slower than degradation of substrate using proteasomes with the ubiquitin-independent artificial recruitment system introduced in Chapter 2, suggesting that ubiquitin processing is rate limiting.

Discussion

To dissect the impact of different substrate characteristics on proteasomal degradation, we developed a substrate design that allows careful modulation of different input parameters. Moreover, we were able to ubiquitinate the substrate using a native ubiquitination machinery instead of relying on linear fusions, and we were able to separate the ubiquitination components from the substrate to ensure there is no re-ubiquitination in the degradation reaction. This approach results in a substrate with a single ubiquitin chain in a defined location relative to the degradation initiation sequence and the folded domains. However, *in vitro* ubiquitination results in a population of ubiquitinated substrates with variable numbers of linked ubiquitin moieties. This heterogeneity makes it difficult to ensure similar extent of ubiquitination, similar degradability, and proteasome affinity for different substrate preparations and thus complicates the interpretation of results. Nonetheless, we were able to discover novel findings regarding the connection between different processing steps in proteasomal degradation.

Here we show biochemically that deubiquitination by Rpn11 is coupled to the translocation of a substrate. Preventing conformational changes of the base unfoldase by using non-hydrolyzable ATPγS or preventing substrate engagement by deleting the unstructured initiation region resulted in loss of deubiquitination by Rpn11. EM structures of substrate-translocating proteasomes show Rpn11 poised directly above the entrance to the N-ring of the unfoldase. This allows the DUB to scan for any isopeptide bonds on the substrate in order to remove ubiquitin. It also means that substrate translocation into the central pore delivers the isopeptide bond directly to the active site of Rpn11. Biochemical investigation of Rpn11 activity reports a maximal isopeptide cleavage rate for the model substrate ubiquitin -lysine-TAMRA at ~1min^{-1}, which is faster than rates reported here, but close to degradation rates others have reported for various substrates[42,55].

Interestingly, unfolding was not rate limiting for the substrates we assayed. This is in contrast to other ATP-dependent unfoldases, like the motor ClpXP, that do not have the extra burden of removing targeting signals like polyubiquitin from their substrates[110,111]. Moreover, degradation rates by the proteasome were markedly slower than those for ClpXP, potentially suggesting a different rate-limiting step unique to substrate processing at the proteasome. Engagement of the unstructured region or removal of polyubiquitin could instead be rate limiting. Without a method to concretely probe engagement, which happens after initial ubiquitin binding but prior to every other processing step in proteasomal degradation, it is difficult to definitely determine if deubiquitination or engagement is rate

limiting. Although the artificial recruitment system shows faster rates than those for native proteasomes, it is possible that the polyubiquitin chains attached to our model substrates are not ideal to properly position the substrates for engagement by the ATPase ring. Moreover, it is possible that the rate-limiting step in degradation differs from substrate to substrate. Our results do, however, allow us to speculate on the cellular ramifications of either deubiquitination or engagement being rate limiting.

There are instances when unfolding is known to play a role in determining the degradation of substrates. A handful of proteins have been identified to be specifically partially degraded and released. This partial degradation gives altered activity to the substrate, resulting in a change in cellular function. Work from the lab of Andreas Matouschek has shown that a combination of a stably folded domain and a glycine-rich 'slippery sequence' is necessary for release of substrate from the proteasome. However, without a comprehensive understanding of the mechanical stability of proteasome substrates, these few examples of partial degradation would suggest that the rate of unfolding affects substrate turnover by the 26S proteasome.

Structure-function studies of Rpn11 have shown that it is a promiscuous DUB that can cleave any linkage type of ubiquitin[55]. However, its placement right above the ATPase hexamer in the assembled proteasome also means that near the active site there is only room for an unfolded polypeptide linked to the C-terminus of ubiquitin, which agrees with the translocation-dependence for Rpn11 activity in the holoenzyme. However it would be interesting if Rpn11 cleavage were rate limiting, since we know substrates can have multiple ubiquitin chains, requiring multiple cleavage events. Moreover other proteasomal factors, like the deubiquitinase Ubp6, can affect the activity of Rpn11, which would provide an opportunity for an additional layer of regulation in proteasomal degradation.

Substrate translocation begins with a step we define as engagement, which happens once the unstructured region of the substrate contacts the pore loops of the base. While difficult to measure, some studies have suggested that engagement can be rate limiting. Work from Andreas Matouschek's lab has shown that substrates with "slippery" sequences consisting of repetitive amino-acid sequences at the initiation region affect substrate degradation, presumably by hindering engagement and translocation by the base[18]. Preliminary data from a translocation assay in our lab, using unfolded titin I27-domain concatamers, suggest that engagement may be rate-limiting (Beckwith, unpublished). Although some proteasomal substrates have been shown to have regions of intrinsic disorder, the presence of an initiation region for all *in vivo* substrates has not been demonstrated. It has been speculated that upstream processing complexes, for example the AAA+ Cdc48, use ATP hydrolysis to create the requisite unstructured initiation region for substrate engagement by the proteasome. This extra layer of signaling would allow regulation of cellular degradation dependent on p97 as well as the proteasome. There may also be differential degradation rates by the proteasome depending on the placement, length, and sequence of the unstructured region generated by p97. The lack of an initiation region also protects

proteasome-associated cofactors from degradation, as they prevent substrate entry to the pore and subsequent engagement by the AAA+ motor [64].

Methods and Materials

Yeast strains

Yeast holoenzyme, lid, and core were purified from the strains listed in chapter 2.

Recombinant base purification

Base was purified as described in chapter 2.

Holoenzyme and subcomplex purification

All proteasome complexes were purified as described in chapter 2.

GFP degradation

GFP degradation was assayed by measuring GFP fluorescence as described in Chapter 2.

Expression and purification of N1 fusion substrates

N1 fusion substrates were cloned into pet28a vectors with an N-termianl His_6 tag and a C-terminal lysineless Strep II tag. BLR DE3 cells were transformed with constructs and grown at 37 ˚C until an OD_{600} of 0.6-1.0. Expression was induced at 18˚C overnight with 0.4mM IPTG. Cells were harvested and resuspended in lysis buffer, (60mM HEPES 8.0, 150mM NaCl, 150mM KCl, 10% Glycerol) supplemented by protease inhibitors, lysozyme, and benzonase (see Chapter 2). Cells were thawed by freeze-thaw and sonication before clarifying lysate by centrifugation. Substrates were purified using tandem Ni-NTA/Strep affinity chromatography followed by size-exclusion chromatography on a Superdex 200 (GE) in substrate gel filtration buffer (60mM Hepes 7.6, 50mM NaCl, 50mM KCl, 5% glycerol, 1mM DTT).

Substrates were labeled using a 5x molar excess of Alexa 647 (Life Technologies) or Cy5 (GE) maleimide dyes. Substrates were exchanged into labeling buffer (PBS, pH 7.2) prior to labeling. Reactions proceeded in the dark at room temperature for 3 hours, and then run over a Superdex 75 (GE) column to remove any aggregate and free dye.

Purification and labeling of ubiquitin

Ubiquitin was purified according to published protocols. Ubiquitin containing an N-terminal cysteine was labeled with Alexa 555 dye and run over a Superdex 75 using the same conditions and protocol as for substrate.

Ubiquitination of substrates

Purified Uba1, Ubc1, and chimeric ligase were purified according to published protocols. 20μM substrate was ubiquitinated with 5μM E1, E2, and E3 enzymes, with 500μM WT ubiquitin or 700μM Alexa-555 Ubiquitin in the presence of 1X ATP regeneration system (chapter 2). Reactions proceeded for 4 hours at 25 ˚C, and were never frozen. After

ubiquitination, 1μL of 4 U/mL Thrombin (Roche) was added to the mixture for 5 min at RT. 40μL of paramagnetic Ni particles (Promega) were washed into pulldown buffer (60mM HEPES, 7.6, 50mM NaCl, 50mM KCl, 5% glycerol, 0.05% tergitol (Sigma)) and was added to 20μL substrate ubiquitination reaction. Mixture was mixed by tapping at RT for 5 minutes before isolating flow through from the beads. Concentration was determined using absorbance$_{650}$ of Alexa 647 or Cy5 and predetermined labeling efficiency of substrate. Prior to degradation, substrate ubiquitination was assessed by SDS-PAGE and imaging on a Typhoon-Trio (GE).

FRET based DUB assay conditions

Deubiquitination of substrates was assayed by measuring loss of signal at 650nm upon excitation at 527nm, at 30˚C in a PTI fluorimeter (see chapter 2). Reactions were done in holoenzyme GF buffer (see chapter 2) with 1X ATP regeneration system or 1mM ATPγS. Reactions were incubated at 30˚C for 10 minutes prior to the addition of substrate.

Quantitation of gels for SDS-PAGE analysis

Ubiquitinated substrates were mixed with 60nM holoenzyme at various concentrations to determine Michaelis-Menten kinetics. Reactions contained 0.2mg/mL Cy-3 BSA as a loading control, and were performed in holoenzyme GF buffer with 1X ATP regeneration system. Timepoints were taken every 2 minutes, and run on a 12% Nu-PAGE SDS-PAGE gel in MOPS running buffer. Gels were imaged on a Typhoon Trio, and bands were quantified using Image-Quant software by using the line function to generate a graph and integrating under peaks to determine area.

Chapter 4

Conclusions

4. Conclusions

Summary

This work investigates two distinct modulators of proteasome function. First I showed that Ubp6 deubiquitination strongly responds to interactions with the base ATPase and the conformational state of the proteasome. Electron-microscopy studies revealed that ubiquitin-bound Ubp6 contacts the N-ring and AAA+ ring of the ATPase hexamer, placing it in close proximity to the deubiquitinase Rpn11. In complex with ubiquitin, Ubp6 inhibits substrate deubiquitination by Rpn11, stabilizes the substrate-engaged conformation of the proteasome, and allosterically interferes with the engagement of a subsequent substrate. Ubp6 may thus act as an ubiquitin-dependent timer to coordinate individual processing steps at the proteasome and modulate substrate degradation.

Secondly, although the mechanism of substrate proteolysis has been well characterized, little was known about how the processing steps prior to degradation culminate to give an overall degradation rate. The complexity of substrate processing and the requisite of proteasome function for cell viability pose a significant challenge to quantitative analysis. The *in vitro* system I developed to prepare defined proteasomal substrates and the assays I designed allowed me to determine the rates of degradation and deubiquitination for a given substrate input. I used these tools to show that deubiquitination by Rpn11depends on translocation of the substrate polypeptide by the ATPase. Moreover I also observed that unlike prokaryotic ATP dependent protease ClpXP, unfolding is not rate limiting in degradation by the proteasome. Overall these studies reflect how the complex 26S proteasome functions to degrade such a diversity of substrates and is integral to the cell. Nonetheless, many questions about the 26S proteasome remain for future study.

Why is the 26S proteasome so slow?

Degradation by the proteasome is much slower than substrate turnover by other ATP dependent proteases. Even with the faster, ubiquitin-independent degradation reactions, the proteasome turns over substrates on the order of 1 $min^{-1}enzyme^{-1}$, which is almost five-fold slower than degradation of the same substrate by ClpXP. In comparison to its prokaryotic counterparts, the proteasome is a much more tightly regulated protease that is involved in a far wider range of cellular activities, and therefore it is possible that the slow turnover rate is the consequence of intense regulation. However, the slow rate of proteasomal degradation is not only slow for enzymes in general, but perplexing given that there are signaling events, like the transition from metaphase to anaphase in cell division, that are dependent on proteasomal degradation and that occur on a minute timescale. Moreover, given reports that there are ten-fold more ribosomes than proteasomes in both yeast and mammalian cells and that 1-5% of synthesized nascent chains are either incompletely translated or do not fold properly and are therefore marked for degradation, the proteasome would already be occupied with these substrates even in the absence of cell signaling or stress[112-113,114]. However, Asano *et al.* recently observed in the cell bodies of neurons that the majority of proteasomes were not actively degrading substrates and were in an apo conformation[70]. The

simplest explanation for this discrepancy is that *in vivo* degradation rates are faster due to accessory factors or environmental conditions lost in the purification process, but so far no one in the field has been able to identify other associated proteins that result in a higher *in vitro* degradation rate. *In vitro* degradations with high concentrations of BSA had no effect on the proteasome degradation rate (data not shown), suggesting that molecular crowding is likely not a factor in accelerating protein turnover.

Another explanation is that substrate delivery to the proteasome *in vivo* is much more efficient, resulting in faster turnover rates in the cell. In ER-associated degradation (ERAD) misfolded polypeptides are extracted out of the ER and targeted to the proteasome for degradation. It is thought that the remodeling motor Cdc48 and its associated cofactors facilitate efficient delivery of polypeptides from the ER to the proteasome. Tomography studies in whole cells show extra electron density at substrate-processing neurons that is larger than the average proteasomal substrate, and these factors may not necessarily speed up the proteasome degradation itself, but rather mediate the efficient delivery of polyubiquitinated substrates to the proteasomal ubiquitin receptors. A number of ubiquitin conjugating and ligating enzymes, including the anaphase promoting complex/cyclosome, are reported to associate with the proteasome, suggesting coordinated substrate ubiquitination and degradation[115-118]. Proteasomes have also been observed to co-migrate with translating ribosomes in sucrose gradients, suggesting recruitment of the proteasome to misfolded polypeptide chains that are marked for degradation by ribosome-associated ubiquitin ligases[114].

It is also possible that the observed *in vitro* degradation rates are physiologically relevant, and overall high substrate turnover is accomplished through high concentrations of proteasome during degradation-dependent signaling events. Proteasome concentrations measured in the nucleus, for example, are reported in the high nM range[119]. Park *et al.* suggested that the polyQ regions of mutant variations of the hungtintin drive aggregation stress in the cell by preventing interaction with chaperone sis1p, which imports misfolded proteins into the nucleus for enhanced degradation by concentrated proteasomes[120]. Proteasomes also migrate into the nucleus during mitosis, which would increase their local concentrations near cell-cycle substrates. A high concentration of proteasomes could suggest that a single round of substrate degradation might be sufficient to induce the signaling change. It would be interesting to take a systems-based approach and computationally model cell signaling at specific established signaling events, such as the transition out of metaphase to anaphase. Modeling of securin degradation could give an idea as to how a given proteasome degradation rate would affect the switch-like signaling needed for efficient separation of sister chromatids.

Conformational dynamics and substrate degradation

Structural studies from multiple labs depict distinct proteasomal conformations, both *in vitro* and in cells[42,68-70]. In chapter 2, I show using biochemical approaches that trapping the engaged conformation using ubiquitin-bound Ubp6 state results in failure to degrade more than one substrate, suggesting that both the substrate free and substrate translocating states

are required for processive and repeated substrate turnover. However, it remains to be seen if other proteasome conformations are important for substrate degradation, and how dynamic is the transitions between these states in a single round of protein degradation. More structural and biochemical studies, as well as single-molecule measurements of the proteasome will lend insight to these questions.

Effect of lysine placement on degradation rate and processivity

The number and positioning of modified lysines could have a major impact on the kinetics of substrate degradation in the cell. Mass spectrometry studies have identified ubiquitination sites on proteins that are stabilized upon proteasome inhibition and show that most substrates contain multiple modified lysines[121]. Single-molecule studies of cyclin-B variants revealed that eliminating different lysines in cyclin B has differential effects on turnover rates.[122]cc The placement of the ubiquitin chain could influence the binding to receptors and the substrate arrangement on the 19S regulatory particle, which may affect the engagement of the initiation region. Moreover, if deubiquitination by Rpn11 were rate-limiting, the number of isopeptide bonds that need to be cleaved prior to complete substrate translocation would also have a major impact on the degradation rate. The orientation and number of chains attached to a substrate docked on the proteasome could also affect Ubp6 as it trims polyubiquitin. If ubiquitin binding to Ubp6 affects Rpn11 affect, the coordination of dismantling multiple chains could prove to be an added layer of modulation in substrate degradation.

Regulating ordered protein degradation

Aside from its crucial role in proteome quality control, the proteasome mediates the ordered degradation of proteins to drive signaling processes. A complex network of phosphorylation and ubiquitination pathways coordinate the tagging of substrates for proteasomal degradation to ensure properly timed degradation. However, given the proteasome's role in multiple signaling pathways and cellular housekeeping, it remains to be seen whether the substrate affinities and therefore the order or the kinetics of proteasome processing differ between signaling events and quality control. It will be interesting and important to elucidate if the proteasome processed substrates differently based on the nature of the polyubiquitin targeting signal and the unstructured region, both of which may vary depending on the involved pathways.

References

1. Finley, D. Recognition and Processing of Ubiquitin-Protein Conjugates by the Proteasome. *Annu. Rev. Biochem.* **78,** 477–513 (2009).
2. Goldberg, A. L. Protein degradation and protection against misfolded or damaged proteins. *Nature* **426,** 895–899 (2003).
3. Goldberg, A. L. Functions of the proteasome: from protein degradation and immune surveillance to cancer therapy. *Biochem. Soc. Trans.* **35,** 12–17 (2007).
4. Verma, R., Oania, R. S., Kolawa, N. J. & Deshaies, R. J. Cdc48/p97 promotes degradation of aberrant nascent polypeptides bound to the ribosome. *eLife* **2,** e00308 (2013).
5. Wolff, S., Weissman, J. S. & Dillin, A. Differential scales of protein quality control. *Cell* **157,** 52–64 (2014).
6. Hampton, R. Y. *ER-associated degradation in protein quality control and cellular regulation*. **14,** 476–482 (2002).
7. Shcherbik, N. & Haines, D. S. Cdc48pNpl4p/Ufd1p Binds and Segregates Membrane-Anchored/Tethered Complexes via a Polyubiquitin Signal Present on the Anchors. *Mol. Cell* **25,** 385–397 (2007).
8. Spokoini, R. *et al*. Confinement to organelle-associated inclusion structures mediates asymmetric inheritance of aggregated protein in budding yeast. *Cell reports* **2,** 738–747 (2012).
9. Kaganovich, D., Kopito, R. & Frydman, J. Misfolded proteins partition between two distinct quality control compartments. *Nature* **454,** 1088–1095 (2008).
10. Ng, A. H. M., Fang, N. N., Comyn, S. A., Gsponer, J. O. R. & Mayor, T. System-wide analysis reveals intrinsically disordered proteins are prone to ubiquitylation after misfolding stress. *Mol. Cell. Proteomics* **12,** 2456–2467 (2013).
11. Brandman, O. *et al*. A ribosome-bound quality control complex triggers degradation of nascent peptides and signals translation stress. *Cell* **151,** 1042–1054 (2012).
12. Shen, P. S. *et al*. elongation of nascent chains. *Science* **347,** 75–78 (2015).
13. Rosenbaum, J. C. *et al*. Disorder targets misorder in nuclear quality control degradation: a disordered ubiquitin ligase directly recognizes its misfolded substrates. *Mol. Cell* **41,** 93–106 (2011).
14. Bloom, J. & Cross, F. R. Multiple levels of cyclin specificity in cell-cycle control. *Nature reviews. Molecular cell biology* **8,** 149–160 (2007).
15. Morgan, D. O. SnapShot: cell-cycle regulators I. *Cell* **135,** 764–764.e1 (2008).
16. Watanabe, Y. Shugoshin: guardian spirit at the centromere. *Curr. Op. Cell Biol.* **17,** 590–595 (2005).
17. Matyskiela, M. E., Rodrigo-Brenni, M. C. & Morgan, D. O. Mechanisms of ubiquitin transfer by the anaphase-promoting complex. *Journal of biology* **8,** 92 (2009).
18. Tian, L., Holmgren, R. A. & Matouschek, A. A conserved processing mechanism regulates the activity of transcription factors Cubitus interruptus and NF-kappaB. *Nat. Struct. Mol. Biol.* **12,** 1045–1053 (2005).
19. Thrower, J. S., Hoffman, L., Rechsteiner, M. & Pickart, C. M. Recognition of the polyubiquitin proteolytic signal. *EMBO J.* **19,** 94–102 (2000).
20. Ye, Y. *et al*. Ubiquitin chain conformation regulates recognition and activity of

interacting proteins. *Nature* **492,** 266–270 (2012).
21. Xu, P. *et al*. Quantitative proteomics reveals the function of unconventional ubiquitin chains in proteasomal degradation. *Cell* **137,** 133–145 (2009).
22. Lander, G. C. *et al*. Complete subunit architecture of the proteasome regulatory particle. *Nature* **482,** 186–191 (2012).
23. Kim, H. C. & Huibregtse, J. M. Polyubiquitination by HECT E3s and the determinants of chain type specificity. *Mol. Cell. Biol.* **29,** 3307–3318 (2009).
24. Deshaies, R. J. & Joazeiro, C. A. P. RING domain E3 ubiquitin ligases. *Annu. Rev. Biochem.* **78,** 399–434 (2009).
25. Matyskiela, M. E. & Martin, A. Design principles of a universal protein degradation machine. *J. Mol. Biol.* **425,** 199–213 (2013).
26. Marques, A. O. N. J., Palanimurugan, R., Matias, A. C., Ramos, P. C. & Dohmen, R. J. U. R. Catalytic mechanism and assembly of the proteasome. *Chemical reviews* **109,** 1509–1536 (2009).
27. Heinemeyer, W., Fischer, M., Krimmer, T., Stachon, U. & Wolf, D. H. The active sites of the eukaryotic 20 S proteasome and their involvement in subunit precursor processing. *J. Biol. Chem.* **272,** 25200–25209 (1997).
28. Smith, D. M. *et al*. Docking of the proteasomal ATPases' carboxyl termini in the 20S proteasome's alpha ring opens the gate for substrate entry. *Mol. Cell* **27,** 731–744 (2007).
29. Orlowski, M. & Wilk, S. Catalytic activities of the 20 S proteasome, a multicatalytic proteinase complex. *Archives of biochemistry and biophysics* **383,** 1–16 (2000).
30. Kim, T., Hofmann, K., Arnim, von, A. G. & Chamovitz, D. A. PCI complexes: pretty complex interactions in diverse signaling pathways. *Trends in plant science* **6,** 379–386 (2001).
31. Lingaraju, G. M. *et al*. Crystal structure of the human COP9 signalosome. *Nature* (2014). doi:10.1038/nature13566
32. Beck, F. *et al*. Near-atomic resolution structural model of the yeast 26S proteasome. *Proc. Natl. Acad. Sci. USA* **109,** 14870–14875 (2012).
33. Estrin, E., Lopez-Blanco, J. E. R. O. N., Chac o n, P. & Martin, A. Formation of an intricate helical bundle dictates the assembly of the 26S proteasome lid. *Structure* **21,** 1624–1635 (2013).
34. Tomko, R. J., Funakoshi, M., Schneider, K., Wang, J. & Hochstrasser, M. Heterohexameric ring arrangement of the eukaryotic proteasomal ATPases: implications for proteasome structure and assembly. *Mol. Cell* **38,** 393–403 (2010).
35. Augustin, S. *et al*. An intersubunit signaling network coordinates ATP hydrolysis by m-AAA proteases. *Mol. Cell* **35,** 574–585 (2009).
36. Gardner, B. M., Chowdhury, S., Lander, G. C. & Martin, A. The Pex1/Pex6 complex is a heterohexameric AAA+ motor with alternating and highly coordinated subunits. *J. Mol. Biol.* **427,** 1375–1388 (2015).
37. Beckwith, R., Estrin, E., Worden, E. J. & Martin, A. Reconstitution of the 26S proteasome reveals functional asymmetries in its AAA+ unfoldase. *Nat. Struct. Mol. Biol.* **20,** 1164–1172 (2013).
38. Lam, Y. A., Lawson, T. G., Velayutham, M., Zweier, J. L. & Pickart, C. M. A proteasomal ATPase subunit recognizes the polyubiquitin degradation signal. *Nature* **416,** 763–767 (2002).

39. He, J. *et al*. The structure of the 26S proteasome subunit Rpn2 reveals its PC repeat domain as a closed toroid of two concentric α-helical rings. *Structure* **20,** 513–521 (2012).
40. Rosenzweig, R., Bronner, V., Zhang, D., Fushman, D. & Glickman, M. H. Rpn1 and Rpn2 coordinate ubiquitin processing factors at proteasome. *J. Biol. Chem.* **287,** 14659–14671 (2012).
41. Elsasser, S. *et al*. Proteasome subunit Rpn1 binds ubiquitin-like protein domains. *Nat. Cell Biol.* **4,** 725–730 (2002).
42. Matyskiela, M. E., Lander, G. C. & Martin, A. Conformational switching of the 26S proteasome enables substrate degradation. *Nat. Struct. Mol. Biol.* **20,** 781–788 (2013).
43. Kusmierczyk, A. R., Kunjappu, M. J., Kim, R. Y. & Hochstrasser, M. A conserved 20S proteasome assembly factor requires a C-terminal HbYX motif for proteasomal precursor binding. *Nat. Struct. Mol. Biol.* **18,** 622–629 (2011).
44. Riedinger, C. *et al*. Structure of Rpn10 and its interactions with polyubiquitin chains and the proteasome subunit Rpn12. *J. Biol. Chem.* **285,** 33992–34003 (2010).
45. Zhang, N. *et al*. Structure of the s5a:k48-linked diubiquitin complex and its interactions with rpn13. *Mol. Cell* **35,** 280–290 (2009).
46. Husnjak, K. *et al*. Proteasome subunit Rpn13 is a novel ubiquitin receptor. *Nature* **453,** 481–488 (2008).
47. Schreiner, P. *et al*. Ubiquitin docking at the proteasome through a novel pleckstrin-homology domain interaction. *Nature* **453,** 548–552 (2008).
48. Sahtoe, D. D. *et al*. Mechanism of UCH-L5 Activation and Inhibition by DEUBAD Domains in RPN13 and INO80G. *Mol. Cell* **57,** 887–900 (2015).
49. VanderLinden, R. T. *et al*. Structural Basis for the Activation and Inhibition of the UCH37 Deubiquitylase. *Mol. Cell* **57,** 901–911 (2015).
50. Elsasser, S., Chandler-Militello, D., M u ller, B., Hanna, J. & Finley, D. Rad23 and Rpn10 serve as alternative ubiquitin receptors for the proteasome. *J. Biol. Chem.* **279,** 26817–26822 (2004).
51. Raasi, S., Varadan, R., Fushman, D. & Pickart, C. M. Diverse polyubiquitin interaction properties of ubiquitin-associated domains. *Nat. Struct. Mol. Biol.* **12,** 708–714 (2005).
52. Yao, T. & Cohen, R. E. A cryptic protease couples deubiquitination and degradation by the proteasome. *Nature* **419,** 403–407 (2002).
53. Verma, R. *et al*. Role of Rpn11 metalloprotease in deubiquitination and degradation by the 26S proteasome. *Science* **298,** 611–615 (2002).
54. Tronrud, D. E., Roderick, S. L. & Matthews, B. W. Structural basis for the action of thermolysin. *Matrix Suppl* **1,** 107–111 (1992).
55. Worden, E. J., Padovani, C. & Martin, A. Structure of the Rpn11–Rpn8 dimer reveals mechanisms of substrate deubiquitination during proteasomal degradation. *Nat. Struct. Mol. Biol.* **21,** 220–227 (2014).
56. Leggett, D. S. *et al*. Multiple associated proteins regulate proteasome structure and function. *Mol. Cell* **10,** 495–507 (2002).
57. Zhang, N.-Y., Jacobson, A. D., Macfadden, A. & Liu, C.-W. Ubiquitin chain trimming recycles the substrate binding sites of the 26 S proteasome and promotes degradation of lysine 48-linked polyubiquitin conjugates. *J. Biol. Chem.* **286,** 25540–25546 (2011).
58. Chen, P.-C. *et al*. The proteasome-associated deubiquitinating enzyme Usp14 is essential for the maintenance of synaptic ubiquitin levels and the development of neuromuscular

junctions. *J. Neurosci.* **29,** 10909–10919 (2009).
59. Kravtsova-Ivantsiv, Y., Cohen, S. & Ciechanover, A. Modification by single ubiquitin moieties rather than polyubiquitination is sufficient for proteasomal processing of the p105 NF-kappaB precursor. *Mol. Cell* **33,** 496–504 (2009).
60. Kim, W. *et al.* Systematic and quantitative assessment of the ubiquitin-modified proteome. *Mol. Cell* **44,** 325–340 (2011).
61. Saeki, Y., Isono, E. & Toh e, A. in *Ubiquitin and Protein Degradation, Part B* **399,** 215–227 (Elsevier, 2005).
62. Nathan, J. A., Kim, H. T., Ting, L., Gygi, S. P. & Goldberg, A. L. Why do cellular proteins linked to K63-polyubiquitin chains not associate with proteasomes? *EMBO J.* **32,** 552–565 (2013).
63. Prakash, S., Inobe, T., Hatch, A. J. & Matouschek, A. Substrate selection by the proteasome during degradation of protein complexes. *Nat. Chem. Biol.* **5,** 29–36 (2009).
64. Fishbain, S., Prakash, S., Herrig, A., Elsasser, S. & Matouschek, A. Rad23 escapes degradation because it lacks a proteasome initiation region. *Nat. Comm.* **2,** 192 (2011).
65. Fishbain, S. *et al.* Sequence composition of disordered regions fine-tunes protein half-life. *Nat. Struct. Mol. Biol.* **22,** 214–221 (2015).
66. Inobe, T., Fishbain, S., Prakash, S. & Matouschek, A. Defining the geometry of the two-component proteasome degron. *Nat. Chem. Biol.* **7,** 161–167 (2011).
67. Piwko, W. & Jentsch, S. Proteasome-mediated protein processing by bidirectional degradation initiated from an internal site. *Nat. Struct. Mol. Biol.* **13,** 691–697 (2006).
68. Sledz, P. & Unverdorben, P. Structure of the 26S proteasome with ATP-γS bound provides insights into the mechanism of nucleotide-dependent substrate translocation. *Proc. Natl. Acad. Sci. USA* **110,** 7264–7269 (2013).
69. Unverdorben, P. *et al.* Deep classification of a large cryo-EM dataset defines the conformational landscape of the 26S proteasome. *Proc. Natl. Acad. Sci. USA* **111,** 5544–5549 (2014).
70. Asano, S. *et al.* A molecular census of 26S proteasomes in intact neurons. *Science* **347,** 439–443 (2015).
71. Hu, M. *et al.* Structure and mechanisms of the proteasome-associated deubiquitinating enzyme USP14. *EMBO J.* **24,** 3747–3756 (2005).
72. Hanna, J. *et al.* Deubiquitinating enzyme Ubp6 functions noncatalytically to delay proteasomal degradation. *Cell* **127,** 99–111 (2006).
73. Peth, A., Besche, H. C. & Goldberg, A. L. Ubiquitinated proteins activate the proteasome by binding to Usp14/Ubp6, which causes 20S gate opening. *Mol. Cell* **36,** 794–804 (2009).
74. Peth, A., Kukushkin, N., Boss e, M. & Goldberg, A. L. Ubiquitinated proteins activate the proteasomal ATPases by binding to Usp14 or Uch37 homologs. *J. Biol. Chem.* **288,** 7781–7790 (2013).
75. Lee, B.-H. *et al.* Enhancement of proteasome activity by a small-molecule inhibitor of USP14. *Nature* **467,** 179–184 (2010).
76. Lee, M. J., Lee, B.-H., Hanna, J., King, R. W. & Finley, D. Trimming of ubiquitin chains by proteasome-associated deubiquitinating enzymes. *Mol. Cell. Proteomics* **10,** R110.003871 (2011).
77. Wu, N. *et al.* Over-expression of deubiquitinating enzyme USP14 in lung adenocarcinoma promotes proliferation through the accumulation of β-catenin.

International Journal of Molecular Sciences **14,** 10749–10760 (2013).
78. D'Arcy, P. A. D. *et al*. Inhibition of proteasome deubiquitinating activity as a new cancer therapy. *Nature Medicine* **17,** 1636–1640 (2011).
79. Groll, M. *et al*. Structure of 20S proteasome from yeast at 2.4Å resolution. *Nature* **386,** 463–471 (1997).
80. Martin, A., Baker, T. A. & Sauer, R. T. Pore loops of the AAA+ ClpX machine grip substrates to drive translocation and unfolding. *Nat. Struct. Mol. Biol.* **15,** 1147–1151 (2008).
81. Maillard, R. A. *et al*. ClpX(P) generates mechanical force to unfold and translocate its protein substrates. *Cell* **145,** 459–469 (2011).
82. Aubin-Tam, M.-E., Olivares, A. O., Sauer, R. T., Baker, T. A. & Lang, M. J. Single-molecule protein unfolding and translocation by an ATP-fueled proteolytic machine. *Cell* **145,** 257–267 (2011).
83. Saeki, Y. *et al*. Lysine 63-linked polyubiquitin chain may serve as a targeting signal for the 26S proteasome. *EMBO J.* **28,** 359–371 (2009).
84. Zhang, D. *et al*. Together, Rpn10 and Dsk2 can serve as a polyubiquitin chain-length sensor. *Mol. Cell* **36,** 1018–1033 (2009).
85. Mayor, T., Graumann, J., Bryan, J., MacCoss, M. J. & Deshaies, R. J. Quantitative profiling of ubiquitylated proteins reveals proteasome substrates and the substrate repertoire influenced by the Rpn10 receptor pathway. *Mol. Cell. Proteomics* **6,** 1885–1895 (2007).
86. Torres, E. M. *et al*. Identification of aneuploidy-tolerating mutations. *Cell* **143,** 71–83 (2010).
87. Dephoure, N. *et al*. Quantitative proteomic analysis reveals posttranslational responses to aneuploidy in yeast. *eLife* e03023 (2014).
88. Walters, B. J. *et al*. A catalytic independent function of the deubiquitinating enzyme USP14 regulates hippocampal synaptic short-term plasticity and vesicle number. *J. Physiol.* **592,** 571–586 (2014).
89. Levchenko, I. A Specificity-Enhancing Factor for the ClpXP Degradation Machine. *Science* **289,** 2354–2356 (2000).
90. Dong, K. C. *et al*. Preparation of distinct ubiquitin chain reagents of high purity and yield. *Structure* **19,** 1053–1063 (2011).
91. Borodovsky, A. *et al*. A novel active site-directed probe specific for deubiquitylating enzymes reveals proteasome association of USP14. *EMBO J.* **20,** 5187–5196 (2001).
92. Chu, B. W. *et al*. The E3 ubiquitin ligase UBE3C enhances proteasome processivity by ubiquitinating partially proteolyzed substrates. *J. Biol. Chem.* **288,** 34575–34587 (2013).
93. Marshall, A. G. *et al*. Genetic background alters the severity and onset of neuromuscular disease caused by the loss of ubiquitin-specific protease 14 (Usp14). *PLOS ONE* **8,** 1–18 (2013).
94. Crosas, B. *et al*. Ubiquitin chains are remodeled at the proteasome by opposing ubiquitin ligase and deubiquitinating activities. *Cell* **127,** 1401–1413 (2006).
95. Aviram, S. & Kornitzer, D. The ubiquitin ligase Hul5 promotes proteasomal processivity. *Mol. Cell. Biol.* **30,** 985–994 (2010).
96. Inobe, T., Fishbain, S., Prakash, S. & Matouschek, A. Defining the geometry of the two-component proteasome degron. *Nat. Chem. Biol.* (2011).
97. Gomez, T. A., Kolawa, N., Gee, M., Sweredoski, M. J. & Deshaies, R. J. Identification

of a functional docking site in the Rpn1 LRR domain for the UBA-UBL domain protein Ddi1. *BMC Biol*. **9,** 33 (2011).
98. Verma, R. *et al*. Proteasomal Proteomics: Identification of Nucleotide-sensitive Proteasome-interacting Proteins by Mass Spectrometric Analysis of Affinity-purified Proteasomes. *Mol. Biol. Cell* **11,** 3425–3439 (2000).
99. Kather, I., Bippes, C. A. & Schmid, F. X. A stable disulfide-free gene-3-protein of phage fd generated by in vitro evolution. *J. Mol. Biol*. **354,** 666–678 (2005).
100. Worden, E. J., Padovani, C. & Martin, A. Structure of the Rpn11-Rpn8 dimer reveals mechanisms of substrate deubiquitination during proteasomal degradation. *Nat. Struct. Mol. Biol*. **21,** 220–227 (2014).
101. Pickart, C. M. & Raasi, S. Controlled synthesis of polyubiquitin chains. *Met. Enz*. **399,** 21–36 (2005).
102. Carragher, B. *et al*. Leginon: an automated system for acquisition of images from vitreous ice specimens. *J. Struct. Biol*. **132,** 33–45 (2000).
103. Lander, G. C. *et al*. Appion: an integrated, database-driven pipeline to facilitate EM image processing. *J. Struct. Biol*. **166,** 95–102 (2009).
104. Roseman, A. M. FindEM--a fast, efficient program for automatic selection of particles from electron micrographs. *J. Struct. Biol*. **145,** 91–99 (2004).
105. Scheres, S. H. W. RELION: implementation of a Bayesian approach to cryo-EM structure determination. *J. Struct. Biol*. **180,** 519–530 (2012).
106. Goddard, T. D., Huang, C. C. & Ferrin, T. E. Visualizing density maps with UCSF Chimera. *J. Struct. Biol*. **157,** 281–287 (2007).
107. Gur, E. & Sauer, R. T. Recognition of misfolded proteins by Lon, a AAA(+) protease. *Genes Dev*. **22,** 2267–2277 (2008).
108. Brocca, S. *et al*. Compaction properties of an intrinsically disordered protein: Sic1 and its kinase-inhibitor domain. *Biophysical journal* **100,** 2243–2252 (2011).
109. Martin, A. & Schmid, F. X. The Folding Mechanism of a Two-domain Protein: Folding Kinetics and Domain Docking of the Gene-3 Protein of Phage fd. *J. Mol. Biol*. **329,** 599–610 (2003).
110. Kenniston, J. A., Baker, T. A., Fernandez, J. M. & Sauer, R. T. Linkage between ATP consumption and mechanical unfolding during the protein processing reactions of an AAA+ degradation machine. *Cell* **114,** 511–520 (2003).
111. Sauer, R. T. *et al*. Sculpting the proteome with AAA(+) proteases and disassembly machines. *Cell* **119,** 9–18 (2004).
112. Haar, von der, T. A quantitative estimation of the global translational activity in logarithmically growing yeast cells. *BMC Syst Biol* **2,** 87 (2008).
113. Russell, S. J., Steger, K. A. & Johnston, S. A. Subcellular localization, stoichiometry, and protein levels of 26 S proteasome subunits in yeast. *J. Biol. Chem*. **274,** 21943–21952 (1999).
114. Duttler, S., Pechmann, S. & Frydman, J. Principles of cotranslational ubiquitination and quality control at the ribosome. *Mol. Cell* **50,** 379–393 (2013).
115. Seeger, M. *et al*. Interaction of the anaphase-promoting complex/cyclosome and proteasome protein complexes with multiubiquitin chain-binding proteins. *J. Biol. Chem*. **278,** 16791–16796 (2003).
116. Xie, Y. & Varshavsky, A. Physical association of ubiquitin ligases and the 26S proteasome. *Proc. Natl. Acad. Sci. USA* **97,** 2497–2502 (2000).

117. Kleijnen, M. F. *et al*. The hPLIC proteins may provide a link between the ubiquitination machinery and the proteasome. *Mol. Cell* **6,** 409–419 (2000).
118. Chandra, A., Chen, L., Liang, H. & Madura, K. Proteasome assembly influences interaction with ubiquitinated proteins and shuttle factors. *J. Biol. Chem.* **285,** 8330–8339 (2010).
119. Pack, C.-G. *et al*. Quantitative live-cell imaging reveals spatio-temporal dynamics and cytoplasmic assembly of the 26S proteasome. *Nat. Comm.* **5,** 3396 (2014).
120. Park, S.-H. *et al*. PolyQ proteins interfere with nuclear degradation of cytosolic proteins by sequestering the Sis1p chaperone. *Cell* **154,** 134–145 (2013).
121. Lu, Y., Lee, B. H., King, R. W., Finley, D. & Kirschner, M. W. Substrate degradation by the proteasome: A single-molecule kinetic analysis. *Science* **348,** 1250834–1250834 (2015).
122. Kirkpatrick, D. S. *et al*. Quantitative analysis of in vitro ubiquitinated cyclin B1 reveals complex chain topology. *Nat. Cell Biol.* **8,** 700–710 (2006).